AN ABSTRACT OF THE DISSERTATION OF

Kimberly H. Halsey for the degree of Doctor of Philosophy in Molecular and Cellular Biology presented on January 9, 2007.

Title: Investigating the Basis of Substrate Specificity in Butane Monooxygenase and Chlorinated Ethene Toxicity in *Pseudomonas butanovora*

Abstract approved: _____

Daniel J. Arp

Pseudomonas butanovora, Mycobacterium vaccae, and *Nocardioides* sp. CF8 utilize distinctly different butane monooxygenases (BMOs) to initiate degradation of recalcitrant chlorinated ethenes (CEs) that pollute aquifers and soils. BMO-dependent degradation of CEs such as trichloroethylene (TCE) can lead to cellular toxicities. The type and severity of TCE transformation-dependent damage can have different impacts on the bacterial host and community, potentially allowing for tolerance to TCE transformation. The physiological consequences of TCE transformation by the three butane-oxidizers were examined. Although the primary toxic event resulting from TCE cometabolism by these three strains was loss of BMO activity, species differences were observed. BMO of *P. butanovora* is the only member of the soluble methane monooxygenase (sMMO) subfamily of soluble diiron monooxygenases in which methane oxidation had not been measured. To investigate the fundamental differences in substrate specificity between BMO and MMO, single amino acid substitutions were made to the hydroxylase α-subunit of BMO (BMOH-α). Striking differences in specific activities and regiospecificity were observed for mutant strains G113N and L279F. The predominantly sub-terminal oxidation of propane and butane by strain G113N suggests the single amino acid substitution caused a significant alteration of BMOH-α active site geometry. The

sensitivity of methane oxidation by BMO to methanol may have significant implications associated with product release. The differences in regiospecificity of *P. butanovora* mutant strains relative to wild-type extend to CEs. Although the wild-type strain released nearly all available chlorine during CE exposures, strain G113N released less than 25% of available DCE chlorine and only 56% of available TCE chlorine. Half the amount of CE epoxide was formed by strain G113N during CE degradation as compared to the wild-type strain. Furthermore, differences in CE epoxide degradation suggest the mutant strains have altered activity towards epoxides. Lactate-dependent O_2 uptake rates were differentially affected by DCE degradation, providing evidence that different products or product ratios are released by the altered BMOs that have remarkable impacts on cellular toxicity. The use of CEs as mechanistic probes in combination with *P. butanovora* BMOH-α mutants provided unexpected insights to the catalytic mechanism of BMO.

Investigating the Basis of Substrate Specificity in Butane Monooxygenase and Chlorinated Ethene Toxicity in *Pseudomonas butanovora*

by
Kimberly H. Halsey

A DISSERTATION

submitted to

Oregon State University

in partial fulfillment of
the requirements for the
degree of

Doctor of Philosophy

Presented January 9, 2007
Commencement June 2007

Doctor of Philosophy dissertation of Kimberly H. Halsey presented on January 9, 2007.

APPROVED:

_____

Major Professor, representing Molecular and Cellular Biology

_____

Director of the Molecular and Cellular Biology Program

_____

Dean of the Graduate School

I understand that my dissertation will become part of the permanent collection of Oregon State University libraries. My signature below authorizes release of my thesis to any reader upon request.

_____

Kimberly H. Halsey, Author

ACKNOWLEDGEMENTS

The mentoring of my advisor, Dr. Daniel J. Arp, has been a constant source of positive and directed guidance. His approach to science is with a true sense of scholarship for which I am grateful to have experienced. In my first year of research, Dan suggested I apply for participation in the NSF GK-12 fellowship program to enhance science education in Oregon schools. It proved to be a particularly enriching experience that served to instill a desire to communicate aspects of scientific discovery through outreach activities. Dan has taught me to be careful with the use of scientific language and his weekly lab meetings provided the opportunity to become more comfortable with sharing scientific ideas.

I am thankful that Dr. Peter Bottomley has willingly advised me through two post-graduate degrees. Peter has provided avenues for creative approaches to scientific questions, and I am especially grateful that he has challenged me to critically analyze scientific data. I have been able to count on his unwavering encouragement.

From the first day that Dr. Luis Sayavedra-Soto taught me to grow bacteria with butane, he has been a constant source of professional assistance. Without fail, Luis was available to discuss results, experimental design, and rationale. He is also a tremendous resource for instrumental assistance, result celebration, and frustration management.

I am grateful to all of my committee members, Dan, Peter, Dr. Lewis Semprini, Dr. Lynda Ciuffetti, and Dr. Jerry Heidel for graciously giving their time and interest to this project and process.

The members of the Arp and Bottomley labs have been a pleasure to work with. They have been generous in the sharing of ideas, and patient in the sharing of space and equipment. We have been a lucky group to have had the opportunity to work together on interesting projects with freedom of investigation – thanks for sharing in the ride.

Finally, I would like to express my deepest appreciation to my family for their constant encouragement and interest in all things scientific, creative, and mysterious. My parents have inspired me to pursue a productive life that combines the joys of work and play. Anybody in the vicinity of the Arp lab at a “Eureka!” moment, cannot miss the enthusiasm I have for research; so I am very fortunate to have found a workplace and

playground in the lab! Together in their own endeavors, my parents have demonstrated their passion for lifelong learning, curiosity, and generosity of spirit. They have taught me to Wonder and Wander with purpose and reverence. And, of course my children, Ellen and Chase! They were 9 and 7 years old when I started this project. Now, 5 (and 1/2) years later, I am amazed at their own strength of characters. There have been many hurried, uninspired dinners, high-strung finals' weeks, and afternoons they were bribed to stuff pipette-tip boxes or sort test-tube caps in order to give me just a few more hours with the GC. Most awe-inspiring; however, is being present at moments of ***their*** learning that demonstrate their potential as individuals in this world. I am most humbled by their sheer openness to questioning the universe.

CONTRIBUTION OF AUTHORS

Dr. Daniel J. Arp contributed scientific discussion and manuscript preparation for chapters 2, 3, and 4. Dr. Arp provided particular expertise with kinetic analyses in chapter 2 and biochemical interpretation of methanol inhibition of methane oxidation by sBMO in chapter 3. Dr. Luis A. Sayavedra-Soto contributed scientific discussion and ideas for experimental design to chapters 2, 3, and 4. Dr. Peter J. Bottomley contributed scientific discussion, critical data analysis, and manuscript preparation for chapters 2, 3, and 4. David M. Doughty provided ideas for experimental design and mechanistic modeling with the specific suggestion of the use of 1,1 dichloroethene as a substrate probe of sBMO and altered sBMO oxidation in chapter 4. All experiments were financially supported and conducted in the laboratory of Dr. Daniel J. Arp at Oregon State University.

TABLE OF CONTENTS

TABLE OF CONTENTS (Continued)

TABLE OF CONTENTS (Continued)

TABLE OF CONTENTS (Continued)

LIST OF FIGURES

LIST OF FIGURES (Continued)

LIST OF TABLES

LIST OF TABLES (Continued)

INVESTIGATING THE BASIS OF SUBSTRATE SPECIFICITY IN BUTANE MONOOXYGENASE AND CHLORINATED ETHENE TOXICITY IN *Pseudomonas butanovora*

CHAPTER 1.

INTRODUCTION

SHORT-CHAINED ALKANES IN THE ENVIRONMENT

Saturated hydrocarbons having the general formula C_nH_{n+2} are referred to as alkanes. Methane, ethane, propane, and butane (C1-C4) are gasses at room temperature. Alkanes that are 5-carbons in length and greater are in the liquid state at room temperature. The water solubility of alkanes decreases as their chain length increases. Methane is released from subsurface anaerobic environments by methanogens, and if it is not consumed by methanotrophs before being released into the atmosphere is an important contributor to the "greenhouse effect" and global warming. Therefore, significant research energy has been put forth to understand the biochemistry and regulation of methane oxidation. Short-chained alkanes (C2-C8) are present in the earth's crust and are found in their highest concentrations in petroleum reservoirs (Hunt, 1996). Trace amounts of gaseous alkanes are also detected at the aerobic-anaerobic interface where they are released by methanogens during biodegradative processes (Belay and Daniels, 1987).

The commensurate step in the aerobic metabolism of short-chained alkanes by aerobic microorganisms is activation of the stable hydrocarbon by insertion of oxygen derived from dioxygen into the substrate. The enzymes that carry out this process are complex and powerful oxidative systems, and they are of particular interest for their involvement in carbon cycling and their potential in bioremediation and bioindustrial catalysis.

Methanotrophs

Methane-oxidizing bacteria, or methanotrophs, are a specialized subset of alkane-oxidizers that are capable of growth on methane as their sole source of carbon and energy. Methanotrophs are grouped according to physiologic characteristics including unique metabolic pathways for formaldehyde assimilation (Hanson and Hanson, 1996). Interestingly, methanotrophs are restricted to growth on methane; that is, they do not possess metabolic pathways for the metabolism of alkanes greater than 1-carbon in chain length.

Metabolism of methane proceeds following the initial NADH dependent oxidation of methane by methane monooxygenase (MMO) to methanol. Methanol dehydrogenase further oxidizes methanol to formaldehyde. As mentioned above, formaldehyde assimilation may proceed via different pathways including the ribulose monophosphate pathway (Type I Methanotrophs) and the Serine pathway (Type II Methanotrophs) (Hanson and Hanson, 1996). Type X Methanotrophs utilize enzymes of both pathways and are unique in producing ribulose-1,5-bisphosphate carboxylase. Type I and X Methanotrophs belong to the γ subdivision of proteobacteria, and Type II Methanotrophs belong to the α subdivision of proteobacteria.

Two distinct MMOs are expressed under conditions of copper availability. Most methanotrophs express an integral membrane, 94 kDA copper containing MMO termed pMMO. Under copper-limiting conditions, some methanotrophs express a soluble, non-haem, diiron-containing MMO (sMMO).

Short-chain alkane-oxidizing bacteria

Because alkane-oxidizing bacteria have been isolated from pristine and industrial soils, freshwater sediments, contaminated aquifers and sewage sludge, it is not surprising that the diversity of bacteria recovered from these sites is remarkable (Shennan, 2006). Enrichment and isolation of aerobic bacteria capable of growth

using alkanes as their sole source of carbon and energy are primarily Gram positives of the CMNR genera *Corynebacterium, Mycobacterium, Nocardia,* and *Rhodococcus*. Several gram negative species identified as pseudomonads and species of *Burkholderia* have been isolated and are among the best studied of the alkane oxidizing bacteria. *Pseudomonas butanovora* was originally isolated from an oil refining plant for its relatively high levels of biomass production (Takahashi, 1980). Original taxonomic classification of this organism, based primarily on morphology and physiology, as a pseudomonad was incorrect; 16S rRNA sequencing suggests it is more closely related to the genera *Thauera* and *Azoarcus* of the β subdivision of proteobacteria (Sayavedra-Soto *et al.*, 2001). *Burkholderia cepacia* and *Burkholderia* LB400 have proven to be useful model systems due to their relatively high transfomation efficiencies and metabolic diversity (Mahendra and Alvarez-Cohen, 2006; Seah *et al.*, 2001; Urgun-Demirtas *et al.*, 2003). The ability to utilize short-chained alkanes as growth compounds is conferred by a monooxygenase reaction; that is, the insertion of one oxygen atom from dioxygen into the alkane by a monooxygenase enzyme.

Pseudomonas butanovora

P. butanovora is a gram-negative, rod-shaped, aerobic bacterium capable of growth on C2 to C8 alkanes as its sole source of carbon and energy. Growth is most rapid on *n*-butane (Takahashi *et al.*, 1980). Metabolism of butane is initiated by butane monooxygenase (BMO) (Arp, 1999; Hamamura *et al.*, 1997). The pathway for butane oxidation in *P. butanovora* was determined and is depicted in Figure 1.1.

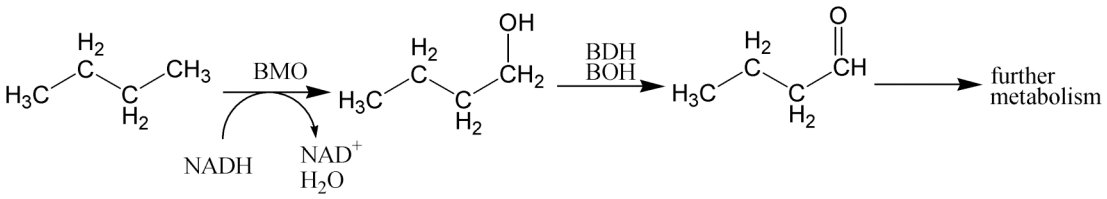

Figure 1.1. Pathway of butane metabolism by *P. butanovora*

1-butanol is the predominant product of butane oxidation by BMO (Arp, 1999; Dubbels *et al.*, accepted; Halsey *et al.*, 2006) which is subsequently oxidized by the alcohol dehydrogenases (ADHs) BOH and BDH (Vangnai *et al.*, 2002) yielding butyraldehyde. Oxidation of butyraldehyde yields butyrate which likely undergoes beta-oxidation entering central metabolism (Arp, 1999; Vangnai *et al.*, 2002). Interestingly, although 96% of the butane oxidation product is 1-butanol, *P. butanovora* is capable of growth on 2-butanol and 2-butanone (Halsey *et al.*, 2006). Two soluble NAD+-dependent ADHs were identified during growth on 2-butanol (Vangnai and Arp, 2001). Propane oxidation also proceeds via terminal oxidation. However, the downstream metabolites of subterminal oxidation of propane, 2-propanol and acetone, are not metabolized under normal growth conditions (minimal media with no yeast extract). Recent experiments demonstrated that addition of yeast extract to the growth media promoted growth of *P. butanovora* on 2-propanol and acetone (Davidson *et al.*, unpublished), implying that a carboxylation reaction enables growth on subterminally activated C3 compounds. *P. butanovora* also utilizes carboxylic acids of C2-C4, but it cannot utilize alkanes of C10 and higher, C1 compounds, *n*-alkenes, or sugars for growth.

Other alkane oxidizers

Gram positive bacteria dominate the strains that have been cultivated from environmental samples by enrichment in the presence of short-chained alkanes (Shennan, 2006). Species of *Mycobacterium*, *Nocardioides*, *Gordonia*, and *Rhodococcus* have been isolated on propane or butane from oil sludge, soil, and aquifer solids (Coleman *et al.*, 2002; Hamamura *et al.*, 2006; Kotani *et al.*, 2006).

Mycobacterium vaccae JOB5 grows on alkanes C2 to C40 in length, organic acids, and sugars. Growth on propane or butane is initiated by subterminal oxidation of the alkane; although terminal oxidation of butane was also noted (Phillips and Perry, 1974). Other alkane oxidizing *Mycobacterium* species have been isolated by ethylene enrichment of environmental samples. These strains have remarkable metabolic versatility, and one strain, NBB4 was recently found to have four different monooxygenases (Coleman *et al.*, 2006).

Nocardioides sp. CF8 was isolated from aquifer solids from the Hanford DOE site in Washington state, and it can utilize alkanes C2-C16 (Hamamura and Arp, 2000). Characterization of the monooxygenase initiating butane oxidation in this species revealed an integral membrane, copper containing monooxygenase. Inhibitor and inactivation profiles demonstrated that this monooxygenase bears similarity to particulate methane monooxygenase (pMMO) and ammonia monooxygenase (AMO) (Hamamura *et al.*, 1999; Hamamura and Arp, 2000). Interestingly, growth of *Nocardioides* sp. CF8 on alkanes greater than C6 in length induced the expression of a second integral membrane, binuclear-iron monooxygenase (Hamamura *et al.*, 2001).

SOLUBLE DIIRON MONOOXYGENASES

Initiation of alkane metabolism occurs by oxidation of the alkane by a monooxygenase. Extensive interest in a group of monooxygenases that activates

alkanes, referred to as soluble diiron monoooxygenases (SDIMOs), has followed several lines of research: (1) structural aspects of the multicomponent enzyme complexes, (2) biochemical nature of stable compound oxidation, and (3) environmental and ecological contexts including involvement in carbon cycling and intrinsic and bioaugmented bioremediation activities. All SDIMOs have a hydroxylase consisting of 2 or 3 subunits, a reductase, and an effector protein. The diiron centers are coordinated by residues in the form of a Glu-Xxx-Xxx-His motif. SDIMOs are structurally related to other enzymes that use carboxylate-bridged diiron centers for substrate oxidation, including the R2 subunit of class I ribonucleotide reductase and stearoyl-ACP Δ^9 desaturase (Merkx *et al.*, 2001). Structural comparisons, sequence identity, operon organization, and to a lesser degree, substrate specificity allowed for organization of the SDIMOs into 6 subgroups (Coleman *et al.*, 2006; Leahy *et al.*, 2003). Three of these subgroups containing enzymes of interest to both the fundamental understanding of hydrocarbon oxidation and structure/function relationships as well as bioindustrial applications are described below.

The sMMOs

The soluble methane monooxygenase (sMMO) subgroup is the most well-characterized of the SDIMOs. Intense interest has focused on the unique ability of enzymes in this group to preferentially oxidize methane to methanol. Purification and crystallography of sMMOs from the flagship species, *Methylococcus capsulatus* Bath and *Methylosinus trichosporium* OB3b, has provided evidence for the manner in which these enzymes selectively oxidize methane. However, SDIMOs from methanotrophs are no longer considered to be the only members of the sMMO subgroup. Following sequence analysis and initial biochemical characterization, soluble butane monooxygenase (sBMO) from *Pseudomonas butanovora* was included with the sMMO subgroup (Sluis *et al.*, 2002). *Brachymonas petroleovorans* was found to utilize a sBMO for initiation of growth on cyclohexane. Interestingly, despite the

difference in growth substrate, the sBMO from *B. petroleovorans* has 90% sequence identity to sBMO from *P. butanovora* (Brzostowicz *et al.*, 2005). More recently, environmental enrichments from lake sediments yielded 3 clones with 60-66% amino acid sequence identity to sBMO (Coleman *et al.*, 2006).

The SDIMOs in the sMMO subgroup are three-component enzymes consisting of a hydroxylase, reductase, and an effector protein. The hydroxylase itself consists of three unique subunits of approximately 60, 45, and 20 kDa arranged in a $\alpha_2\beta_2\gamma_2$ configuration. Crystallization and biochemical analyses confirmed that the α-subunit contains the diiron active site and interacts with both the reductase and effector protein (Merkx *et al.*, 2001; Sluis *et al.*, 2002). The reductase is 39 kDa and transfers electrons from NADH to the hydroxylase via FAD and [2Fe-2S] clusters. In sMMO, while oxidative activity occurs in the absence of the 15 kDa effector protein, it has substantial effects on substrate specificity, rate and regiospecificity of oxidation, and stability of enzyme intermediates (Murrell *et al.*, 2000). The effector protein apparently affects influence on catalysis through conformational changes in the hydroxylase. The role of the effector protein in sBMO is less clear. It does not appear to affect rates of substrate oxidation or product distribution, and only modestly improves overall coupling of the overall reaction (Dubbels *et al.*, accepted).

SDIMOs of the sMMO subgroup are widely distributed phylogenetically. The sMMOs are genetically similar; the protein component that harbors the active-site is 65% identical among those that have been completely sequenced. However, the sMMOs often carry out oxidation of very different growth substrates (compare methane, butane, and cyclohexane) with different metabolic pathways, suggesting that enzymes of this subgroup were independently incorporated into distinct metabolic pathways by diverse hosts (Coleman *et al.*, 2006). Evolutionarily, it has been suggested that horizontal transfer events have distributed the genes encoding sMMOs allowing for successful adaptation to a range of habitats (Leahy *et al.*, 2003; Murrell *et al.*, 2000).

The phenol hydroxylases

The SDIMOs of the phenol hydroxylase (PH) subgroup initiate oxidation of phenolic substrates to their corresponding catechols. The PH from *Pseudomonas* CF600 and toluene-*o*-monooxygenase (T2MO) from *Burkholderia cepacia* have been well characterized. PHs have also been found in *Acinetobacter* spp., *Commamonas testosteroni* R5, and *Ralstonia eutropha* E2. The multicomponent organization of the PHs is the same as described for the sMMOs above, and the genetic organization of these enzymes is identical among the PHs.

The effector protein (P2) in PH from *Pseudomonas sp.* CF600 was the first of the SDIMO effector proteins to be structurally characterized by NMR (Qian *et al.*, 1997), and the conformation of P2 is unusual upon three dimensional comparison with sMMO effector proteins. P2 has a unique "donut" structure in which the "donut hole" has been hypothesized to funnel the hydrophobic substrate to the active site of the hydroxylase (Qian *et al.*, 1997).

T2MO from *B. cepacia* was one of the first to be utilized for SDIMO mutagenesis studies. T2MO was heterologously expressed in *E. coli*. The hydroxylase α-subunit was altered using DNA shuffling and saturation mutagenesis techniques. Clones of interest were selected by colorimetric identification. Strains demonstrating changes to rate and regiospecificity of oxidation were sequenced, and key residues were identified that were postulated to affect substrate-positioning at the active site (Canada *et al.*, 2002; Fishman *et al.*, 2005; Rui *et al.*, 2005; Vardar and Wood, 2004, 2005). Wood and colleagues successfully exploited this methodology to conduct many studies using other toluene monooxygenases (T4MO, T3MO, and toluene/*o*-xylene monooxygenase; see below) to describe changes to the oxidation activity of many substrates that are either environmental contaminants or precursors to industrially relevant products (for example, (Rui *et al.*, 2005)).

The alkene/aromatic monooxygenases

SDIMOs containing four components are currently grouped together in the alkene/aromatic subgroup. The fourth component is an iron-sulfur (Rieske-type) ferredoxin component that transfers electrons from the reductase to the hydroxylase. The effector protein in this subgroup has roles in affecting regiospecificity and possibly, electron passage to the hydroxylase. Species containing enzymes from this subgroup have overlapping substrate ranges: ie, T4MO in *P. mendocina* KR1 oxygenates toluene and C3-C8 alkenes, but not phenolic compounds; toluene/o-xylene monooxygenase in *P. stutzeri* OX1 oxygenates phenolic compounds and toluene, but not unactivated aromatics; and alkene monooxygenase from *Xanthobacter* sp. Py2 oxidizes C2-C6 alkenes, benzene, toluene, and phenol (Leahy *et al.*, 2003).

In agrichemicals and pharmaceuticals, activation of biologically relevant reactions often depends upon complementary stereospecificity between activator and catalyst. Alkene monooxygenase is of particular commercial interest due to interest in "green synthesis" reactions, specifically with regards to the production of stereospecific epoxides.

BUTANE MONOOXYGENASE

Diversity of butane monooxygenases

Several butane monooxygenases (BMOs) have been characterized at the molecular and/or biochemical level. While several of the BMOs were identified as SDIMOs by sequence analysis (Coleman *et al.*, 2006; Sluis *et al.*, 2002), other BMOs include the pBMO of *Nocardioides* sp. CF8 (Hamamura *et al.*, 1999), and a BMO of *M. vaccae* JOB5 that has not been genetically or biochemically characterized. The role

of BMO in initiating butane oxidation in the three strains, *P. butanovora*, *Nocardioides* sp. CF8, and *M. vaccae* was verified experimentally: (1) O_2 was required for butane oxidation, (2) 1-butanol was produced during butane oxidation (2) incubation of the butane-grown strains with acetylene, a monooxygenase inhibitor of sMMO, pMMO, and ammonia monooxygenase (Hyman and Wood, 1985; Prior and Dalton, 1985) resulted in complete inactivation of butane oxidation. However, the BMOs of *Nocardioides* sp. CF8 and *M. vaccae* were distinguished from each other and from sBMO of *P. butanovora*. [^{14}C] from [^{14}C]acetylene was incorporated into different cellular proteins of the three butane-grown strains. Furthermore, the protein banding patterns of butane-induced cells of each of the three strains were different. Incubation with ATU (a copper-selective chelator) or ethylene resulted in differential inhibition of butane oxidation among the three strains (Hamamura *et al.*, 1999). These results demonstrated that the butane monooxygenases from three different genera could be discriminated from each other based on remarkably different inactivation and inhibition profiles and [^{14}C]acetylene labeling studies.

Certain substrates have also been shown to discriminate among BMOs; for example, *Nocardioides* sp. CF8 readily degraded 1,1,2 trichloroethane, but *P. butanovora* did not. Furthermore, rates of substrate oxidation vary among the BMOs (Halsey *et al.*, 2005; Hamamura *et al.*, 1997).

Substrate range of butane monooxygenase

The substrate range of most BMOs includes alkanes, alkenes, alkynes, cyclohexane, some aromatics, chlorinated ethenes, chloroform, ammonia, and possibly naphthalene (Hamamura *et al.*, 1997; Hamamura *et al.*, 1999; Rouviere and Chen, 2003). Although the list above is extensive, it is by no means exhaustive, as undoubtedly many compounds that are probably substrates of BMO have not been tested. Perchloroethylene is not a substrate of BMO (Hamamura *et al.*, 1997). Until the research presented here (Chapter 3), methane was not considered to be a substrate for BMO. The apparent exclusion of methane from the list of substrates for BMO was a

clear distinction between MMO from methylotrophs and BMO since the broad substrate ranges of MMO and BMO are likely otherwise shared. The largest substrate tested with sMMO is 2,2-diphenyl-1-methylcyclopropane (Sazinsky and Lippard, 2006) demonstrating the exceptionally broad range of substrates fortuitously oxidized by members of the soluble methane monooxygenase subfamily.

Biochemical characterization of BMO of *P. butanovora*

Partial purification of BMO and reconstitution of oxidation activity required the combination of different protein components and NADH. Acetylene-treated cell extracts were combined with different protein components to identify the specific component harboring the active site. One acetylene-sensitive component containing three polypeptides of 54, 43, and 25 kDa and referred to as α, β, and γ-subunits, was named butane monooxygenase hydroxylase (BMOH). By analogy to the sMMO system, the BMO "reductase" component (BMOR) was identified by measurement of NADH:potassium ferricyanide oxidoreductase activity (Sluis *et al.*, 2002). Initial efforts to restore butane oxidation required the inclusion of a third protein component of 15 kDa (BMOB). Recently, purification of BMO to homogeneity showed that BMOH, BMOR, and NADH are sufficient to catalyze butane oxidation in vitro (Dubbels *et al.*, accepted). These conflicting results may resolve by further optimization of in vitro assays such that the role of BMOB in affecting hydrocarbon catalysis is clarified.

The BMO structural genes encoding the α, β, and γ-subunits of BMOH (*bmoX*, *bmoY*, and *bmoz*), BMOB (*bmoB*), and BMOR (*bmoC*) are ordered as shown in Fig 1.2. The genetic organization of these structural genes is identical to the other members of the sMMO SDIMOs.

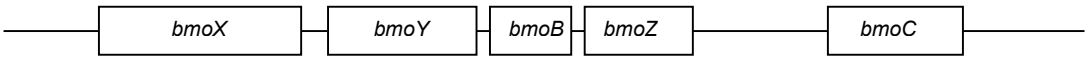

Figure 1.2. Genetic organization of structural genes of BMO

Amino acid sequence alignment of the peptides described above revealed that they are most closely related to the peptides of sMMO with the highest identity in the α-subunit of BMOH (65%). Residues in the α-subunit involved in coordination of the diiron active site in sMMO are strictly conserved in sBMO. The *bmoX* gene was specifically disrupted by insertional mutagenesis to confirm its role in growth of *P. butanovora* on butane (Sluis *et al.*, 2002). Furthermore, the residues involved in hydrogen-bonding in sMMO are conserved in sBMO as well. BMOB is 53-54% identical to MMOB, and although MMOB plays a significant role in the selective oxidation of methane in sMMO (Zhang *et al.*, 2006a), the role of BMOB has not yet been clarified (Dubbels *et al.*, accepted). Although the sequence identity between BMOR and MMOR is less than the identity noted between the other sBMO and sMMO components, the cysteine ligands to ferredoxin iron-sulfur centers are conserved between the two reductases. Other structural motifs present in BMOR confirm its homology to MMOR (Sluis *et al.*, 2002).

More detailed characterization of purified sBMO has confirmed its strong bias towards terminal oxidation of alkanes and branched alkanes (Dubbels *et al.*, accepted). Assays were conducted using the optimal BMOH:BMOR ratio of 1:2 in the presence of excess NADH. For C3-C6 substrates, >82% of the total product was accounted for as the primary oxidation product. Whereas addition of MMOB causes a remarkable shift in product distribution towards primary hydroxylation (Froland *et al.*, 1992), addition of BMOB at (1:2 BMOH:BMOB ratio) did not shift the product distribution. Excess BMOB depressed the rate of BMO activity as measured by ethylene oxide

accumulation (an alternative assay for butane oxidation activity) which is a noted characteristic of effector proteins from other SDIMOs (Cadieux *et al.*, 2002; Dubbels *et al.*, accepted; Fox *et al.*, 1989; Green and Dalton, 1985). BMO is highly sensitive to H_2O_2 produced during the uncoupled turnover of NADH even in the presence of butane (Dubbels *et al.*, accepted). Addition of BMOB did not significantly reduce H_2O_2 production. Surprisingly, BMOB only increased the activity of sBMO by at most 30%. Activity measurements are increased 30-150-fold by the addition of the effector protein in all other SDIMOs (Sazinsky and Lippard, 2006).

Regulation of BMO of *P. butanovora*

The DNA sequence immediately upstream of *bmoX* contains a putative sigma 54-dependent promoter (Sluis *et al.*, 2002). Promoters of this type typically participate with an enhancer DNA-binding protein in the upregulation of gene expression. Initial reports described butane, the natural substrate of BMO, as the inducer of butane oxidation activity in *P. butanovora* (Sayavedra-Soto *et al.*, 2001; Sluis *et al.*, 2002). RNA was extracted from *P. butanovora* cells following growth on lactate and citrate. RNA was also extracted from similar cells that had been exposed to butane for 3 h following growth on lactate. Transcripts of the BMO structural genes identified above were hybridized to individual *bmo* probes only under 'butane-exposed' conditions (Sluis *et al.*, 2002). BMO was also induced in response to 1-butanol and butyraldehyde, the immediate downstream metabolites of butane oxidation (Sayavedra-Soto *et al.*, 2001). A reporter strain of *P. butanovora* containing *lacZ::kan* inserted into *bmoX* provided more detailed characterization of BMO induction. In fact, butane did not induce expression of β-galactosidase activity, but both 1-butanol and butyraldehyde induced β-galactosidase activity (Sayavedra-Soto *et al.*, 2005). Importantly, a low (3.0 ± 1 nmol ethylene oxide (mg protein)$^{-1}$ min^{-1}), product-independent, level of BMO activity was measured in wild-type *P. butanovora* grown with citrate or lactate. Following depletion of lactate or citrate, product-independent

BMO induction, as measured by β-galactosidase expression in the reporter strain, increased 3-7 fold (Sayavedra-Soto *et al.*, 2005).

Regulation of BMO was further investigated in terms of catabolite repression. BMO activity is repressed during growth on lactate (Doughty *et al.*, 2005, 2006; Sayavedra-Soto *et al.*, 2001). Incubation of lactate-grown cells with butane induced BMO activity as measured by ethylene oxide accumulation (an alternative assay for BMO activity). Surprisingly, a lag in induction of BMO activity was measured when lactate grown cells were incubated with propane, or a mixture of propane and butane, suggesting that propane had a repressive effect on BMO. Pentane, but not ethane, was also capable of stilting BMO activity of butane-induced cells. These results seemed contrary to the fact that *P. butanovora* grows on C2-C9 alkanes. Using the *P. butanovora bmoX::lacZ::kan* reporter strain, propane itself was shown to induce transcriptional activity of the BMO promoter, but its metabolites, 1-propanol, propionaldehyde, and propionate repressed 1-butanol-dependent induction of the BMO promoter as measured by β-galactosidase activity (Doughty *et al.*, 2006). Work to understand propane metabolism in *P. butanovora* revealed that in ethane or butane grown cells, propionate accumulates as the product of 1-propanol transformation by alcohol and aldehyde dehydrogenases (Doughty *et al.*, 2006; Vangnai *et al.*, 2002). The enzymatic pathways required for propionate consumption were induced within 2h of exposure to propionaldehyde (Doughty *et al.*, 2006).

The complexity of the regulation of BMO in *P. butanovora* is just being realized. However, it seems rational that an organism that harbors a broad substrate-range energy-dependent monooxygenase would maintain several layers of regulation including positive and negative controls. Even more recent work by Doughty, *et al*., demonstrates reversible and irreversible inhibition of BMO by propionate (manuscript in preparation). Clearly, management of BMO is required at the promoter and mature enzyme level where substrate access and turnover is delicately controlled, possibly in effort to avoid excess energy drain or dead-end products.

sMMO

Structural characterization of sMMOH

The sMMO enzymes isolated from *M. capsulatus* Bath and *M. trichosporium* OB3b have been extensively studied at the structural and biochemical levels (Merkx *et al.*, 2001; Smith and Dalton, 2004; Zhang *et al.*, 2006b). Crystal structures of the hydroxylase components (MMOH) from both organisms in different crystal forms, oxidation states, and in the presence of various substrates and products have been solved ((Elango *et al.*, 1997; Rosenzweig *et al.*, 1997) and others). This vast collection of data provides details of the diiron active site and suggestions for protein interactions, substrate access, product egress, and dioxygen activation. The overall structure of MMOH resembles a heart-shaped, dimerized bundle of alpha helices (Fig. 1.3). The α, β, and γ subunits are arranged as two trimers related by a noncrystallographic, two-fold symmetrical axis.

The diiron centers coordinated by 2 His and 4 Glu residues, universally conserved among all SDIMOs, reside within the α-subunits approximately 12 Å from the surface (Fig 1.4). The diiron center is bridged by Glu 144, a hydroxide ion and a third bridging ligand. The distance between the iron atoms is variable depending on oxidation state and the ligand occupying the third bridging position (Whittington and Lippard, 2001). In product-bound crystal structures methanol and ethanol occupy the bridging position (Whittington *et al.*, 2001b).

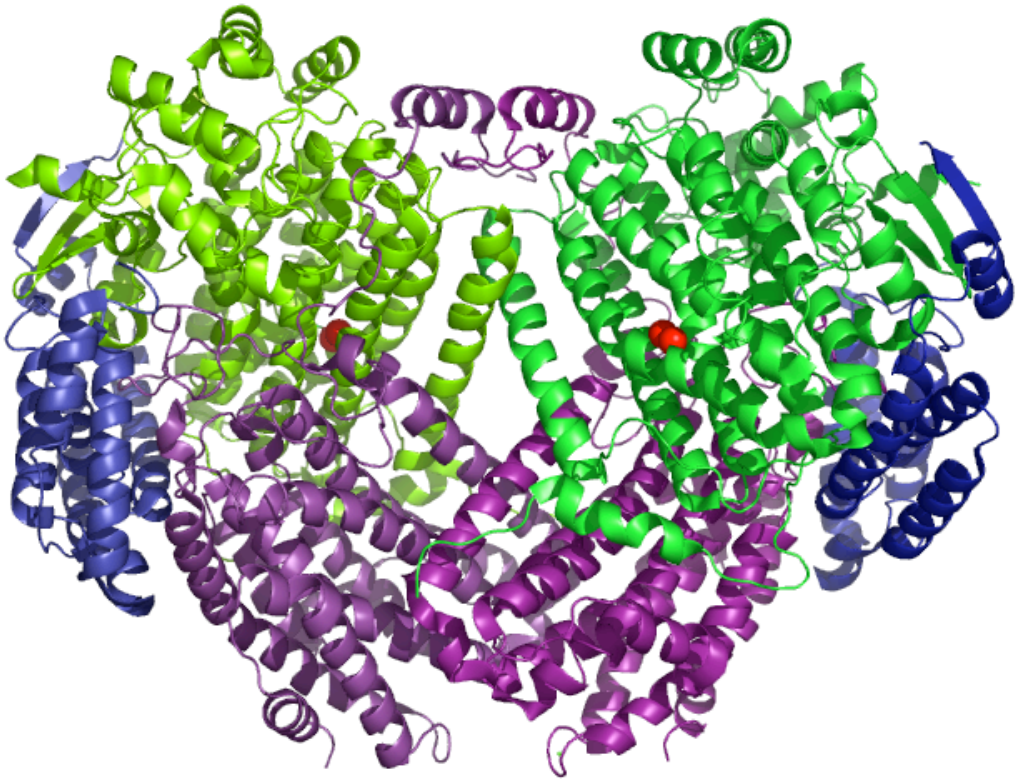

Figure 1.3. Cartoon depiction of the structure of MMOH from *M. capsulatus* Bath (PDB 1FZ1). Structure of αβγ the dimer. The two fold axis is vertical. α chains are colored in two shades of green, β chains are colored as two shades of purple, γ chains are colored as two shades of blue. Iron atoms are shown as red spheres. This figure was created using Pymol (DeLano, 2002)

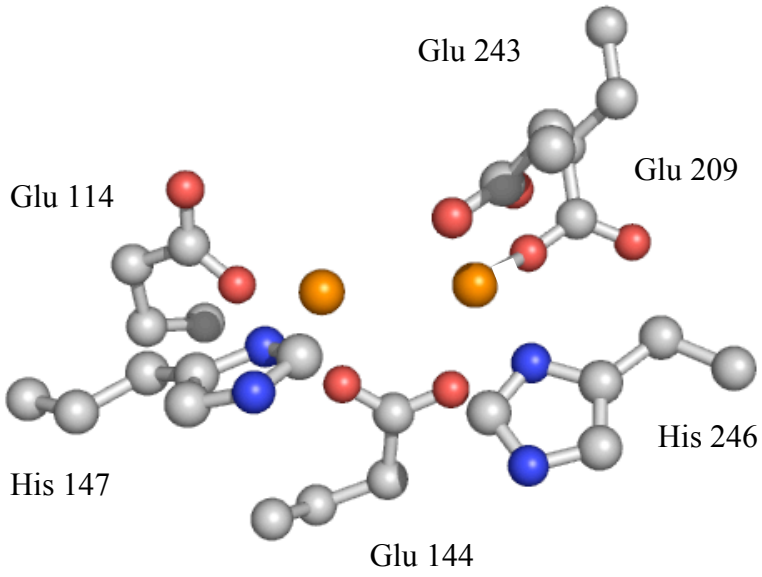

Figure 1.4. Ball and stick representation of the sMMOH diiron center from *M. capsulatus* Bath (PDB 1FZ1). The residues coordinating the geometry of the Fe atoms are labeled, and the Fe atoms are colored orange. This figure was created using Pymol software (DeLano, 2002).

The diiron center is surrounded by hydrophobic side chains (designated cavity 1), and it faces another, somewhat circuitous, longer cavity (cavity 2) that is completely lined with hydrophobic side chains and which may guide hydrophobic substrates such as methane and O_2 into the active site (Rosenzweig *et al.*, 1997). Because methane is not detected in crystallography, Xe serves as a useful methane-surrogate because its van der Waals radius is about the same as methane (~2.15 Å). Xenon-pressurized MMOH crystals revealed Xe in cavity 2 (Whittington *et al.*, 2001a). Three residues (Leu 110, Thr 213, Phe 188) contribute to the formation of the "leucine gate". Leu 110 adopts different rotameric conformations under different oxidation states and in the product-bound state (Rosenzweig *et al.*, 1997; Sazinsky and Lippard, 2005). These observations led to the suggestion that the leucine gate monitors substrate access to the diiron center (Rosenzweig *et al.*, 1997).

The crystal structure of a hydroxylase-effector protein complex from phenol hydroxylase (PH) has been solved very recently (Sazinsky *et al.*, 2006). The effector protein binding face on the hydroxylase is in a slightly different location than that previously proposed for sMMOH and MMOB. Nevertheless, the effector protein from PH interacts with α-subunit helices A, E, F and H via ionic and hydrophobic interactions (Sazinsky *et al.*, 2006). PH effector protein residues involved in hydroxylase interactions are not conserved in the sMMO subfamily, suggesting that differences in component intereactions between subfamilies may impact substrate specificity and oxidative mechanisms. Evidence exists for the site of MMOB interaction with BMOH. First, the geometrical coordination of Fe2 is markedly different when comparing oxidized and reduced MMOH crystal structures. Likewise, Asn 214 changes rotameric conformations under oxidized and reduced conditions. Binding of MMOB to MMOH may affect the position of Fe2 by impacting the conformation of Helices E and F, which contain the Fe2 coordinating residues and Asn 214. Spectroscopic and chemical cross-linking experiments showed MMOB interacts with the α-subunit of MMOH altering its structure (Fox *et al.*, 1991; Froland *et al.*, 1992). Other studies identified charged residues on the surfaces of MMOB that are required for MMOB-MMOH interaction (Balendra *et al.*, 2002; Brazeau *et al.*,

2003). Modeling the interaction using the charged residues as targets provided additional confirmation that MMOB binds to the region of the MMOH α-subunit that forms a canyon with the second αβγ protomer (Brazeau *et al.*, 2003).

Catalytic cycle of sMMO

The catalytic cycle of sMMO is exceptionally impacted by MMOB. For example, (1) the rate of substrate turnover is increased 150-fold (Liu *et al.*, 1994), (2) regiospecificity of substrate oxidation is altered (Froland *et al.*, 1992), (3) the redox potential is shifted by over -130 mV (Paulsen *et al.*, 1994), (4) coupling of NADH consumption to substrate hydroxylation is most efficient when MMOB is present (Blazyk *et al.*, 2005; Gassner and Lippard, 1999). These observations suggest a powerful role for MMOB in regulating the catalytic cycle of sMMO such that methane is selectively oxidized.

The fact that some sMMO catalytic intermediates exhibit unique spectroscopic characteristics prompted the development of a catalytic cycle and has provided experimental evidence regarding the catalytic mechanisms of sMMO (Fig 1.5) (Zhang *et al.*, 2006b).

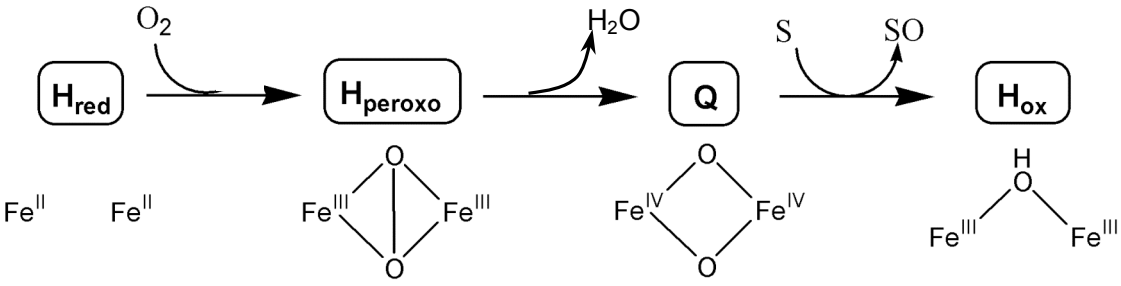

Figure 1.5. sMMO catalytic cycle adapted from (Beauvais and Lippard, 2005a, 2005b; Zhang *et al.*, 2006a; Zheng and Lipscomb, 2006).The boxed sMMO intermediates have been detected spectroscopically and refer to the different oxidative states of the diiron center. H_{ox} is reduced by the transfer of electrons from NADH restoring H_{red}.

Oxygen binds to the diiron cluster yielding a bridging peroxo-adduct, H_{peroxo}. Following the input of two protons, the bis-μ-oxo dinuclear Fe(IV) compound Q, with its characteristically intense yellow chromophore, is detected. Q has only been identified in sMMO. Mossbauer studies showed that Q has an assymetric diamond core structure with two bridging oxo-groups between the two Fe(IV)s. Q reacts with methane as well as other substrates yielding the product-bound compound H_{ox}. Heretofore, the rate-limiting step in the catalytic cycle is product release. The cycle regenerates by the transfer of electrons from NADH restoring the diferrous MMOH (H_{red}) (Merkx *et al.*, 2001; Zhang *et al.*, 2006b). It is important to note that H_{peroxo} is also capable of activating some substrates. For example H_{peroxo} effects propylene epoxidation (Beauvais and Lippard, 2005b).

BIOREMEDIATION

In 2002, the United States Environmental Protection Agency reported that human exposure to the industrial solvent trichloroethylene (TCE) could result in more severe toxic consequences, ranging from nerve damage to cancer, than earlier reports indicated (EPA, 2001). Chlorinated ethenes are now common contaminants of soils and groundwater due to improper disposal and storage of industrial solvents.

Bioremediation is receiving considerable attention as a cost-effective, publicly accepted, and environmentally considerate method to remove toxic contaminants. As yet, no microorganisms have been isolated that can utilize TCE as their primary carbon and energy source. However, bacterial species and mixed cultures that can cometabolize TCE have been isolated from contaminated aquifers (Brzostowicz *et al.*, 2003; Coleman *et al.*, 2002; Hamamura and Arp, 2000). Because these isolates are naturally occuring microorganisms, their use in bioremediation strategies is especially appealing. Initial results from field trials utilizing bacterial bioremediation are encouraging (Beeman and Bleckmann, 2002; Kao and Prosser, 1999; Lenczewski *et al.*, 2003; Semprini *et al.*, 1994), but long-term success hinges on the maintenance of healthy and active cometabolic bacterial communities.

COMETABOLISM

The broad substrate range of monooxygenases makes them susceptible to fortuitous reactions that do not necessarily support growth. Reactions such as these that cause energetic drain with no energetic return are referred to as cometabolic. Organisms that activate methane, propane, butane, ethylene, ammonia, toluene, and phenol using monooxygenases have also been shown to degrade chlorinated xenobiotics (Arciero *et al.*, 1989; DiSpirito *et al.*, 1992; Ensign *et al.*, 1992; Hamamura *et al.*, 1997; Shields *et al.*, 1991; Tsein *et al.*, 1989). Degradation of these compounds occurs at various rates and sustainabilities depending on the organism,

presence of an exogenous source of reductant, enzyme inducibility, and degree of toxicity associated with compound turnover (Arp *et al.*, 2001; van Hylckama Vlieg and Janssen, 2001). The rate of cometabolic degradation of chlorinated ethenes by methanotrophs decreases over time, thus limiting the total amount of substrate degradation (Alvarez-Cohen and McCarty, 1991a; Alvarez-Cohen and McCarty, 1991b). For the practical purposes of predicting maximal contaminant degradation, the term 'transformation capacity' (T_c) was introduced to describe the maximum mass of cometabolized compound that can be transformed per unit mass of cells (Chu and Alvarez-Cohen, 1999).

Transformation of trichloroethylene

TCE is effectively degraded via cometabolic pathways. Bacteria that can efficiently transform TCE under anaerobic conditions have received considerable research attention (Lovley, 2001; Semprini, 1995). However, a primary product of anaerobic dehalogenation is vinyl chloride which is more soluble in water than TCE, and itself poses serious health hazards (Infante and Tsongas, 1983). The first step in aerobic cometabolism of TCE is initiated by an oxygenase that activates the recalcitrant TCE molecule to TCE epoxide. TCE epoxide is a highly reactive intermediate that can spontaneously decompose yielding dichloroacetate, glyoxylate, or formate. TCE epoxide also damages the transforming oxygenase (van Hylckama Vlieg *et al.*, 1997). For example, studies with *Nitrosomonas europaea* showed that [14C]TCE binds to a 27-kDa polypeptide of ammonia monooxygenase which supports the idea that TCE epoxide may act as a mechanism based inactivator (Rasche *et al.*, 1991). sMMO of *M. trichosporium* OB3b and T2MO of *P. putida* F1 suffered irreversible loss of enzyme activity following TCE transformation (Fox *et al.*, 1990; Newman and Wackett, 1997; van Hylckama Vlieg *et al.*, 1996). Interestingly, Yeager *et al.* (Yeager *et al.*, 2001) showed that oxidation of TCE by *Burkholderia cepacia* G4 resulted in losses of cellular viability of two-orders in magnitude whereas T2MO

activity decreased by 52%. TCE transformation by *B. cepacia* G4 also caused death of T2MO-deficient *B. cepacia* mutant cells. TCE transformation by the wild-type cells resulted in a 63% reduction in viability of the surrounding mutant cells. Taken together, research has shown that the range of toxicity that can occur during TCE cometabolism includes inactivation of the transforming oxygenase, loss of respiratory activity, death of the cells performing the cooxidation, as well as death of neighboring bacterial cells.

Transformation of dichloroethenes

Reductive dechlorination of PCE and TCE under anaerobic groundwater conditions has been demonstrated (Beeman and Bleckmann, 2002), but dechlorination can be incomplete, leaving persistant DCEs and VC in the contaminated plumes (Semprini, 1997). Very few organisms have been isolated that can utilize DCE or VC for growth (Coleman *et al.*, 2002). As is the case with TCE, exploiting the fortuitous oxidations of aerobic cometabolism is a viable option for bioremediation. DCEs are interesting substrates for study because they represent different stereoisomeric forms, are differentially oxidized by monooxygenase-dependent turnover, and may be oxidized to their corresponding DCE-epoxides which have half-lives that vary from <2 s for 1,1 DCE epoxide to 31 h for *cis*-DCE epoxide and 72 h for *trans*-DCE epoxide (van Hylckama Vlieg and Janssen, 2001).

Cometabolic processes typically require the presence of the monooxygenase-inducing and energy-yielding hydrocarbon. Several studies sought to investigate the possibility that chlorinated hydrocarbons could serve to induce their own degradation. For example, 1,2 *cis*-DCE and *trans*-DCE induced alkene monooxygenase activity in *Xanthobacter* sp. Strain Py2, and 1,2 *cis*-DCE also induced toluene oxygenase in *P. mendocina* KR1, albeit in all cases, to low levels of activity (Ensign, 1996; McClay *et al.*, 1995). 1,2 *trans*-DCE was determined to be a gratuitous inducer of sBMO activity in *P. butanovora* (Doughty *et al.*, 2005). Both MMO-expressing methanotrophs and

sBMO-expressing *P. butanovora* oxidize the 3 forms of DCE, but there are interesting turnover-dependent differences. Although 1,2 *cis*-DCE degradation caused more rapid loss of cellular viability and enzymatic inactivation in *M. trichosporium* OB3b (van Hylckama Vlieg *et al.*, 1997), less 1,2 *trans*-DCE turnover was needed to inactivate sBMO in *P. butanovora* (Doughty *et al.*, 2005; van Hylckama Vlieg *et al.*, 1997).

In sMMO, DCEs are oxidized to their corresponding epoxides, which either covalently modify cellular components, or are themselves degraded by sMMO resulting in inactivation of the enzyme (van Hylckama Vlieg and Janssen, 2001). The fate of DCE epoxides has important consequences to cellular physiology. Both 1,1 DCE and 1,2 *trans*-DCE are potent inhibitors of cellular respiration in *P. butanovora*. For example, degradation of the available 1,1 DCE was complete after less than 0.5 min, and 1,2 *trans* DCE was completely consumed in 5 min, but in both cases <25% of the initial lactate-dependent respiration remained after only 5 min. In contrast, the available 1,2 *cis*-DCE was consumed within 2.5 min, but retained nearly 100% lactate-dependent respiration for 14 min before declining dramatically (Doughty *et al.*, 2005). It is likely that 1,2 *cis*-DCE epoxide turnover is required for the cells to experience severe physiological toxicity.

SUMMARY

Butane monooxygenase was shown to have a broad substrate range, that could be exploited for the purposes of bioremediation. Research by Hamamura, *et al*., (1997), demonstrated marked biochemical diversity among BMOs from different butane oxidizers. Chlorinated ethylene turnover-dependent cellular toxicities, including enzymatic inactivation and loss of cellular viability, were described in different monooxygenase-expressing systems. These reports provided the basis for Chapter 2 of this dissertation which describes the physiological consequences of BMO-dependent TCE degradation by three different strains of butane oxidizing bacteria known to express biochemically distinct BMOs. Experiments to ascertain

kinetic constants and transformation capacities were done to contribute useful predictive parameters for bioremediation purposes.

Previous work to understand substrate oxidation by butane monooxygenase (BMO) from *P. butanovora* primarily focused on substrate range, regulation of BMO expression, and genetic and biochemical characterization of the downstream metabolism. Sluis *et al.* (2002) demonstrated the genetic and biochemical homology of sBMO from *P. butanovora* to the sMMOs from methanotrophs. The most obvious distinction between sBMO and sMMO, was the apparent exclusion of methane from the sBMO substrate range. Chapter 3 of this dissertation describes research conducted to address the fundamental basis of substrate specificity of sBMO using site-directed mutagenesis targeting key functional regions of the diiron-containing α-subunit of BMOH. For this study, whole cell experiments were carried out to determine differences in substrate oxidation and fortuitously, provided insights into cellular metabolic management of multiple products produced by a single monooxygenase.

Development of the final phase of research for this dissertation utilized the combination of tools developed in the third chapter, observations from the second chapter, and concepts derived from both. Differences in substrate oxidation can have strikingly different impacts on cellular physiology. Therefore, we were interested in determining if different oxidative products of sBMO-dependent chlorinated ethene turnover would result in the exhibition of different phenotypes in mutant strains containing single amino acid substitutions in BMOH. Chlorinated ethenes were used as probes for mechanistic differences in BMOH-α in the mutant strains.

The research questions presented here developed gradually, using the work from previous and current researchers in the Arp laboratory at Oregon State University as much of the foundation. Much of the literature cited in this introduction became available during my term of research at OSU, and has been included along with relevant research discoveries during the same time period, as it was used not only to develop the research project, but also to make relevant conclusions that are broadly discussed in the final chapter.

CHAPTER 2.

TRICHLOROETHYLENE DEGRADATION BY BUTANE-OXIDIZING BACTERIA CAUSES A SPECTRUM OF TOXIC EFFECTS

Kimberly H. Halsey, Luis A. Sayavedra-Soto, Peter J. Bottomley
and Daniel J. Arp

Published in *Applied Microbiology and Biotechnology*
Springer-Verlag, London
2005, Vol. 68, p. 794-801

ABSTRACT

The physiological consequences of TCE transformation by 3 butane-oxidizers were examined. *Pseudomonas butanovora, Mycobacterium vaccae,* and *Nocardioides* sp. CF8 utilize distinctly different butane monooxygenases (BMOs) to initiate degradation of the recalcitrant TCE molecule. Although the primary toxic event resulting from TCE cometabolism by these three strains was loss of BMO activity, species differences were observed. *P. butanovora* and *Nocardioides* sp. CF8 maintained only 4% residual BMO activity following exposure to 165 μM TCE for 90 and 180 min, respectively. In contrast, *M. vaccae* maintained 34% residual activity even after exposure to 165 μM TCE for 300 min. Culture viability was reduced 83% in *P. butanovora*, but was unaffected in the other 2 species. Transformation of 530 nmoles TCE by *P. butanovora* (1.0 mg total protein) did not affect viability of BMO-deficient *P. butanovora* cells, whereas transformation of 482 nmoles of TCE by toluene-grown *Burkholderia cepacia* G4 caused 87% of BMO-deficient *P. butanovora* cells to lose viability. Together, these results contrast with those previously reported for other bacteria carrying out TCE cometabolism and demonstrate the range of cellular toxicities associated with TCE cometabolism.

INTRODUCTION

After years of industrial use accompanied by accidental spills and deliberate dumping, trichloroethylene (TCE) is now a common contaminant of soils and groundwater. Aerobic cometabolism is an effective means of transforming TCE thus providing a promising approach to the bioremediation of contaminated sites. Bacterial species and mixed cultures that can cometabolize TCE have been isolated from contaminated aquifers (Brzostowicz *et al.*, 2003; Coleman *et al.*, 2002; Hamamura and Arp, 2000). One of the factors limiting the effectiveness of cometabolism is the cytotoxicity of the TCE transformation product(s). Previously, TCE cometabolism was shown to cause inactivation of the transforming oxygenase in several classes of bacteria including ammonia-oxidizing (*Nitrosomonas europaea*), methane-oxidizing (*Methylosinus trichosporium* OB3b), and toluene-oxidizing (*Pseudomonas putida* F1) (Newman and Wackett, 1997; Rasche *et al.*, 1991; van Hylckama Vlieg *et al.*, 1996). Additionally, research with *M. trichosporium* OB3b, toluene-oxidizing *Burkholderia cepacia* G4, and a mixed culture of soluble MMO (sMMO)-containing methane-oxidizers, showed significant losses in cellular viability during TCE transformation (Alvarez-Cohen and McCarty, 1991b; van Hylckama Vlieg *et al.*, 1997; Yeager *et al.*, 2001). Exposure of *B. cepacia* G4 to 250 μM TCE for 90 min resulted in only partial (52%) decrease in toluene monooxygenase (T2MO) activity, while acetate-coupled respiration decreased 98%, and the number of viable cells was reduced by three orders of magnitude (Yeager *et al.*, 2001).

Butane-oxidizing bacteria are an attractive choice for augmentation of indigenous microbial communities at sites requiring bioremediation (Kim *et al.*, 1997; Kim *et al.*, 2000). While several butane-oxidizing bacteria have been shown to be capable of TCE cometabolism (Hamamura *et al.*, 1999; Wackett and Householder, 1989), the kinetic properties of TCE transformation by these bacteria have not been examined. Further, the nature and extent of transformation-dependent TCE toxicity on butane-oxidizing bacteria has not been studied. The enzyme butane monooxygenase (BMO) initiates butane oxidation. Like other catabolic monooxygenases, BMO has a

relatively wide substrate range including certain gaseous and liquid alkanes and a number of chlorinated hydrocarbons. However, BMOs in different organisms have been shown to be biochemically distinct. For example, soluble BMO from *Pseudomonas butanovora* has been biochemically and genetically characterized, and is similar to soluble methane monooxygenase (sMMO) from methanotrophs (Arp, 1999; Hamamura *et al.*, 1999; Sluis *et al.*, 2002). In contrast, *Nocardioides* sp. CF8 appears to maintain a copper-containing BMO that is associated with the cell membrane (Hamamura *et al.*, 2001). The BMO of *Mycobacterium vaccae* is distinguished from the BMOs of *P. butanovora* and *Nocardioides* sp. CF8 by its distinct [^{14}C]acetylene labeling pattern and its partial inhibition by the copper chelator, allylthiourea (ATU) (Hamamura *et al*. 1997). Since the BMOs from these three organisms were shown to be biochemically diverse, it was intriguing to study the physiological responses of their hosts to TCE exposure and to compare them with other well-studied systems.

The type and severity of TCE transformation-dependent damage occurring in bacterial systems has various implications. For example, the regioselectivity of different transforming monooxygenases can have very different impacts on the bacterial host and its community, or the host may utilize epoxidases or other repair mechanisms allowing for greater tolerance to TCE transformation. The objective of this study was to examine the physiological consequences of TCE transformation by three butane-oxidizers, *P. butanovora, M. vaccae,* and *Nocardioides* sp. CF8, that have distinctly different BMOs, and to compare the results with previously published work on other bacteria.

MATERIALS AND METHODS

Bacterial strains and growth conditions

P. butanovora (ATCC 43655) was cultured in sealed bottles (720 ml) containing 300 ml of liquid medium and 420 ml of air, with 30 ml of *n*-Butane gas (99.0%) (Airgas, Inc., Randor, Pa.) added as an overpressure. The growth medium consisted of 2 mM $MgSO_4 \cdot 7H_2O$, 400 μM $CaCl_2 \cdot 2H_2O$, phosphate [pH 7.2; 60 mM $(NH_4)_2HPO_4$, 7 mM $Na_2HPO_4 \cdot 7H_2O$, and 15 mM KH_2PO_4], and the trace elements described previously (Wiegant and deBont, 1980). The *P. butanovora* mutant strain *bmoX::lacZ::kan* has a DNA cassette disrupting *bmoX* rendering the host BMO-deficient and kanamycin resistant (unpublished results). *P. butanovora bmoX::lacZ::kan* was grown in 50 ml of the medium described above with 5 mM sodium citrate and 25 μg/ml kanamycin. *M. vaccae* JOB5 (ATCC 29678) was grown in medium previously described (Hamamura *et al.*, 1997). Cultures (300 ml) were grown in 720 ml sealed bottles with 180 ml of butane gas and 150 ml of O_2 added as overpressure. *Nocardioides* sp. CF8 was grown in 300 ml of the same medium used for *M. vaccae* with 180 ml of butane gas added as overpressure. *B. cepacia* G4 was grown as described previously (Yeager *et al.*, 2001) in sealed 160 ml vials containing 60 ml minimal media and 94 μmoles toluene. At 4 h prior to harvest, an additional 94 μmoles of toluene was added. All cultures were incubated at 30°C in an orbital shaker at 150 rpm and harvested during the log or late log growth phase for experimental use. Prior to experiments, cells were washed three times with the same phosphate buffers used for growing the individual cultures, and resuspended in the same buffers as concentrated cell suspensions.

TCE exposure

TCE degradation was monitored by gas chromatography. Teflon-faced butyl septa (Supelco) were used to seal serum vials (7.7 ml) containing 5 mM sodium butyrate or sodium lactate, TCE (2.2, 3.3, 5.5, 10.9, 21.9, 54.8, 110, or 165 μM initial aqueous concentration after addition of cells), and sufficient phosphate buffer to bring the volume to 800 μl, were equilibrated for at least 30 min in a reciprocating shaker with constant shaking at 30°C. Concentrated cell suspensions (200 μl containing 1.0 mg total protein *P. butanovora*, and *Nocardioides* sp. CF8, or 0.75 mg *M. vaccae*) were added to initiate the experiments. To monitor TCE consumption, samples of the gas phase (20 to 100 μl) were removed using a gas-tight syringe (Hamilton) for analysis by gas chromatography (see below). TCE concentration and exposure time were selected to maximize TCE transformation. Cometabolism (e.g. ethylene oxidation (Hamamura *et al*. 1999)) can be slower if the cellular reductant supply is limiting. Therefore, an exogenous source of reductant was provided in the form of sodium lactate (10 mM) for *P. butanovora,* and sodium butyrate (10 mM) for *M. vaccae* and *Nocardioides* sp. CF8. These reductants were the most effective among those studied (lactate, citrate, butyrate, and acetate). Acetylene is a potent inactivator of BMO (Hamamura *et al.*, 1999). Cells that had been exposed to acetylene were included to confirm the function of BMO in TCE transformation. After the desired incubation period, the reaction mixture was transferred to a microcentrifuge tube and the cells were sedimented. Cells were resuspended, washed three times, and then resuspended in fresh phosphate buffer for post-exposure assays for residual BMO activity, O_2 uptake, and cellular viability (see below for assay descriptions).

For determination of TCE degradation kinetics, vials of butane-grown cells containing different initial TCE concentrations were monitored for TCE degradation. The rate of degradation by *P. butanovora* was linear over the first 20 minutes of exposure and determined with 0, 12, and 20 min time points. Likewise, the rate of degradation by *M. vaccae* was linear over the first 60 min and determined with 0, 20, 40, and 60 min time points; and the rate of degradation by *Nocardioides* sp. CF8 was

linear over the first 30 min and determined with 0, 15, and 30 min time points (data not shown).

Assays for BMO activity, O_2 uptake, and cellular viability

BMO activity was measured using the ethylene oxidation assay (Hamamura *et al.*, 1999). This method exploits ethylene as an alternative substrate for BMO in the presence of an exogenous source of reductant. Cell suspensions (1 ml) were incubated for up to 30 minutes at 30°C with shaking in 7.7 ml sealed serum vials containing phosphate buffer and supplemented with 5 mM sodium lactate (*P. butanovora*) or 5 mM sodium butyrate (*Nocardioides* sp. CF8 and *M. vaccae*). Ethylene gas (20% v/v) was added to initiate the assay. Samples of the gas phase (100 μl) were removed for analysis by gas chromatography for ethylene oxide accumulation (see below).

Aeration in the absence of enzyme substrate has been suggested to cause inactivation of monooxygenases (Alvarez-Cohen and McCarty, 1991b; Chu and Alvarez-Cohen, 1999). Therefore, treatments were included with no TCE added (0 μM) to establish if any loss of BMO activity occurred from aeration alone. To help determine if the presence of O_2 was responsible for loss of BMO activity, reaction vials containing cells were purged of air and exposed to N_2 during the incubation period ("N_2-exposed").

O_2 uptake measurements were made using a Clark-style O_2 electrode (Yellow Springs, Ohio) mounted in a glass water-jacketed reaction vessel (1.6 ml) at 30°C. The reaction chamber was filled with phosphate buffer. Following TCE exposure, cells were washed and resuspended in phosphate buffer to 200 μl. Cells (50 μl) were added to the reaction vessel and the endogenous O_2 uptake rate was determined. Sodium butyrate (5 mM) (*P. butanovora*) or 1-butanol (5 mM) (*Nocardioides* sp. CF8 and *M. vaccae*) was added to the vessel to determine a substrate-dependent O_2 uptake rate. Butyrate and 1–butanol are metabolites of butane oxidation (Arp, 1999) and do not require functional BMO for their further metabolism (Vangnai *et al.*, 2002). Several

other substrates were tested to determine their ability to promote rates of O_2 uptake. Sodium lactate, sodium citrate, sodium acetate, sodium formate, and ethanol were also tested, but generally did not support rates of O_2 uptake above endogenous levels.

To account for any toxicity associated with exposure to TCE in the absence of TCE transformation, acetylene-treated cells were exposed to 22 μM and 165 μM initial TCE concentrations for the pre-determined exposure times prior to washing and plating. To determine residual cellular viability following TCE exposure, cells were washed and resuspended in phosphate buffer to 1.0 ml. Serial dilutions of the resuspended cells were made and aliquots (100 μl) were plated onto R2A agar plates (Difco). R2A agar contains pyruvate to degrade H_2O_2, a primary causative agent of oxidative stress. Colonies were counted after 2-3 days of incubation at 30°C.

Effect of TCE degradation on viability of surrounding cells

Butane-grown *P. butanovora* or toluene-grown *B. cepacia* G4 cells were mixed with *P. butanovora bmoX::lacZ::kan* (9:1 ratio for *P. butanovora* wild type to mutant; 9:1 or 6:1 ratio for *B. cepacia* G4 to *P. butanovora bmoX::lacZ::kan*) and exposed to TCE for 90 minutes as described above. Following TCE exposure, cells were washed and resuspended in phosphate buffer to 1 ml. The number of viable *P. butanovora bmoX::lacZ::kan* cells remaining was determined by preparing serial dilutions to 1×10^{-6} in sterile phosphate buffer and plating 100 μl aliquots onto R2A agar plates with kanamycin (25 μg/ml). Colonies (*P. butanovora bmoX::lacZ::kan*) were counted after 2-3 days of incubation at 30°C.

Analytical and other methods

Ethylene oxide accumulation was analyzed with a Shimadzu (Kyoto, Japan) GC-8A chromatograph equipped with a flame ionization detector and a stainless steel column (0.3 by 61 cm) packed with Porapak Q 80 to 100 mesh (Alltech, Deerfield, Ill). TCE transformation was monitored using the same GC-8A FID chromatograph with a capillary column (15 m x 0.53 mm) (Alltech). Ethylene oxide and TCE calibration curves were obtained by performing a headspace gas analysis with vials containing known amounts of each compound. A dimensionless Henry's constant, 0.494 at 30°C (Gossett, 1983), was used to account for aqueous and gaseous partitioning of the total TCE mass in the vials. Protein concentrations were determined by the Biuret assay (Gornall *et al.*, 1949) following cell solubilization in 3M NaOH for 30 min at 65°C.

RESULTS

TCE-exposure results in severe loss of BMO activity

Time courses of TCE transformation are shown for each of the three butane-grown species (Fig. 2.1). An initial concentration of 165 μM TCE (initial aqueous concentration) was used for determining the time course of TCE transformation for *P. butanovora.* Since the initial rate of TCE transformation by *M. vaccae* and *Nocardioides* sp. CF8 is approximately 5 times less than that of *P. butanovora,* an initial TCE concentration of 22 μM was used to accurately measure TCE disappearance by GC. The rate of TCE transformation decreased with time for all three strains. Even after 4 h of exposure, TCE transformation by *M. vaccae* remained measurable. In contrast, TCE transformation by *P. butanovora* and *Nocardioides* sp.

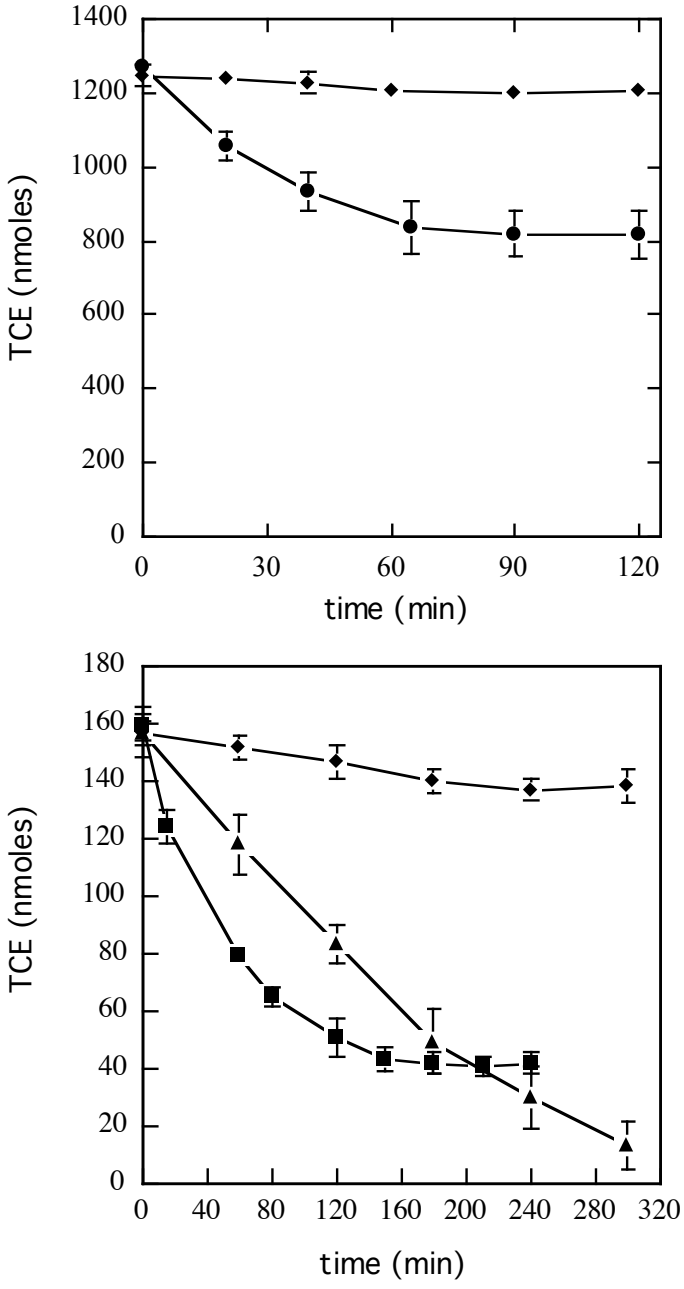

Figure 2.1. Time courses for TCE disappearance by butane-grown *P. butanovora* (●), 165 μM initial TCE concentration; *Nocardioides* sp. CF8 (■), *M. vaccae* (▲), and acetylene-inactivated control cells, (♦), 22 μM initial TCE concentration. Cells were grown on butane, harvested, and washed 3-times prior to incubation with TCE at 30°C.

CF8 ceased after 90 and 180 minutes, respectively. Supplementing the reaction vials with additional reductant (sodium lactate or sodium butyrate) did not stimulate additional TCE disappearance, suggesting that reductant limitation was not the reason for the time-dependent decrease in TCE disappearance.

Following exposure to TCE, residual BMO activities for butane-grown *P. butanovora*, *Nocardioides* sp. CF8, and *M. vaccae* were measured and are summarized in Table 2.1. Incubation in the absence of substrate (0 μM TCE) caused a significant reduction in BMO activity in all three species. The same loss in BMO activity was measured when the air in the vials was replaced with N_2. It appearsthat BMO can be partially inactivated by the mechanical disturbance experienced during wash procedures and shaking. To determine if BMO activity was affected by TCE transformation, BMO activity was measured before and after incubation of each butane-grown species with different initial concentrations of TCE. Because cellular damage is imparted by a toxic intermediate(s) formed during TCE transformation (most likely TCE-epoxide), exposure conditions were selected that would allow maximal TCE transformation (see Fig. 2.1). Exposure to TCE concentrations as low as 5.5 μM resulted in loss of BMO activity, and the residual BMO activity decreased with increasing TCE concentrations for all three bacteria. While incubation of all three strains in the presence or absence of air resulted in the loss of BMO activity, exposure to TCE consistently resulted in even further reduction of BMO activity. These results showed that BMO activities in *P. butanovora* and *Nocardioides* sp. CF8 were very sensitive to TCE transformation. The fact that BMO activity in *M. vaccae* suffered only a modest decline following TCE transformation is reminiscent of T2MO activity in *B. cepacia* G4 which was also relatively unaffected by TCE transformation (Chu and Alvarez-Cohen, 1999).

Transformation capacity (T_cs) is defined as the mass of a compound that can be degraded prior to enzyme inactivation by a given amount of non-growing cells (Chu and Alvarez-Cohen, 1999). *P. butanovora* (1.0 mg total protein) was exposed to an

Table 2.1. Residual BMO activity following exposure of cells to TCE[a]

		Residual BMO activity (%)							
					TCE Concentration[c]				
	Initial BMO activity[b]	Following wash steps	Butane Protected[c]	N_2-exposed[c]	0 μM	5.5 μM	22 μM	55 μM	165 μM
P. butanovora	15.5 ± 0.8	71 ± 1.9	65 ± 2.1	49 ± 2.2	50 ± 1.1	35 ± 1.5	27 ±1.6	13 ± 1.1	4.3 ± 1.2
M. vaccae	41.1 ± 1.9	86 ± 2.0	65 ± 2.5	61 ± 1.0	62 ± 2.1	58 ± 2.2	39 ± 1.7	34 ± 1.5	34 ± 2.1
Nocardiodes sp. CF8	12.0 ± 0.4	85 ± 0.9	75 ± 1.3	63 ± 1.6	64 ± 0.7	31 ± 0.7	11 ± 0.2	6.0 ± 0.3	3.6 ± 0.1

[a]All data expressed as means ± standard deviations of at least 3 trials

[b]Activity measurements expressed as nmoles $(min \cdot mg\ protein)^{-1}$

[c]Exposure times were selected to ensure maximal TCE transformation (*P. butanovora*, 90 min; *M. vaccae*, 300 min; *Nocardiodes* sp. CF8, 180 min)

initial TCE concentration of 165 μM (1265 nmoles TCE) for 90 min, and *Nocardioides* sp. CF8 (1.0 mg total protein) was exposed to an initial TCE concentration of 165 μM for 180 min. Because only 4% of the initial BMO activities remained in *P. butanovora* and *Nocardioides* sp. CF8 under these exposure conditions, their transformation capacities were determined. T_cs for *P. butanovora* was 475 ± 30 nmoles/mg total protein, and T_cs for *Nocardioides* sp. CF8 was 214 ± 27 nmoles/mg total protein. We could not determine a transformation capacity for *M. vaccae* because it retained over 30% of its initial BMO activity following TCE exposure.

TCE degradation follows Michaelis-Menten enzyme kinetics

Whole cell kinetics for TCE cooxidation have been determined for a number of physiologically diverse bacteria including ammonia-, phenol-, methane-, and toluene-oxidizers (Arp *et al.*, 2001). Here we contribute information about TCE degradation kinetics of pure cultures of butane-oxidizers. For all three species of bacteria, initial rates of degradation were plotted against TCE concentration and fitted to the Michaelis-Menten model of enzyme velocity versus substrate concentration (Fig. 2.2), and the corresponding V_{max} and K_s values were determined.

The maximal rate of TCE transformation by *P. butanovora* was over 5 times faster than rates of TCE transformation by *Nocardioides* sp. CF8 and *M. vaccae*. K_s values ranged from a low of 6 μM for *M. vaccae* to 22 μM for *Nocardioides* sp. CF8. Despite the phylogenetic and biochemical diversity of these three butane-oxidizing species and their respective BMOs, the kinetic parameters for TCE transformation were comparable.

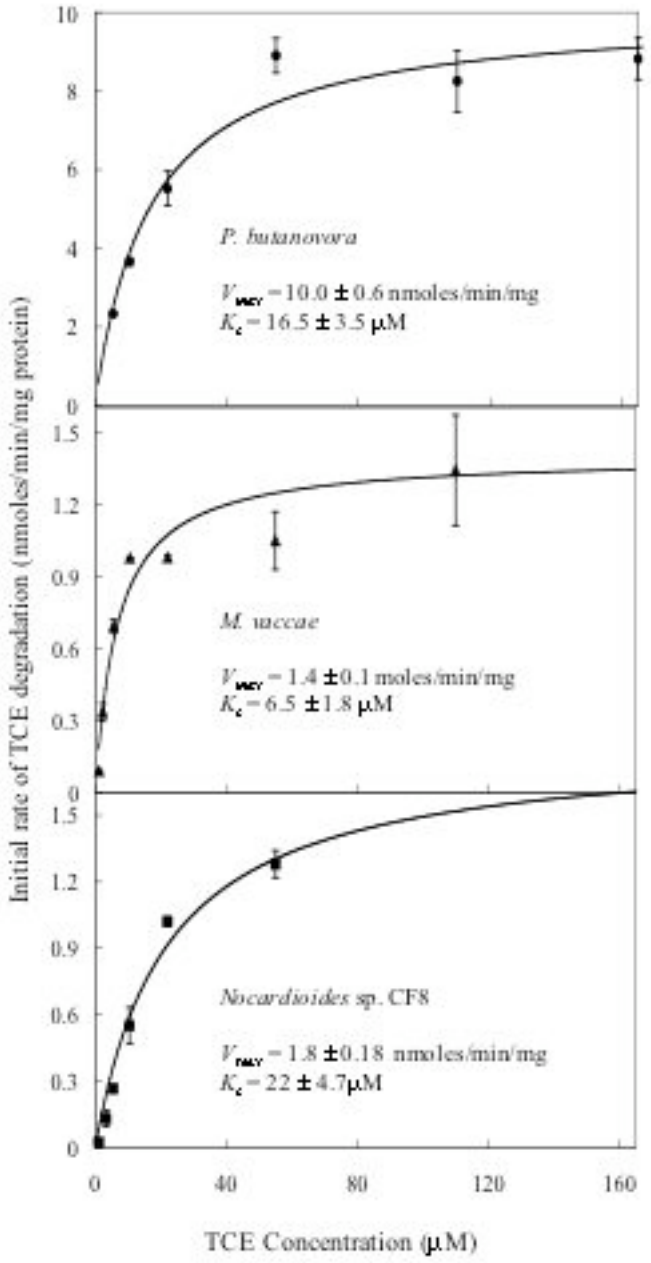

Figure 2.2. K_s and V_{max} determinations for TCE degradation by *P. butanovora*, *M. vaccae,* and *Nocardioides* sp. CF8. Initial rates of TCE degradation for butane grown *P. butanovora* (●), *M. vaccae* (▲), and *Nocardioides* sp. CF8 (■) are plotted against TCE concentration. The symbols represent the means for three experiments and the lines represent the Michaelis-Menten model fit for each species tested.

Effect of TCE cometabolism on cellular respiration and viability

Although BMO inactivation during TCE cometabolism occurred with all three butane-grown bacteria, there remained the possibility of other adverse cellularresponses. Residual substrate-dependent O_2 uptake rates and cellular viability of cells exposed to two different concentrations of TCE were determined. 83% of *P. butanovora* cells lost viability when exposed to 165 μM initial TCE concentration whereas only 32% of butyrate-dependent O_2 uptake was lost (Table 2.2). In contrast, no loss in viability was detected at an initial TCE concentration of 22 μM. Cells of *Nocardioides* sp. CF8 and *M. vaccae* that were exposed to 22 μM and 165 μM TCE did not appear to lose viability, but 1-butanol-dependent O_2 uptake rates decreased about 32% in *Nocardiodes* sp. CF8 cells exposed to 165 μM initial TCE concentration. Substrate-dependent O_2 uptake rates for cells of *M. vaccae* following incubation with TCE were similar to O_2 uptake rates of cells incubated in the absence of TCE. Substrate-dependent O_2 uptake rates for acetylene-treated cells of all three strains were intermediate to cells incubated in the absence of TCE and TCE-treated cells.

Because significant transformation-dependent TCE toxicities, including severe loss of sBMO activity and loss of viability, were detected in *P. butanovora*, we determined if the TCE transformation-dependent toxicities observed in *P. butanovora* were manifested in neighboring cells not expressing sBMO. Yeager et al. (2001) showed that *B. cepacia* G4 reduces viability of neighboring T2MO-inactivated *B. cepacia* TCS-100 cells when incubated with TCE. When wild type *P. butanovora* was mixed 9 to 1 with citrate-grown *P. butanovora bmoX::lacZ::kan* and exposed to 165 μM TCE for 90 minutes, the BMO-deficient mutant remained viable (Table 2.3). On the other hand, when toluene-grown *B. cepacia* G4 was mixed 9 to 1 with *P. butanovora bmoX::lacZ::kan*, 97% of the BMO-deficient mutant cells lost viability. To determine if the viability of neighboring *P. butanovora bmoX::lacZ::kan* cells were sensitive to lower levels of TCE transformation, toluene-grown *B. cepacia* G4 was mixed 6 to 1 with *P. butanovora* mutant cells and exposed to 165 μM TCE for 90

TABLE 2.2. Remaining viability and substrate dependent O_2–uptake rates of TCE-exposed *P. butanovora*, *M. vaccae*, and *Nocardioides* sp. CF8

	Acetylene-treated prior to TCE exposure	Exposure time (min)	Initial [TCE] (μM)	TCE transformed (nmoles)	Number of viable cells ($x10^7$ CFUs ml^{-1}) [a]	Substrate dependent O_2-Uptake Rate (nmoles O_2/mg·min)[b]
P. butanovora	No	90	22	165 ± 0	76 ± 4	15.0 ± 2.0
	No	90	165	451 ± 62	13 ± 3	12.9 ± 1.1
	Yes	90	165	38 ± 8	76 ± 5	16.6 ± 0.8
	No	90	0	0	75 ± 6	19.3 ± 1.9
M. vaccae	No	300	22	155 ± 12	49 ± 17	18.0 ± 1.7
	No	300	165	346 ± 40	44 ± 14	17.1 ± 1.7
	Yes	300	165	49 ± 10	47 ± 12	18.5 ± 0.4
	No	300	0	0	46 ± 10	19.8 ± 1.5

Table 2.2. (Continued)

Nocardioides CF8	No	180	22	125 ± 10	73 ± 12	35.6 ± 7.3
	No	180	165	236 ± 30	67 ± 12	28.6 ± 4.9
	Yes	180	165	42 ± 8	75 ± 13	37.2 ± 1.3
	No	180	165	0	77 ± 16	42.1 ± 2.0

[a]Viability reported as means of at least 3 samples ± standard deviations

[b]Substrate used for determination of O_2-uptake rates was butyrate for *P. butanovora* and 1-butanol for *Nocardioides* sp. CF8 and *M. vaccae.*

TABLE 2.3. Loss of viability of BMO-deficient cells[a] in the presence of TCE transforming cells

TCE transforming strain	Acetylene-treated prior to TCE exposure	Ratio TCE transforming strain: BMO-deficient strain	TCE transformed (nmoles)	Number of viable BMO-deficient cells ($x10^6$ CFUs ml^{-1})[b]
P. butanovora	No	9:1	530 ± 25	39 ± 5
P. butanovora	Yes	9:1	35 ± 12	41 ± 2
B. cepacia G4	No	9:1	1065 ± 61	1.0 ± 0.2
B. cepacia G4	Yes	9:1	41 ± 8	40 ± 4
B. cepacia G4	No	6:1	482 ± 21	5.5 ± 4
B. cepacia G4	Yes	6:1	30 ± 11	42 ± 2

[a]BMO-deficient strain: *P. butanovora bmoX::lacZ::kan*

[b]Viability reported as means of at least 3 samples ± standard deviations

minutes. While the amount of TCE transformed by *B. cepacia* G4 was equivalent to that transformed by wild type *P. butanovora,* 87% of *P. butanovora bmoX::lacZ::kan* cells were no longer viable. Either wild type *P. butanovora* does not release a toxic product extracellularly, or the toxic product(s) do not accumulate to concentrations that would cause damage to other bacterial community members. These results emphasize the intriguing possibility that T2MO and sBMO produce or release different products or different ratios of products during the transformation of TCE.

DISCUSSION

Toxicity resulting from TCE cometabolism can be viewed as a continuum from specific damage (to the transforming enzyme itself) to general damage (affecting cellular respiration, viability, and the bacterial community). The results of this study present a somewhat different picture of toxicity associated with TCE degradation than has emerged from studies with methanotrophs and the toluene-oxidizing bacterium, *B. cepacia* G4. Whereas the predominant TCE transformation-dependent toxicity measured in MMO- and T2MO- expressing cells is loss of cellular viability, the three butane-oxidizing bacteria studied here cometabolize TCE with toxic consequences that are either modest or severe and either specific or broadly-based depending on the parameters considered.

Our results also contribute kinetic constants for three more bacteria, and these allow some general trends to be noted. Interestingly, the kinetic parameters for butane-oxidizing bacteria are similar to those determined for other organisms that carry out TCE cometabolism. As with the characterized BMOs, the closely related MMOs can be expressed as either a soluble MMO (when copper is limiting) or as a particulate MMO. Other soluble monooxygenases include T2MO from *B. cepacia* G4 and alkene monooxygenase from *Xanthobacter* Py2. The maximal rates reported for organisms expressing these soluble monooxygenases range from 2.4 – 580 nmoles of TCE transformed min^{-1} mg of $protein^{-1}$ with the majority of measurements falling between

8 – 38 nmoles min^{-1} mg of $protein^{-1}$. The corresponding K_s values range from 3-225 μM (reviewed in (Arp *et al.*, 2001)). The kinetic constants determined for *P. butanovora* compare most favorably with those of *B. cepacia* G4 which has a maximum TCE oxidation rate of 10 nmoles min^{-1} mg of $protein^{-1}$ (Landa *et al.*, 1994). The half-saturation constant (K_s) for *B. cepacia* G4 is 6 μM compared to 16.5 μM for *P. butanovora*. Organisms expressing membrane-associated, copper-containing monooxygenases appear to have slightly lower kinetic constants: V_{max} values range from 4.1-10.9 nmoles min^{-1} mg of $protein^{-1}$, and K_s values range from 7.9 – 30 μM in *Nitrosomonas europaea* expressing AMO and *Methylosinus trichosporium* expressing pMMO (reviewed in (Arp *et al.*, 2001)). The kinetic constants determined for *Nocardioides* sp. CF8 expressing pBMO and *M. vaccae* are similar to those of bacteria expressing copper-containing monooxygenases. Although the BMO in *M. vaccae* has not been shown to be copper-containing, its partial sensitivity to ATU and low V_{max} towards TCE suggests it may have some properties that are similar to the BMO of *Nocardioides* sp. CF8.

The primary toxic event resulting from TCE transformation by all three of these butane-oxidizing bacteria appears to be loss of BMO activity. Reduction of BMO activity in *Nocardioides* sp. CF8 and *P. butanovora* was particularly striking. Both of these bacteria maintained less than 5% of their initial BMO activity after exposure to 165 μM TCE as described in Table 2.1. We considered the possibility that TCE acts as a mechanism-based inactivator. Indeed, many of the requirements for describing TCE as a mechanism-based inactivator were met (Silverman, 1988): inactivation of BMO by TCE is irreversible, the active catalyst, BMO, is required for inactivation, the presence of substrate (butane) protects against inactivation (data not shown), and the rate of inactivation is proportional to the concentration of TCE at low concentrations and approaches a maximum at higher concentrations. Attempts to determine first-order rates of inactivation were confounded by loss of activity due to washing procedures and mechanical disturbance and (in the case of *P. butanovora*) demonstrable secondary toxicities (ie: reduced cellular viability) at high TCE concentrations. Regardless of whether or not all the criteria were met for classifying

TCE as a mechanism-based inactivator of the BMOs, the data are consistent with the idea that TCE transformation by BMO leads to the loss of BMO activity.

While loss of BMO activity was the primary toxic event in butane-grown cells, secondary toxicity was only measured in *P. butanovora*. Both toluene-grown *B. cepacia* G4 and methane-grown *M. trichosporium* OB3b lose culturability following TCE exposure (Yeager *et al.*, 2001). In fact, in both cases, overall cellular damage is considered to be the principal toxic effect associated with TCE oxidation while damage to the monooxygenases is secondary. Considering the severe loss of BMO activity incurred during TCE transformation coupled with the modest decrease in cellular respiratory activity, we did not expect viability to be significantly reduced. However, the number of viable *P. butanovora* cells was markedly decreased when exposed to high concentrations of TCE. Presumably, at the higher initial TCE concentration, *P. butanovora* attained the toxicity threshold introduced by Chu and Alvarez-Cohen (1999), which directly correlates T_c with general cellular damage. In this case, the T_c was achieved (478 nmoles TCE degraded/mg protein) resulting in sufficient accumulated cellular damage to render the cells irreparable. The toxicity threshold was also achieved by *Nocardioides* sp. CF8 (as predicted by the amount of TCE transformed per milligram of protein). However, the corresponding loss in viability was not detected. It is curious that no loss in viability was measured in *Nocardioides* sp. CF8 or *M. vaccae* cells following TCE exposure. There are several possible explanations for these disparate results. First, the maximal rates of TCE degradation for both *Nocardioides* sp. CF8 and *M. vaccae* are lower than those of *P. butanovora, M. trichosporium* OB3b, and *B. cepacia* G4. Therefore, it is possible that repair of general cellular damage keeps pace with toxicity imparted by a reactive intermediate such as TCE epoxide. This idea would suggest that bacteria with higher V_{max} values experience a "dosage effect" resulting from the formation of high concentrations of a toxic intermediate in a short time period. Second, the BMOs of *M. vaccae* and *Nocardioides* sp. CF8 may catalyze formation of different, non-toxic products during TCE transformation; or alternatively, different ratios of the same

products (including the toxic intermediates) may be formed resulting in less accumulation of the more destructive intermediates.

It is also conceivable that the partition ratio of TCE transformation products by pBMO in *Nocardioides* sp. CF8 is smaller than that of strains exhibiting losses in cellular viability. The transformation of a mechanism-based inactivator (I) into its activated form (I') is described by the equation below.

$$E + I \underset{k_{-1}}{\overset{k_1}{\rightleftarrows}} E \bullet I \xrightarrow{k_2} E \bullet I' \xrightarrow{k_4} E\text{–}I''$$
$$\qquad\qquad\qquad\qquad\qquad\qquad\quad \downarrow k_3$$
$$\qquad\qquad\qquad\qquad\qquad\qquad\quad E + P$$

The partion ratio, k_3/k_4, is an indicator of the efficiency of the inactivator (Silverman, 1988). A low partition ratio describes a system in which most inactivator molecules lead to enzyme inactivation (E–I") and fewer molecules are converted and released as (potentially damaging) product (P). TCE transformation by *Nocardioides* sp. CF8 results in a lack of general respiratory damage, maintenance of full cellular viability, and a striking sensitivity of pBMO. Taken together, these results suggest that there is minimal release of toxic intermediates from the E·I' complex and supports the presumption of a low partition ratio.

It appears that higher rates of TCE cometabolism can cause rapid accumulation of cellular damage. The maintenance of BMO activity and overall cellular health in *M. vaccae* following TCE transformation encourages consideration of this and other strains that have slower rates of TCE degradation. Unfortunately, these “plodding” bacterial strains are often overlooked in favor of speedier but potentially less robust strains. Interestingly, several strains of aerobic, vinyl chloride-degrading *Mycobacterium* and one *Nocardioides* strain were recently isolated from sites contaminated with chlorinated ethenes (Coleman *et al.*, 2002) indicating the importance of these particular genera in remediation of xenobiotic compounds in the environment.

ACKNOWLEDGEMENTS

This work was supported by the office of Research and Development, U.S. Environmental Protection Agency, under Agreement R-828772 through the Western Region Hazardous Substance Research Center.

CHAPTER 3.

SITE-DIRECTED AMINO ACID SUBSTITUTIONS IN BMOH-α OF BUTANE MONOOXYGENASE FROM *Pseudomonas butanovora*: IMPLICATIONS FOR SUBSTRATES KNOCKING AT THE GATE

Kimberly H. Halsey, Luis A. Sayavedra-Soto, Peter J. Bottomley,
and Daniel J. Arp

Published in *Journal of Bacteriology*
American Society for Microbiology
July, 2006, Vol. 188, p. 4962-4969

ABSTRACT

Butane monooxygenase (BMO) from *Pseudomonas butanovora* has high homology to soluble methane monooxygenase (sMMO), and both oxidize a wide range of hydrocarbons; yet previous studies have not demonstrated methane oxidation by BMO. Studies to understand the basis for this difference were initiated by making single amino acid substitutions to the hydroxylase α-subunit of butane monooxygenase (BMOH-α) in *P. butanovora*. Residues likely to be within hydrophobic cavities, adjacent to the diiron center, and on the surface of BMOH-α were altered to the corresponding residues from the α-subunit of sMMO. *In vivo* studies of five site-directed mutants were carried out to initiate mechanistic investigations of BMO. Growth rates of mutant strains G113N and L279F on butane were dramatically slower than the control *P. butanovora* wild-type strain (Rev WT). The specific activities of BMO in these strains were 7-fold lower than Rev WT. Strains G113N and L279F also showed 277 and 5.5-fold increases in the ratio of rates of 2- to 1-butanol production as compared to Rev WT. Propane oxidation by strain G113N was exclusively sub-terminal, and led to accumulation of acetone, which *P. butanovora* could not further metabolize. Methane oxidation was measurable for all strains, although accumulation of 23 μM methanol led to complete inhibition of methane oxidation in Rev WT. In contrast, methane oxidation by strain G113N was not completely inhibited until the methanol concentration reached 83 μM. The structural significance of the results obtained in this study is discussed using a three-dimensional model of BMOH-α.

INTRODUCTION

Pseudomonas butanovora utilizes an alkane monooxygenase, commonly referred to as butane monooxygenase (BMO), to initiate growth on C2-C9 alkanes. BMO, like soluble methane monooxygenase (sMMO), consists of three protein components: a hydroxylase (BMOH) consisting of three unique subunits ($\alpha_2\beta_2\gamma_2$), a reductase (BMOR), and an effector protein (BMOB). The genes encoding the α, β, and γ subunits of BMOH, *bmoX, bmoY, bmoZ,* have 65, 42, and 38% amino acid identity with the corresponding subunits of MMOH from *M. capsulatus* (Bath) (Sluis *et al.*, 2002). There is 86.3% sequence identity among the MMOH-α subunits of six strains of sequenced methanotrophs (reviewed in (Leahy *et al.*, 2003)). Although BMO and sMMO share extended substrate ranges including alkanes, alkenes, aromatics, and chlorinated xenobiotics, BMO is the only member of the soluble methane monooxygenase (sMMO) subfamily of soluble diiron monooxygenases in which methane oxidation has not been observed. Because BMO and sMMO comprise a group of powerful oxidative systems capable of activating highly stable hydrocarbons, they garner serious attention for their potential in bioremediation and bioindustrial catalysis (Lipscomb, 1994; Smith and Dalton, 2004).

The crystal structure of MMOH has led to identification of five hydrophobic cavities that extend from the surface of the α-subunit to the diiron active site (Rosenzweig *et al.*, 1997). Cavity 1 is the hydrophobic pocket containing the active site, and cavity 2 comprises a substantial pocket extending from the active site. Evidence that these cavities bind substrates and provide passage to the active site was provided by crystallization of MMOH in the presence of the methane surrogates, xenon or dibromomethane (Whittington *et al.*, 2001a). Since longer chained halogenated alcohols were also found to bind in cavities 1 and 2 of MMOH-α, it is presumed that the hydrophobic cavities provide passage to and from the active site (Sazinsky and Lippard, 2005). MMOH-α residues L110, T213, and F188 are conserved residues that contribute to the formation of the "leucine gate" which

apparently allows substrate access to the active site from hydrophobic cavity 2 (Rosenzweig *et al.*, 1997). Crystallization of oxidized and reduced MMOH and alcohol soaked structures revealed changes in the rotameric conformations of L110 and T213 (Rosenzweig *et al.*, 1997; Sazinsky *et al.*, 2004). Alteration of Thr213 to Ser in MMOH-α resulted in lower specific activity towards different substrates including methane (Smith *et al.*, 2002). DNA shuffling and saturation mutagenesis of the corresponding gating residues in the more distantly related toluene *ortho*-monooxygenase (TOM), toluene *para*-monooxygenase (TpMO), and toluene-*o*-xylene monooxygenase (ToMO) resulted in variants that have new regiospecificities (Canada *et al.*, 2002; Fishman *et al.*, 2005; Vardar and Wood, 2004).

Sequence alignment of BMOH-α and MMOH-α allowed a comparison to be made of residues lining hydrophobic cavities 1 and 2. All but 5 of the 19 residues lining cavity 2 are identical in BMOH-α and MMOH-α (Sluis *et al.*, 2002). Although the residues coordinating the diiron center and comprising the leucine gate in BMOH-α are identical to those in MMOH-α, several residues adjacent to the active site are different. The amino acid differences in the hydrophobic cavities and adjacent to the active site provided clear targets for exploration of the fundamental differences in substrate specificity between BMO and sMMO. Analogous to sMMO, the effector protein of BMO (BMOB) is likely to affect the rate and regioselectivity of hydroxylation as well as the redox potential of the active site (Merkx *et al.*, 2001). Site-directed mutagenesis of the gene encoding MMOB and *in vitro* analysis has continued to clarify the influence of the effector protein (Brazeau *et al.*, 2003; Chang *et al.*, 2001; Wallar and Lipscomb, 2001). Although crystal structures of bacterial multicomponent monooxygenases in complex have not been solved, specific charged residues were determined to be involved in the interaction of MMOH-α and MMOB (Brazeau *et al.*, 2003). We hypothesized that altering BMOH-α surface residues involved in BMOB-BMOH-α interaction could change substrate access or alter regions of structural flexibility such that methane oxidation or other alteration to substrate catalysis would be observed. Sequence alignment of BMOH-α and MMOH-

α in conjunction with a spatial model describing the hydroxylase-effector protein complex for MMO (Brazeau *et al.*, 2003), revealed BMOH-α surface residues that were of particular interest for study.

The development of a bacterial system to investigate the roles of individual residues within MMOH-α has been challenging due to enzyme instability or low enzyme activity when expressed in *Escherichia coli* (Jahng and Wood, 1994; West *et al.*, 1992). One promising system that has circumvented this problem utilizes a plasmid-based expression system for sMMO in *Methylosinus trichosporium* thus avoiding the use of a heterologous host (Smith *et al.*, 2002). In this manuscript, we describe another approach using a homologous expression background by which single amino acid substitutions were created in BMOH-α of *P. butanovora.* Five of these *P. butanovora* mutants permitted investigation of several structural regions of the BMO hydroxylase. The results of these whole cell experiments were applied to a model of BMO derived from MMO crystal structures, and the two enzymes were structurally compared. The mutant phenotypes should be valuable in furthering our understanding of the recently discovered complexities in BMO regulation and downstream alkane metabolism (Doughty *et al.*, 2006; Sayavedra-Soto *et al.*, 2005).

MATERIALS AND METHODS

Bacterial strains and growth conditions

The plasmids and bacterial strains used in this study are described in Table 3.1. *P. butanovora* wild type and *P. butanovora* mutant strains were cultured at 30°C in sealed 160 ml vials containing 33 ml of liquid medium with either 10 ml *n*-butane, 15 ml propane, or 25 ml ethane gas (99.0%) (Airgas, Inc., Randor, Pa.), added as an overpressure. Liquid alkanes (15 mM; pentane, hexane, or octane) or 1- or 2- butanol

Table 3.1. Plasmids and bacterial strains used in this study

Plasmid or strain	Description	Source or reference
Plasmids		
pGEM-T Easy	PCR product TA cloning vector; Amp^r	Promega
pGBKB	pGEM-T Easy carrying the 1973-bp PCR product BmoUP-Kan-BmoDN (*bmox* partially deleted and Kan^r inserted into the deleted region)	This study
pBluescript II SK	Cloning vector, 3.0-kb; Ap^r *lacZ′*	Stratagene
pBSbmoxyb	pBluescript carrying a 3.68-kb *bmoxyz* PCR product cloned with KpnI	This study
Strains		
P. butanovora	ATCC 43655; *n*-butane-assimilating bacteria	(Takahashi *et al.*, 1980)
P. butanovora PBKB	Mutant strain with *bmox* partially deleted and Kan^r inserted into the deleted region. Created by homologous recombination of BmoUP-Kan-BmoDN from pGBKB with *P. butanovora*	This study
Rev WT	Butane-oxidizing control strain used for comparison of *P. butanovora* mutants containing single amino-acid substitutions in BMOH-α. Created by homologous recombination of *bmoxyb* from pBSbmoxyb with *P. butanovora* PBKB replacing Kan^r with wild-type *bmox* sequence	This study
E. coli JM109	cloning host strain; Amp^r	(Yanisch-Perron *et al.*, 1985)
E. coli DH5α	cloning host strain; Amp^r	Invitrogen

(5mM) were added directly to the mineral salts medium which was previously described (Sayavedra-Soto *et al.*, 2005) except that 30 mM KNO_3 was substituted for NH_4Cl. Alternatively, if BMO expression was not required, strains were grown in 30-100 ml of the sterile medium described above with 10 mM sodium lactate as carbon source.

For growth experiments, ethane-grown cells were obtained from early stationary phase, diluted, and grown again to stationary phase for 48 h. A 3% inoculum was transferred to fresh medium containing the specific alkane of interest. Samples were taken periodically using sterile technique for determination of optical density (600 nm).

Engineering *P. butanovora bmoX* mutants

A *P. butanovora bmoX* mutant host strain (*P. butanovora* PBKB) was constructed for use in mutagenesis experiments. Primers used in construction of *P. butanovora* PBKB are listed in Table 3.2. Using PCR ligation mutagenesis (Lau *et al.*, 2002), a 273 bp fragment of *bmoX* containing 161 bp flanking DNA upstream of ATG was amplified by PCR from *P. butanovora* genomic DNA ('BmoUP'). A second fragment 1212 bp in length and containing a kanamycin resistance cassette was amplified by PCR from the pUC4K plasmid (Taylor and Rose, 1988). Both fragments were XbaI digested, ligated, and PCR amplified to yield 'BmoUP-Kan' (1485 bp). A third fragment that was 488 bp in length containing 165 bp of flanking DNA downstream of TGA was PCR amplified from *bmoX* ('BmoDN'). 'BmoUP-Kan' and 'BmoDN' were digested with SacII, ligated, and PCR-amplified to yield the 1973 bp full-length fragment ('BKB'). 'BKB' was cloned into pGEM-EZ to form pBKB (Table 3.1). Following electroporation (1 mm electrode gap cuvette, ISC BioExpress Cat No. E-5010-1; 1600 V, 150 Ω, 50 μF) of pBKB into wild-type *P. butanovora* the 1185 bp fragment of *bmoX* was replaced with the Kan^R cassette from

Table 3.2. Primers used in this study

Name	Sequence (5'-3')[a]
Used in generating pGBKB	
LBMOUPSac130	GGAGCGGCCAAGAGCtCCGCACCTTGCGGC
RBMOUPXba129	GATACTTCGCGGtCtAGACCTTGAAATCC
LKanXba130	CAGTTGGTGATTCTAGACTTTTGCTTTGCC
RKanSac229	TCATTAGGCACCCGCGGCTTTACACTTTA
LBMODNSac220	TATCAAGCCGCGGTTCACTG
RBMODNKpn129	GCTTGGTTTCCAGCGGtaCCTTGGGTACG
Used in generating pBSbmoxyz	
P1UPX	CACACGCCTGGAGCGGtCtAGAGCCCCGCACCTTG
P4DNB	TCCAATTGTATTCCTTCTaGAGATCGTACGTCGTG
Used in mutagenesis of pBSbmoxyz[b]	
T148C top	AAATCCGCCATGTGAACCAG**TGC**GCGTACGTGAAT
T148C bot	CTGGTTCACATGGCGGATTTCGTCGATCACCTG
Q320K top	TGGCTGGGCCGACTGCAG**AAG**TTCGGCGTCAAAACG
Q320K bot	CTGCAGTCGGCCCAGCCAGATGCCAGCCCA
F321Y top	CTGGGCCGACTGCAGCAG**TAC**GGCGTCAAAACGCCA
F321Y bot	CTGCTGCAGTCGGCCCAGCCAGATGCCAGC
G113N top	GAGACCGGCGAATAC**AAC**GCAATCGCCGGTTCTGCT
G113N bot	CTCTGGCCGCTTATG
L279F top	GACGCAGCACAAGTTC**TTC**ACCCCCTTCGTCGGGG
L279F bot	CTGCGTCGTGTTCAAG

[a]Restriction sites are underlined. Changes to the *P. butanovora* sequence are in lower case.

[b]Codons encoding substituted amino acids are bold.

pBKB. *P. butanovora* PBKB was selected by growth in 30 ml of the lactate medium described above containing 25 μg/ml kanamycin.

Site-directed mutagenesis was performed using GeneTailor™ Site-Directed Mutagenesis System (Invitrogen, Carlsbad, CA). Single specific mutations were introduced into *bmoX* using pBSbmoxyz (Table 3.1) as template DNA with pairs of mutagenic primers (Table 3.2). The reaction mixtures were transformed into competent *E. coli* DH5α cells. Mutations in pBSbmoxyz were verified by DNA sequencing (Center for Genome Research and Biocomputing Core Laboratory, Oregon State University; CGRB CL, OSU).

Plasmids containing site-directed mutations of *bmoX* were electroporated into the mutant host strain *P. butanovora* PBKB using conditions described above. pBSbmoxyb with no mutation was also electroporated into the mutant host strain to recover the wild-type genotype (*P. butanovora* Rev WT, Table 3.1). Following electroporation, mutant strains were immediately transferred to 30 ml *P. butanovora* medium containing 1 mM citrate for recovery. Butane (10 ml) was added as overpressure for selection of mutant strains with and without altered amino acids. Growth was observed after 10 to 30 days. Liquid cultures were plated on LB agar and single colonies picked for clonal cell lines. The entire *bmoX* gene was amplified using high fidelity PCR (Platinum *Pfx*, Invitrogen) and sequence changes for each *P. butanovora* mutant cell line were verified by DNA sequencing (CGRB CL, OSU). The amino acids altered in BMOH-α in recovered strains of *P. butanovora* are listed in Table 3.3.

Table 3.3. Amino acids altered in BMOH-α in recovered strains of *P. butanovora*

Targeted amino acid in BMOH-α	**Corresponding amino acid in MMOH-α**	**Putative position in BMOH-α**
Thr 148	Cys	Adjacent to active site
Glu 320	Lys	Surface residue involved in BMOH-α - BMOB interaction
Phe 321	Tyr	Surface residue involved in BMOH-α - BMOB interaction
Leu 279	Phe	Hydrophobic cavity 2
Gly 113	Asn	Hydrophobic cavity 1

BMO induction

Lactate-grown cells were grown overnight and harvested at late-exponential phase (OD_{600} 0.8-1.0). Cells were washed 3 times in phosphate buffer (25 mM KH_2PO_4•25 mM Na_2HPO_4 pH 7.2) and resuspended to OD_{600} 0.65-0.75 in growth medium with 1 mM 1-butanol added to induce expression of BMO (Sayavedra-Soto *et al.*, 2005). Following incubation at 30°C with shaking for 3 h, cells were harvested for analysis of BMO activity using the ethylene oxidation assay (Hamamura *et al.*, 1999). Briefly, following harvest, cells were exposed to ethylene (an alternative substrate for BMO) and ethylene oxide accumulation was measured by gas chromatography (GC).

Butane oxidation

Butane consumption was measured using a 1 ml syringe assay (Arp, 1999). Briefly, 0.025 ml cell suspension was added to 0.75 ml O_2-saturated phosphate buffer and 0.1 ml butane-saturated phosphate buffer. A glass bead within the chamber mixed the contents of the syringe. Samples (5 μl) were taken periodically and butane concentrations measured by GC.

Regiospecificity of BMO mutants towards butane and propane

Butane-grown cells were harvested by centrifugation for analysis at late-exponential phase (OD_{600} 0.60-0.75). Cells were washed 3 times in phosphate buffer and resuspended as a concentrated cell suspension (5 mg total protein/ml). Accumulation of 1- and 2-butanol were measured using 1-propanol or 2-pentanol as inhibitors of butanol consumption (Arp, 1999). Vials (7 ml) containing 0.8 ml phosphate buffer, were capped and sealed, and 1.5 ml butane was added as overpressure to the headspace. Vials were placed in a 30°C water bath with constant

shaking. Assays were initiated by the addition of 0.2 ml concentrated cell suspension, and liquid samples (1 μl) were removed periodically for measurement of butanol accumulation by gas chromatography. Rates of 1- and 2-butanol accumulation were linear during the first 8 and 40 min. We verified that the differences in rates of 1- and 2- butanol production in the *P. butanovora bmox* mutants as compared to Rev WT were attributable to the single amino acid alterations and not to differences in expression levels of BMOH-α. Butane-grown mutant strains were harvested as described above and the relative amounts of the different BMO subunits were evaluated by SDS-PAGE. No apparent differences in expression levels were observed.

To determine regiospecificity of propane oxidation, accumulation of propionate and acetone were monitored as downstream metabolites of 1- and 2-propanol, repectively. In this case, cells were grown in the presence of ethane because the enzymatic pathways required for propionate consumption are not expressed (Doughty *et al.*, 2006). Priopionate accumulates as the product of 1-propanol transformation by alcohol and aldehyde dehydrogenases (Doughty *et al.*, 2006; Vangnai *et al.*, 2002), and no propionaldehyde accumulation was measureable during incubations. Similarly, if propane is oxidized sub-terminally, to 2-propanol, acetone should accumulate. Vials were prepared as described above with 2.0 ml propane added instead of butane, and assays proceeded as above.

Methane oxidation

Vials (7.7 ml) containing 0.8 ml phosphate buffer, 5 mM lactate, and 3 ml methane gas were incubated at 30°C with shaking. Washed cell suspensions (5 mg total protein/ml) were added to the vials to initiate the assays, and liquid samples (1 μl) were removed for measurement of methanol by GC.

Analytical techniques

Ethylene oxide (100 μl headspace samples), methanol, butane, acetone, and propionate (1 μl liquid phase samples) were analyzed by GC with a Shimadzu (Kyoto, Japan) GC-8A chromatograph equipped with a flame ionization detector (FID) and a stainless steel column packed with Porapak Q 80 to 100 mesh (Alltech, Deerfield, Ill). Butanol accumulation (1 μl liquid phase samples) was monitored by GC using a FID and a CarboWax 1500 column (6 ft x 2 mm) (Alltech). Compounds were identified by correspondence to retention times of standards. Compounds were quantified by comparison of peak areas or peak heights obtained from known quantities of standard solutions.

Structural modeling

The BMOH-α subunit was modeled using the Mod Web Server (Fiser *et al.*, 2000; Marti-Renom *et al.*, 2000; Sali and Blundell, 1993) based on MMOH-α templates (PDBs 1FZ1B, 1FZHA, 1FZ8A, 1FZ2A, 1FZ0B) from *Methylococcus capsulatus* (Bath) (Whittington and Lippard, 2001; Whittington *et al.*, 2001a) and viewed using Deep View Swiss-Pdb Viewer and Pymol (DeLano, 2002). BMOH-α with the G113N substitution was modeled using 1MTY (Rosenzweig *et al.*, 1997). Torsion angles for F185 in the BMOH-α, and G113N models were calculated using the Deep View program, and those for MMOH-α F188 were calculated using Deep View program from the coordinates of PDB 1FZ8A. The methanol-bound MMOH crystal structure (PDB 1FZ6) was used for cavity 1 comparisons.

RESULTS

Mutagenesis of *P. butanovora bmoX*

Investigations of regions of the hydroxylase component of BMO were initiated by engineering nine single amino acid substitutions in BMOH-α in *P. butanovora.* By comparison to crystal structures of MMOH-α and sequence alignment with BMOH-α, residues targeted for substitution reside in three key regions: the area adjacent to or contributing to formation of the active site (G113, T148, P179), hydrophobic cavity 2 which leads to the active site (V181, L287, L279), and the surface of BMOH-α that interacts with the effector protein, BMOB (Q319, Q320, F321). BMOH-α residues were changed to residues occupying the equivalent positions in MMOH-α; for example, for *P. butanovora* mutant strain T148C, the Thr148 in wild-type BMOH-α was changed to the corresponding Cys in MMOH-α.

First, mutant strain *P. butanovora* PBKB was constructed containing a selectable kanamycin resistance cassette within partially deleted *bmoX* (Table 3.1). Homologous recombination of *bmoX* sequences flanking the kanamycin cassette facilitated replacement of the kanamycin marker in *P. butanovora* PBKB with plasmid-borne *bmoX* sequences containing site-directed mutations. Because we were interested in studying the roles of individual amino acids in BMO catalysis, mutants were selected that maintained butane oxidation. To verify that the double-crossover event was successful, the entire *bmoX* gene from each recovered clonal line was sequenced. *P. butanovora* mutants were kanamycin sensitive, and PCR analysis using external *bmoX* primers and internal *kan* primers verified removal of *kan* and recovery of full-length *bmoX* (data not shown). Of the nine mutant strains engineered, five were recovered by growth on butane. Mutant strains Q319G, P179K, V181M, and L287F were not recovered and therefore may have yielded altered BMOH-α subunits that could not support sufficient butane oxidation activity for growth on butane or produced products that could not be metabolized further. It is also possible that these residues are each

essential for butane oxidation, or recombination was incomplete. Finally, to ensure that any observed phenotypic differences were not artifacts of the mutagenesis procedures, but instead were attributable to the single amino acid changes, one strain with no amino acid changes was recovered for use as the control "wild-type" BMOH-α phenotype (strain Rev WT; Table 3.1). The 5 mutant strains were studied for the mechanistic and physiological implications of single amino acid substitutions within BMOH-α.

Growth of *P. butanovora* mutants on alkanes

The growth characteristics of the *P. butanovora* mutants on butane were examined (Fig. 3.1). Mutant strains L279F and G113N showed both distinctly longer lag phases and slower growth rates reflecting a diminished ability to grow on butane. All mutant strains reached similar optical densities (OD) as the Rev WT control strain. Generation times of butane-grown mutant strains Q320K and F321Y were not significantly different from Rev WT; however the remaining three mutant strains showed generation times at least 0.75 h longer than Rev WT (Table 3.4). Because BMOH-α was altered to reflect the corresponding residues in MMOH-α, we were interested in determining if growth of the mutant strains on either shorter or longer chain length alkanes was different from Rev WT. While the generation time of Rev WT was longer on ethane than on butane (4.5 h vs. 3.6 h), the slower growth of the mutants on ethane was exacerbated by the single amino acid substitutions present in the mutant strains. The lag phase of mutant strain G113N when grown on ethane was about twice as long as when grown on butane (data not shown). The generation time of mutant strain F321Y was not significantly different than Rev WT when grown on butane, but this strain was able to maintain a shorter generation time than Rev WT when grown on propane and ethane. The growth rate of mutant strain T148C was as slow as L279F on ethane, but nearly the same as Rev WT on propane. While all other mutant strains grew on propane to a final OD with similar growth rates as Rev WT,

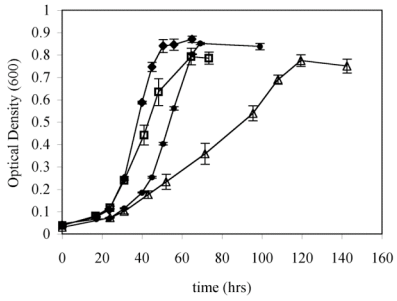

Figure 3.1. Growth of *P. butanovora* mutant strains on butane. Data are presented as the mean OD(600) at each time point for 3 replicate growth curves ± standard deviations. Symbols: ♦, Rev WT; □, T148C; ●, L279F; △, G113N.

Table 3.4. Generation times for *P. butanovora* mutants grown on butane, propane, and ethane[a]

	Growth Substrate		
	Butane	Propane	Ethane
P. butanovora strain	Generation time (hrs)	Generation time (hrs)	Generation time (hrs)
Rev WT	3.6 ± 0.2	4.0 ± 0.4	4.5 ± 0.3
T148C	4.4 ± 0.3	4.2 ± 0.4	7.0 ± 0.1
Q320K	4.1 ± 0.3	3.9 ± 0.1	5.9 ± 0.1
F321Y	3.4 ± 0.3	3.4 ± 0.2	3.8 ± 0.1
L279F	5.7 ± 0.1	4.5 ± 0.1	7.9 ± 0.6
G113N	9.1 ± 0.4	NA	13.1 ± 0.5

[a]Generation times were determined based on exponential increases in optical density of 3 replicate growth curves

mutant strain G113N showed only a slight increase in OD (0.10-0.15) after nearly 8 days. All mutants grew to similar ODs on C5-C8 alkanes. Generation times for wild-type and mutant *P. butanovora* strains increased during growth on C4+ alkanes. Furthermore, differences in lag phases and growth rates for the mutant strains relative to Rev WT on C5-C8 alkanes did not reveal other notable phenotypic differences (data not shown).

BMO specific activity of mutant BMOH-α strains

We chose to alter amino acids in BMOH-α in key areas affecting substrate-binding, active site geometry or chemistry, and interaction with the effector protein with the expectation that they would influence butane oxidation activity. Although growth on butane was diminished in most of the mutant strains (Fig 3.1 and Table 3.4), changes in the specific activity of BMO could have been masked by changes in the amount of total BMO produced. To generate cells with identically induced BMO, cultures were grown on lactate, then washed and exposed to 1-butanol to induce BMO expression (Sayavedra-Soto *et al.*, 2005). Specific activities of the altered BMOs were lower than that of Rev WT. Mutant strains L279F and G113N had specific activities at least 7-fold lower than Rev WT, corroborating the more dramatically diminished growth rates observed for these mutant strains. We also evaluated the relative amounts of the BMO subunits produced by each of the mutant strains by SDS-PAGE following growth to OD_{600} of 0.75. No differences in protein levels were observed in BMOH subunits, BMOR, or BMOB (data not shown) providing further evidence that the differences in growth rates were due to changes in specific activity of BMO.

Regiospecificity of mutant BMOH-α strains

Previous research has shown that alterations to residues within multicomponent monooxygenases can result in specific catalytic effects, including changes to rate of substrate turnover, substrate specificity, and position of oxygen insertion into the substrate ((Fishman *et al.*, 2005; Smith *et al.*, 2002; Vardar and Wood, 2004, 2005) and others). Wild-type *P. butanovora* predominantly oxidizes butane at the terminal carbon (Arp, 1999); likewise, Rev WT oxidized butane to 1-butanol and 2-butanol in a 24:1 ratio. The rates of 1- and 2-butanol accumulation were determined for each of the *P. butanovora* mutant strains (Table 3.5). Substantial differences from Rev WT were observed. Most notably, ninety-two percent of the product of butane oxidation by mutant strain G113N was 2-butanol. The ratio of rates of 2- to 1-butanol accumulation for mutant strains L279F and G113N were 5.5-fold and 278-fold higher than Rev WT. Wild-type *P. butanovora* can grow on both 1- and 2-butanol, although the generation time for growth on 2-butanol (5 mM) is 3.5 times longer than growth on 1-butanol (data not shown). Mutant strain F321Y was the only mutant in which 2-butanol production was not measurable (detection limit: 0.0015 nmoles min^{-1} (mg $protein^{-1}$)).

To further investigate the extent of subterminal oxidation of alkanes by the *P. butanovora* mutant strains, the regiospecificity of propane oxidation was also determined. When butane is the growth substrate, the subsequent oxidation of 1-butanol yields butyraldehyde that is transformed to butyrate, while oxidation of 2-butanol yields butanone (Arp, 1999). When propane is the growth substrate, its terminal oxidation yields propionate, and the subterminal oxidation of propane yields propanone (commonly known as acetone). In *P. butanovora* the further metabolism of the products of propane oxidation, namely propionate and acetone, requires induction of metabolic pathways that are not expressed in lactate, ethane, or butane-grown cells (Doughty *et al.*, 2006). Therefore, cells with BMO induced by ethane and subsequently exposed to propane, should initially accumulate propionate or acetone since the downstream enzymes required for their metabolism are not expressed. Washed ethane-grown cells were exposed to propane and rates of propionate and,

Table 3.5. Regiospecificity of butane oxidation by *P. butanovora* mutant strains

P. butanovora strain	Rate of product accumulation (nmoles min^{-1} (mg $protein^{-1}$))		Rate 2-butanol accumulation/rate 1-butanol accumulation	Fold increase over Rev WT
	1-butanol	2-butanol		
Rev WT	74.0 ± 3.9	2.70 ± 0.91	0.04	--
T148C	41.3 ± 4.0	6.14 ± 0.89	0.15	3.7
Q320K	50.4 ± 7.8	10.3 ± 0.53	0.20	5.6
F321Y	102.4 ± 5.7	ND[a]	NA	NA
L279F	47.0 ± 7.1	10.45 ± 4.2	0.22	5.5
G113N	1.77 ± 0.06	19.67 ± 2.4	11.1	277.5

[a]ND: Not Detected, NA: Not Applicable

acetone accumulation were measured. The rates of propionate and acetone accumulation were linear over the 60 min time-course. The ratio of propionate to acetone accumulation by Rev WT was 17:1 (Table 3.6). In sharp contrast mutant strain G113N oxidized propane exclusively to acetone at a rate of 11.3 nmoles min^{-1} (mg protein)$^{-1}$, and no propionate was detected during the 60 min incubation (detection limit: 0.0033 nmoles min^{-1} (mg $protein^{-1}$)). Because mutant strain G113N oxidized propane to the sub-terminal oxidation product, and yet did not grow on propane, we considered the possibility that although wild type *P. butanovora* grows on propane and 1-propanol, it may not grow on acetone. Indeed, no increase in OD (600) wasmeasured when wild type *P. butanovora* was inoculated to liquid medium with 5 mM, 10 mM, or 25 mM acetone. To verify that acetone is not toxic to *P. butanovora* at these concentrations, we inoculated cells to normal growth medium with acetone (0, 5, 10, 25 mM) and butane. All cultures grew to similar final ODs. Interestingly, 2-butanone (5 mM) and 2-pentanone (5 mM) were growth substrates for *P. butanovora* (data not shown).

Propane oxidation by mutant strains L279F and F321Y did not result in enrichment of the sub-terminal oxidation product as compared to Rev WT. Although acetone was shown to be consumed by *P. butanovora* at approximately 9 nmoles min^{-1} (mg protein)$^{-1}$ ((Arp, 1999) and this study), its consumption was acetylene-sensitive and can be attributed to turnover by BMO (data not shown). Nevertheless, the concentration of propane in the propane oxidation assay is high enough that it out-competes acetone for the active site of BMO.

Table 3.6. Accumulation of propionate and acetone in butane-grown *P. butanovora* mutant strains following removal of butane and exposure to propane

	Rate of product accumulation (nmoles min^{-1} (mg total $protein^{-1}$))	
P. butanovora strain	Propionate	Acetone
Rev WT	70.0 ± 3.0	4.2 ± 1.2
L279F	53.5 ± 2.3	4.4 ± 1.1
F321Y	74.2 ± 3.5	5.4 ± 0.09
G113N	ND	11.3 ± 2.1

ND: None Detected

Methane Oxidation

Given that five specific amino acid substitutions in BMOH-α were changed to reflect the corresponding residues of MMOH-α, it was of interest to determine if rates of methane oxidation by the BMOH-α mutant strains were changed relative to Rev WT. Methanol consumption by wild-type *P. butanovora* and Rev WT was not detected at low concentrations in the presence of methane obviating a need for an inhibitor of methanol consumption. In this study we measured an initial rate of methanol accumulation of 3.6 ± 0.6 nmoles min^{-1} (mg protein)$^{-1}$ for Rev WT (first 2 min; Fig. 3.2), about 5% of the rate of 1-butanol production. However, unlike butane oxidation to 1-butanol, methanol accumulation stopped after 10 min at a final concentration of 23 μM. With the exception of mutant strain G113N, all other BMOH-α mutant strains exhibited kinetic properties of methane oxidation similar to Rev WT. In contrast, mutant strain G113N oxidized methane to methanol at a slower initial rate (2.1 ± 0.1 nmoles min^{-1} (mg protein)$^{-1}$); yet, methanol accumulated to a final concentration 3.5-fold higher than Rev WT (83 ± 2.2 μM vs. 23 ± 1.7 μM).

To determine if methanol accumulation ceased due to enzyme inactivation or methanol inhibition of methane oxidation, Rev WT and mutant strain G113N cells that were exposed to methane were washed three times and exposed again to methane as described above. The rate and extent of methanol accumulation in Rev WT cells were equivalent to that shown in Fig 3.2, indicating that methanol reversibly inhibits methane oxidation by BMO. Although only 75% of the methanol oxidation activity was recovered in mutant strain G113N, mechanical disturbance due to prolonged incubation and wash procedures were previously shown to reduce BMO activity (Halsey *et al.*, 2005). We also determined whether methanol inhibition is turnover-dependent. The methanol accumulation assay was repeated with Rev WT and mutant G113N strain cells, and methanol (20 μM for Rev WT, and 80 μM for G113N) was added to the reaction mixtures at time-zero. No additional methanol accumulated over

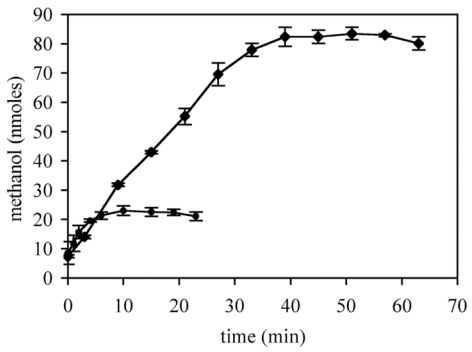

Figure 3.2. Time course of methane oxidation to methanol. Washed butane-grown cells (1 mg total protein) exposed to 3 ml methane in 7.7 ml sealed vials. Data are presented as the mean of at least 3 replicates ± standard deviation. Symbols: ●, Rev WT; ♦, G113N.

a 30 min incubation period for either *P. butanovora* strain. Furthermore, methanol (20 μM) did not inhibit butane or ethylene oxidation by Rev WT cells (data not shown).

DISCUSSION

We have demonstrated that BMO from *P. butanovora* can be altered directly within the native host organism allowing for valuable mechanistic and physiologic studies. Five mutant strains of *P. butanovora* were engineered to initiate investigations of the fundamental differences in substrate specificity between the two closely related enzymes, BMO and MMO. Effects of the single amino acid substitutions in BMOH-α on growth rates and downstream metabolism were evaluated in addition to hydrocarbon oxidation.

Altered BMOH-α residue T148C resulted in slightly slower growth on alkanes and reduced specific activities. T148 corresponds to C151 in MMOH-α and Q141 in toluene 4-monooxygenase (T4MO) from *Pseudomonas mendocina* KR1. Although T148C had little effect on regiospecificity of propane and butane oxidation, Q141C in T4MO resulted in changes to regiospecificity of *m*- and *p*-xylene oxidation (Pikus *et al.*, 1997). Site-directed mutagenesis of Cys 151 in MMOH-α to Glu or Tyr yielded mutant strains of *M. trichosporium* OB3b that were unable to support growth on methane under conditions that favored expression of the mutant enzyme (Smith *et al.*, 2002). However, there is no evidence about the activity of these altered enzymes towards methane since the α, β, and γ subunits of MMOH could not be visualized by SDS-PAGE analysis suggesting that the altered enzymes were unstable (Smith *et al.*, 2002). Because neither mutant strain T148C nor Q141C in T4MO (Steffan and McClay, 2000) promoted methane oxidation, we can conclude that simply acquiring the Cys residue is not sufficient for active site chemistry facilitating methane oxidation.

Mutant strain F321Y oxidized butane even more selectively to 1-butanol than the Rev WT strain as no 2-butanol was detected during the butane regiospecificity

assay. It is possible that the specificity of strain F321Y allowed it to keep pace with the growth of Rev WT on alkanes even though its specific activity was diminished as measured by the ethylene oxide assay. However, propane oxidation by strain F321Y yielded both terminal and sub-terminal oxidation products. It remains to be seen if the terminal oxidation regiospecificity exhibited by strain F321Y with butane extends to other longer-chained alkanes. In methane-oxidizers, MMOB is known to affect the regiospecificity of the enzyme complex (reviewed by (Merkx *et al.*, 2001)). *In vitro* experiments revealed that the product distribution of sMMO-catalyzed butane oxidation is 44% 2-butanol and 56% 1-butanol. The product distribution of butane oxidation shifts to 95% 2-butanol in the absence of MMOB (Froland *et al.*, 1992). The strict terminal oxidation of butane by mutant strain F321Y is consistent with the idea that the interaction between BMOH-α and BMOB was affected. Complementary mutational analysis of BMOB would lead to more detailed understanding of the role of BMOB in affecting the regiospecificity of substrate oxidation.

Two residues, G113 and L279, within hydrophobic cavities 1 and 2 in BMOH-α, were found to have distinct roles in hydrocarbon oxidation. Striking differences in specific activities and regiospecificity were observed for mutant strains G113N and L279F. The predominantly sub-terminal oxidation of propane and butane by strain G113N suggests the single amino acid substitution caused a significant alteration of BMOH-α active site geometry. Likewise, the ratio of rates of 2-butanol to 1-butanol production was increased 5.5-fold by strain L279F relative to the wild-type phenotype. It is also possible that the altered regiospecificities of mutant strains G113N and L279F were conferred by modified interactions with BMOB.

With the availability of site-directed *bmox* mutants that demonstrate interesting changes in enzyme properties, we were in a position to spatially compare the geometry of BMOH-α with MMOH-α. We have modeled BMOH-α using MMOH-α crystal structures as templates and focused attention to the area immediately surrounding the active site and including the leucine gate (Fig 3.3). The crystal structure of MMOH-α reveals that residue F282 contributes both to the strained conformation of gating residue F188 (χ_1 and χ_2 torsion angles are -98° and -168°, respectively) and the

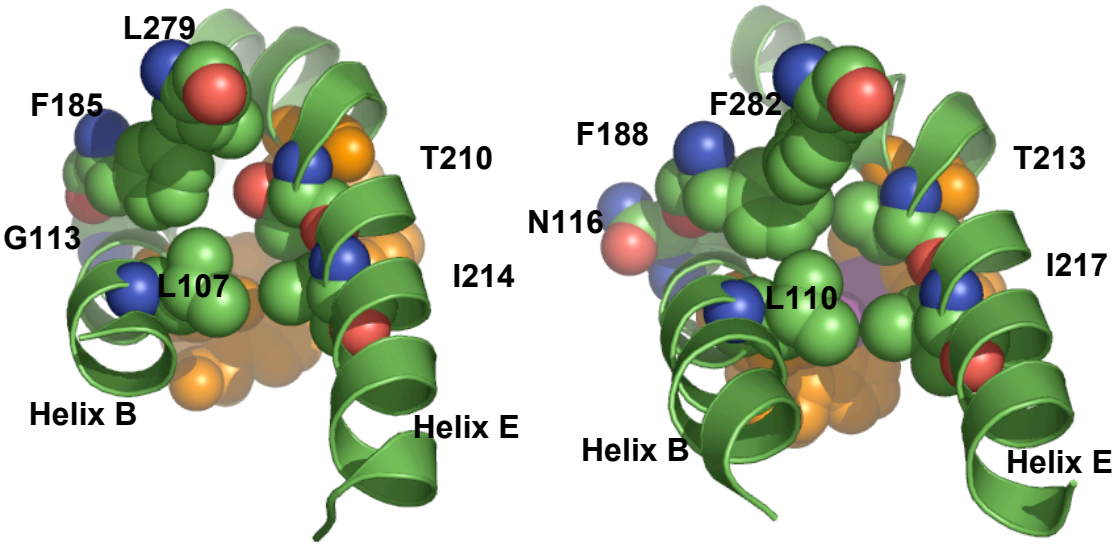

Figure 3.3. Model of BMOH-α (left) compared to the MMOH-α crystal structure (right). Top: BMOH-α residues G113, L279, G186, and L190 affect the conformation of residue F185, opening the leucine gate and shifting the geometry of the active site relative to MMOH-α. The atoms of residues are colored by type, where green is carbon, red is oxygen, blue is nitrogen, purple is iron (MMOH-α only), except for residues coordinating the active site which are colored orange. Bottom: space-filling representations. View is looking through the leucine gate towards the diiron center (depicted in MMOH-α only) Atom colors are the same as in top. Fig created using Pymol.

reduction in size of cavity 1. In the same plane in MMOH-α, N116 borders cavity 1 on the opposite side of helix B from E114 (Fig 3.3, top right). The two residues packing to either side of N116 are S189 and I193. These 3 residues interact with P58 and W83 of MMOH-β. In BMOH-α, the two residues flanking G113 are G186 and L190 (Fig 3.3, top left) that probably interact with N57 and Y82 from the BMOH-β-subunit. Neither of these residues has substantially different space-filling potential as P58 and W83 from MMOH-β. In BMOH-α, the missing or reduced side-chains of G113, G186, and L190 to one side of F185, and L279 to the other, may allow F185 to adopt the more relaxed rotameric conformation present in the BMOH-α model (predicted χ_1 and χ_2 torsion angles are -53° and -156°, respectively, Fig 3.3). The position of F185 shifts the geometry of the active site and the leucine gate to a more open position relative to that of MMOH-α. This opening may favor entry of butane, BMO's natural substrate, to the active site. Likewise, the more restricted access to the active site in MMOH-α appears to favor its natural substrate, methane. We also modeled BMOH-α with the G113N substitution using the MMOH-α crystal structure (not shown). Indeed, the predicted χ_1 and χ_2 torsion angles for F185 in the G113N model (-85° and -124°, respectively) are intermediary to the wild-type BMOH-α model and MMOH-α crystal structure, and result in partial closing of the leucine gate. The model of BMOH-α may suggest a relationship between substrate size and specificity. Recognizing that in the MMO system the effector protein influences substrate access (Wallar and Lipscomb, 2001) as well as active site geometry (Froland *et al.*, 1992) and chemistry (Zheng and Lipscomb, 2006), the single amino acid substitutions in BMOH-α studied here reiterate the importance of the finely tuned structures at the active site of the hydroxylase.

We believe that the sensitivity of methane oxidation by BMO to methanol may have significant implications associated with product release from the active site. Product release is considered to be rate-limiting in the sMMO catalytic cycle (Lee *et al.*, 1993; Zheng and Lipscomb, 2006). Altered MMOB proteins revealed that MMOB affects the rates of specific steps in the catalytic cycle, including product release

(Wallar and Lipscomb, 2001). Product release may comprise more than one definable step, or these multicomponent monooxygenases have regions of flexibility that accommodate unique postures during different steps of the cycle (Brazeau and Lipscomb, 2003). Product-bound MMOH crystal structures revealed positional changes of I217 in addition to the leucine gate residues (Sazinsky and Lippard, 2005; Whittington *et al.*, 2001a). In the methanol-bound MMOH crystal structure, we note that L110 moves 0.8 Å away from F188, and 2.7 Å closer to Fe1, when compared to native MMOH. It was previously suggested that these changes are necessary to allow residence of the oxidation product (Sazinsky and Lippard, 2005). The 3.5-fold increase in methanol accumulation by *P. butanovora* mutant strain G113N compared to Rev WT suggests that geometric alterations to cavity 1 and the leucine gate may make the active site **less** accommodating to the product, thus encouraging its release. In MMOH-α the strained coordination of F188 held in place by the counter-forces of F282 and N116 and its interacting residues, could provide the necessary constraints within cavity 1 such that methanol is released.

The results obtained from the site-directed *bmox* mutants of *P. butanovora* support the idea that the geometric intricacies of the leucine gate influence catalysis at the active site. Furthermore, BMO's striking sensitivity of methane oxidation to methanol inhibition provides a new avenue for exploration of the mechanistic differences between BMO and sMMO. The inability of *P. butanovora* to metabolize acetone exposed vulnerability in its metabolic flexibility. The mutant strains should prove valuable in unraveling the complexities associated with downstream metabolism of products generated from a broad substrate range monooxygenase.

ACKNOWLEDGEMENTS

This research was funded through a grant from the National Institutes of Health (5R01GM56128-06). We gratefully acknowledge P. Andrew Karplus at OSU for helpful discussions regarding protein chemistry and structure.

CHAPTER 4.

MODIFIED MECHANISMS OF CHLORINATED ETHENE OXIDATION IN SITE-DIRECTED BMOH-α *Pseudomonas butanovora* MUTANTS

Kimberly H. Halsey, David M. Doughty, Luis A. Sayavedra-Soto,
Peter J. Bottomley, and Daniel J. Arp

In preparation for submission to
Journal of Bacteriology
American Society for Microbiology

ABSTRACT

Mutant strains of *P. butanovora* containing specific amino acid substitutions in the α-subunit of the butane monooxygenase hydroxylase (BMOH-α) were exposed to 1,1 dichloroethene (DCE), 1,2 *cis*-DCE, and trichloroethylene (TCE). Differences in oxidation rates were most pronounced with TCE; the rate of TCE degradation was reduced by one-half in mutant strain L279F and two-thirds in strain G113N relative to the wild-type (Rev WT). Evidence was obtained that the composition of products of chloroethene (CE) oxidation differed between Rev WT and some of the mutant strains. For example, while Rev WT released nearly all available chlorine stoichiometrically during CE oxidation, strain G113N released less than 25% of available DCE chlorine and only 56% of available TCE chlorine. Whereas Rev WT, strain L279F, and strain F321Y formed stoichiometric amounts of 1,2 *cis*-DCE epoxide during oxidation of 1,2 *cis*-DCE, only about 50% of the 1,2 *cis*-DCE oxidized by strain G113N was detected as the epoxide. Evidence was obtained for 1,2 *cis*-DCE epoxide being a substrate for BMO that was oxidized after the parent compound was consumed. Yet, all of the mutant strains released less than 40% of the available 1,2 *cis*-DCE chlorine suggesting they have altered activity towards the epoxide. In addition, strain G113N was unable to degrade the epoxide. TCE epoxide was detected during exposure of Rev WT and strain F321Y to TCE, but not with strains L279F and G113N. Lactate-dependent O_2 uptake rates were differentially affected by DCE degradation among the strains providing evidence that different products or product ratios are released by the altered BMOs during CE degradation that reduce the impacts of CE oxidation on cellular toxicity. The use of CEs as mechanistic probes, in combination with *P. butanovora* BMOH-α mutants might provide insights into the catalytic mechanism of BMO.

INTRODUCTION

Pseudomonas butanovora utilizes a butane monooxygenase (BMO) to initiate oxidation of short-chained alkanes as its sole source of carbon and energy for growth (Arp, 1999). BMO fortuitously activates a wide variety of chemically stable compounds including environmental contaminants such as chlorinated ethenes (CEs) (Arp *et al.*, 2001; Hamamura *et al.*, 1997). Other bacterial genera such as *Nocardioides* and *Mycobacterium* also utilize BMOs that are biochemically distinct from that characterized in *P. butanovora* (Hamamura *et al.*, 1999). For example, trichloroethylene (TCE) turnover-dependent toxicities, including BMO inactivation (66% inactivation in *M. vaccae* compared to 96% in *P. butanovora* and *Nocardioides* sp. CF8) and reduction in cell viability (83% reduced in *P. butanovora* compared to no reduction in *M. vaccae* and *Nocardioides* sp. CF8) varied substantially among these strains (Halsey *et al.*, 2005). The possibility that differences exist among the BMOs in their catalytic attack on TCE and that product profiles from TCE degradation may vary and impact overall CE transformation capacities encouraged additional research aimed at the identification of mechanisms that would allow for more sustainable CE degradation.

Products of CE degradation have been quantified from whole cells of methanotrophs and from purified sMMO (Fox *et al.*, 1990; Lontoh *et al.*, 2000; Shinohara *et al.*, 1998; van Hylckama Vlieg *et al.*, 1996). For example, 80-96% of the products of CE degradation are the result of CE epoxide hydrolysis or enzymatic turnover of CE epoxide. The outcome of epoxide breakdown is primarily liberation of chloride, with the organochlorines chloral (trichloroacetaldehyde) and dichloroacetaldehyde (DCA) accounting for small percentages (6% and 5-17%, respectively) of the total TCE turned over (Fox *et al.*, 1990; Shinohara *et al.*, 1998). In contrast, chloral and DCA comprise the majority of the products formed during oxidation of TCE by the distantly related liver microsomal cytochrome P-450 (Miller and Guengerich, 1982). Retention of the chlorine atoms is a result of electron abstraction followed by halide or hydride shift (NIH shift); an enzymatic mechanism

that does not involve formation of a CE epoxide (Green and Dalton, 1989; Lipscomb, 1994; Miller and Guengerich, 1982). These early experiments using CEs as substrates with purified sMMO and P-450 provided the foundations for development of mechanistic models of the enzymatic catalytic cycles. For example, the atomic migration associated with the formation of chloral during oxidation of TCE was rationally explained by the formation of a carbocation intermediate and radical rebound chemistry (Fox *et al.*, 1990; Liebler and Guengerich, 1983), as was the detection of trace monochloroacetic acid from the oxidation of 1,1 DCE by sMMO (Green and Dalton, 1989).

BMO is a soluble diiron multicomponent monooxygenase with high similarity to soluble methane monooxygenase (sMMO). Genetic and biochemical characterization showed that BMO consists of a hydroxylase (BMOH) in $\alpha_2\beta_2\gamma_2$ configuration, a reductase (BMOR) which transfers electrons from NADH to the active site in the hydroxylase α-subunit, and an effector protein (BMOB) whose function in BMO remains undefined (Sluis *et al.*, 2002). Single amino acid substitutions in the BMO hydroxylase α-subunit (BMOH-α) of *P. butanovora* have provided a glimpse into the basis of its substrate and product specificity (Halsey *et al.*, 2006). For example, the broad substrate range of BMO which includes aromatics, alkenes, alkynes, and CEs (Doughty *et al.*, 2005; Hamamura *et al.*, 1999) was recently shown to include methane (Halsey *et al.*, 2006). In addition, while wild-type BMO terminally oxidizes propane and butane (Arp, 1999), strain G113N in which glycine 113 in BMOH-α was substituted for asparagine to resemble MMOH-α at that position, oxidized propane and butane almost exclusively at the subterminal position (Halsey *et al.*, 2006). Two other mutant strains, L279F and F321Y, were similarly engineered to resemble MMOH-α at the corresponding amino acid positions. The ratio of rates of 2-butanol to 1-butanol accumulation in mutant strain L279F was 5.5-fold higher than in the control strain (Rev WT), and strain F321Y appeared to oxidize butane exclusively at the terminal position (Halsey *et al.*, 2006).

In this study, mutant strains of *P. butanovora* containing altered BMOs were exposed to the CEs, 1,1 dichloroethene (DCE), 1,2 *cis*-DCE, and TCE. Differences in

product formation and physiological responses were measured, and the results were applied to a model describing enzymatic oxidation of CEs by *P. butanovora* and mutant strain G113N. The data obtained in this study demonstrates that experiments with mutant strains of *P. butanovora* containing single amino acid substitutions in the α-subunit of the BMO hydroxylase and CEs as substrate probes, may provide insights into the mechanism of CE oxidation by BMO.

MATERIALS AND METHODS

Bacterial strains and growth conditions

P. butanovora strains were cultured at 30°C in sealed 160 ml vials as previously described (Halsey *et al.*, 2006). Mutant strains F321Y, L279F, and G113N, contain single amino acid substitutions in BMOH-α. Strain Rev WT contains the wild-type amino acid sequence. The construction of these strains was previously described (Halsey *et al.*, 2006). For all experiments, cells were grown on butane and harvested at late-exponential to early-stationary phase (OD_{600}, 0.60-0.80). Cells were washed three times and resuspended in phosphate buffer to a concentrated cell suspension (10 mg/ml total protein).

Chlorinated ethene exposure

1,1 DCE, 1,2 *cis*-DCE, and TCE concentrations were monitored by gas chromatography. Teflon faced butyl septa (Supelco, Bellefonte, PA) were used to seal 7.7 ml vials containing 5 mM sodium lactate, and either 25 μM 1,1 DCE or 1,2 *cis*-DCE (initial liquid concentration) or 40 μM TCE, and sufficient phosphate buffer to bring the volume to 900 μl. Vials were equilibrated for at least 15 min in a

reciprocating shaker at 30°C. Concentrated cell suspensions (100 μl containing 1.0 mg total protein) were added to initiate the experiments. Samples of the gas phase (10 to 40 μl) were removed using a gas-tight syringe for analysis by gas chromatography.

For chloride release measurements, following complete CE consumption, vials were placed on ice for 15 minutes. Cells were sedimented and the supernatant was transferred to a fresh tube and stored at 4°C until analysis by ion chromatography. Chloride concentrations were determined using a Dionex (Sunnyvale, CA) model DX-120 ion chromatograph equipped with an auto-sampler, an electrical conductivity detector and a Dionex AS14 column.

Oxygen-uptake measurements

O_2 uptake measurements were made using a Clark-style O_2 electrode (Yellow Springs, Ohio) mounted in a glass water-jacketed reaction vessel (1.6 ml) at 30°C filled with phosphate buffer (25 mM KH_2PO_4 · 25 mM Na_2HPO_4, pH 7.2). For each experiment, cells (0.3 mg total protein) were added to the reaction vessel and the vessel was capped. Sodium lactate (3 mM) was added to the vessel through the capillary inlet to establish a lactate-dependent O_2 uptake rate. Chlorinated ethenes (13 μM 1,1 DCE; 10 μM 1,2 *cis*-DCE) were added to determine their effects on rates of lactate-dependent O_2 uptake. O_2 uptake rates were determined for each strain during exposure to each CE by measuring the slopes of tangent lines drawn to the resulting progress curves.

Determination of chloroethene epoxides

Reaction vials containing either 1,2 *cis*-DCE (25 μM) or TCE (80 μM) and cell suspension (1 mg total protein) were prepared as described above, and reactions were quenched by addition of 0.5 ml benzene at appropriate time points. 1,2 *cis*-DCE and

TCE epoxides were determined as previously described (Fox *et al.*, 1990; Miller and Guengerich, 1982). Because mutant strains L279F and G113N had slower rates of TCE degradation and because of the relative instability of TCE epoxide (half-life is 21-39 sec) (van Hylckama Vlieg *et al.*, 1996), the quantity of cell suspension was increased for these mutant strains and decreased for Rev WT such that the total TCE epoxide measured would be based on comparable degradation rates and total TCE degraded.

Analytical methods

CE concentrations were monitored with a Shimadzu (Kyoto, Japan) GC-8A chromatograph equipped with a flame ionization detector (FID) and capillary column (15 m x 0.53 mm) (Alltech, Deerfield, Ill) as described above. CE calibration curves were obtained by performing headspace gas analysis with vials containing known amounts of each compound. Dimensionless Henry's constants (1.3 for 1,1 DCE; 0.18 for 1,2 *cis*-DCE; 0.49 for TCE; Gossett, 1983) were used to account for aqueous and gaseous partitioning of the total CE in the vials. Protein concentrations were determined using the Biuret assay following cell solubilization in 3M NaOH for 30 min at 65ºC.

RESULTS

Degradation of chlorinated ethenes by *P. butanovora* mutants

The effect of specific amino acid substitutions in BMOH-α mutant strains of *P. butanovora* on CE oxidation was measured. The mutant strains degraded the three CEs at initial rates that were less than or equivalent to that of the wild-type control

strain (Rev WT) (Table 4.1). Mutant strain F321Y degraded the chloroethenes at rates that were similar to those of Rev WT. Mutant strain G113N degraded all three substrates at slower rates than Rev WT, whereas strain L279F only degraded TCE at a slower rate than Rev WT. For all strains the rates of CE oxidation were slower than the respective rates of butane oxidation (Halsey *et al.*, 2006) except for the oxidation of 1,1 DCE by strain G113N which was equivalent to the rate of butane oxidation.

Chloride release during chloroethene degradation

The amount of chloride released following incubation of the *P. butanovora* mutant strains with the same amounts of each of the CEs was measured. Rev WT released all available chlorine during consumption of each CE (Table 4.1). In contrast, strain G113N released less than 25% of the available chlorine from either of the DCEs, and only 56% of the available chlorine from TCE. Strain F321Y released 100% of the chlorine when exposed to 1,1-DCE, but only about 40% when exposed to 1,2-*cis* DCE and TCE. On the contrary, strain L279F released all of the available chlorine from TCE, which corresponded to a lower rate of TCE degradation than strains F321Y and Rev WT, but only partial amounts when exposed to either of the DCEs. Cells of each strain incubated without TCE released no chlorine. These results provide circumstantial evidence that the altered BMOs created different products during CE oxidation, or, the altered BMOs have different oxidative activities towards the products of initial CE oxidation that account for the variable percentage of chloride released.

Table 4.1. Initial rates of CE oxidation and percent chloride released following exposure to CEs by mutant strains of *P. butanovora*[a]

Strain	Butane oxidation	1,1-DCE (25 μM)[b]		1,2-*cis* DCE (25 μM)		TCE (40 μM)	
	Rate[c]	Rate[d]	Chloride Released (%)[e]	Rate	Chloride released (%)	Rate	Chloride released (%)
Rev WT	76.7 ± 4.0	31.6 ± 3.5	94.5 ± 3.8	8.8 ± 1.9	98.0 ± 7	16.5 ± 2.7	95 ± 1.5
F321Y	102.4 ± 5.7	30.3 ± 3.0	106 ± 2.2	8.4 ± 2.2	39.2 ± 0.9	17.9 ± 3.0	43 ± 1.6
L279F	57.5 ± 7.1	28.5 ± 2.9	70.9 ± 2.3	7.2 ± 2.4	30.5 ± 1.6	8.0 ± 2.5	97 ± 1.6
G113N	21.4 ± 2.4	22.5 ± 2.5	25.1 ± 0.6	4.1 ± 1.8	14.1 ± 1.2	5.6 ± 2.0	56 ± 0.9

[a]Values represent data from at least 3 separate experiments ± standard deviations.

[b]Initial liquid phase chlorinated ethene concentration.

[c]Data modified from (16). Sum of the rates of 1- and 2- butanol accumulation expressed as nmol min^{-1} (mg protein)$^{-1}$.

[d]Rate of CE degradation expressed as nmoles min^{-1} (mg protein)$^{-1}$.

[e]Strains (1 mg total protein) were exposed to CEs. Following complete CE consumption, vials were placed on ice 15 min. Cells were pelleted and supernatant transferred to a fresh tube and stored at 4°C until chloride release was measured as described in methods. Values expressed as percentagess of total chlorine available at the start of each experiment.

Epoxide detection

It is well established that the predominant pathway for 1,2 *cis*-DCE and TCE degradation by sMMO is via epoxide intermediates (1,1 DCE epoxide is thought to have a half-life of <2 s and has not been detected) (Liebler and Guengerich, 1983; van Hylckama Vlieg and Janssen, 2001). We verified that exposure of the Rev WT control strain to 1,2 *cis*-DCE resulted in accumulation of the corresponding epoxide. After 10 min incubation and consumption of 57 nmoles of 1,2 *cis*-DCE, a stoichiometric amount of 1,2 *cis*-DCE epoxide accumulated (Fig 4.1). Subsequently, following consumption of the DCE, 82% of the epoxide was degraded (Fig 4.1). Stoichiometric conversion of 1,2 *cis*-DCE to its epoxide was also detected in strains F321Y and L279F (data not shown), and the epoxide was similarly degraded following consumption of nearly 90% of the 1,2 *cis*-DCE (Table 4.2). However, only 30-40% of available chlorine from 1,2 *cis*-DCE was released by these strains compared to complete chloride release by Rev WT. Together, these results indicate that the mechanism of epoxide oxidation was changed in strains F321Y and L279F. Consumption of 57 nmoles of 1,2 *cis*-DCE by mutant strain G113N resulted in production of only 30 nmoles of the corresponding epoxide (Fig 4.1). Furthermore, 1,2 *cis*-DCE epoxide was not degraded 50 min following complete DCE turnover suggesting that the altered BMO in strain G113N not only produced different oxidized products, but did not attack 1,2 *cis* DCE epoxide. Alternatively, products other than 1,2 *cis*-DCE epoxide that were produced during 1,2 *cis*-DCE oxidation inhibited or inactivated BMO thereby preventing 1,2 *cis*-DCE epoxide turnover. Both of these scenarios would account for the low percent release of chloride by strain G113N during oxidation of 1,2 *cis*-DCE.

TCE epoxide formation was measured during exposure to TCE. While 1,2 *cis*-DCE epoxide is relatively stable, the half-life of TCE epoxide is only 21-39 sec (van Hylckama Vlieg *et al.*, 1996). Therefore, rapid formation of TCE epoxide in sufficient quantity was required for detection. Strains were exposed to 80 μM TCE for 6-7 min. Rev WT consumed TCE at a rate of 44 nmol min^{-1} mg^{-1}. After 6 min, the reaction was

quenched with benzene, and 28 nmoles TCE epoxide was detected (Table 4.2). Interestingly, the rate of TCE consumption for F321Y was at least as fast as Rev WT, but only 15 nmoles TCE epoxide was detected. This result is corroborated by the fact that only 43% of the available chlorine was released during exposure to TCE for strain F321Y (Table 4.1). Because strains L279F and G113N have slower rates of TCE consumption, the total protein used in the assays was adjusted in an attempt to match the rates of these strains with Rev WT. Using 2 mg total protein in each assay, strains G113N and L279F consumed 275-325 nmoles TCE at maximal rates of 32-36 nmoles min^{-1}. TCE epoxide was detected in these assays at about one-fourth the levels detected in strains Rev WT and F321Y per mg total protein. The lower levels of TCE epoxide detected in strains F321Y, L279F and G113N are either a result of less epoxide formed during TCE turnover, or differences in the fate of the TCE epoxide. Since 1,2 *cis*-DCE epoxide consumption commences only after ≥ 85% of the 1,2 *cis*-DCE is consumed (Fig 4.1), it is unlikely that BMO-dependent TCE epoxide consumption would occur in these assays since the reactions are quenched with benzene with approximately 40 μM TCE remaining. This is the first study in which TCE epoxide was detected by BMO-dependent turnover of TCE.

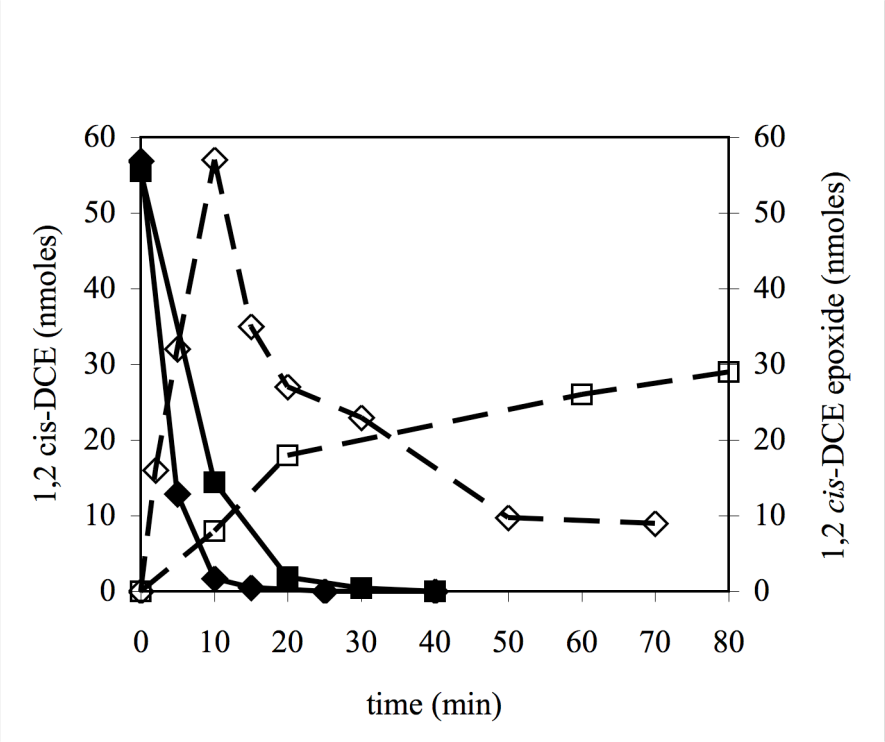

Figure 4.1. 1,2 *cis*-DCE epoxide formation (open symbols and dashed lines) during 1,2 *cis*-DCE degradation (closed symbols and solid lines) by Rev WT (◆, ◇) and mutant strain G113N (■,□).

Table 4.2. 1,2 *cis*-DCE epoxide and TCE epoxide formation and DCE epoxide consumption by BMO

Strain	1,2 *cis*-DCE degraded[a] (nmoles)	1,2 *cis*-DCE epoxide formed[b] (nmoles)	1,2 *cis*-DCE epoxide degraded[c] (nmoles)	TCE degraded[d] (nmoles)	TCE epoxide formed[e] (nmoles)
Rev WT	57	57	48	265	28
	152	149	61		
F321Y	60	60	55	300	15
	159	131	54		

[a]Strains (1 mg total protein) were exposed to either 25 or 75 μM 1,2 *cis*-DCE (initial liquid concentration).

[b]Reaction vials were quenched with benzene following 10 min exposure to 1,2 *cis*-DCE, and 1,2 *cis*-DCE epoxide was measured colorimetrically as described in methods.

[c]Reaction vials were quenched with benzene at appropriate time points to follow disappearance of 1,2 *cis*-DCE epoxide.

[d]Strains (1 mg total protein) were exposed to 80 μM TCE (initial concentration).

[e]Reaction vials were quenched with benzene following 6 min exposure to TCE, and TCE epoxide was measured colorimetrically as described in methods.

Effects of CE degradation on general cellular respiration

Degradation of chlorinated ethenes results in the release of products that may cause cellular toxicities including inactivation of the monooxygenase and attack by nucleophilic groups on macromolecules (Alvarez-Cohen and McCarty, 1991b; Doughty *et al.*, 2005; Halsey *et al.*, 2005; van Hylckama Vlieg *et al.*, 1997; Yeager *et al.*, 2001). Because the ratio of rates of 2- to 1-butanol accumulation for mutant strains L279F and G113N were 5.5-fold and 278-fold higher than Rev WT (Halsey *et al.*, 2006), it was plausible that differences in regiospecific oxidation of CEs by the mutant strains would result in the production of different product profiles leading to changes in toxic effects relative to Rev WT. The effects of DCE turnover on general cellular respiration were determined by measuring lactate-dependent O_2 consumption during exposure to 1,1- or 1,2-*cis* DCE. The DCE concentrations used in the assays were well below transformation capacities to ensure that all available DCE would be consumed (Doughty *et al.*, 2005). For all strains, prior to addition of the DCE, the lactate-dependent O_2 uptake rates were 28 to 32 nmoles min^{-1}. Upon addition of 1,1 DCE, O_2 uptake rates increased 52% for Rev WT and strain F321Y, 33% in strain L279F, and 30% in strain G113N. Although 1,1-DCE was completely consumed by all strains within 3 min, the impact on O_2 uptake rates was remarkably different among strains (Fig 4.2, A). Lactate-dependent respiration by mutant strain G113N appeared insensitive to 1,1-DCE turnover. However, the rate of O_2 uptake was reduced similarly in mutant strains F321Y and Rev WT. In contrast, the O_2 uptake rate in strain L279F was intermediate between G113N and F321Y and Rev WT. Since the chloride release value was similarly intermediate for strain L279F as compared to the other strains, the data imply that different products produced during CE oxidation are less toxic.

Differential effects on lactate-dependent O_2 uptake rates were also measured with 1,2 *cis*-DCE (Fig 4.2, B). Addition of 1,2 *cis*-DCE immediately promoted lactate-dependent O_2 uptake rates 50% in Rev WT and strain F321Y, 30% in strain L279F, and 20% in strain G113N. The O_2 uptake rate of Rev WT was reduced by 50% (equivalent to the original lactate-dependent O_2 uptake rate) within

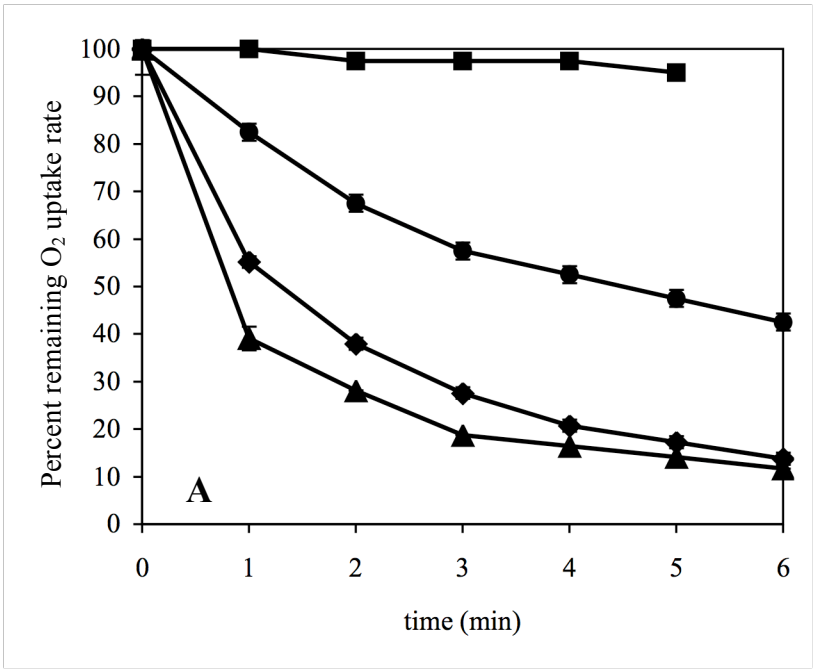

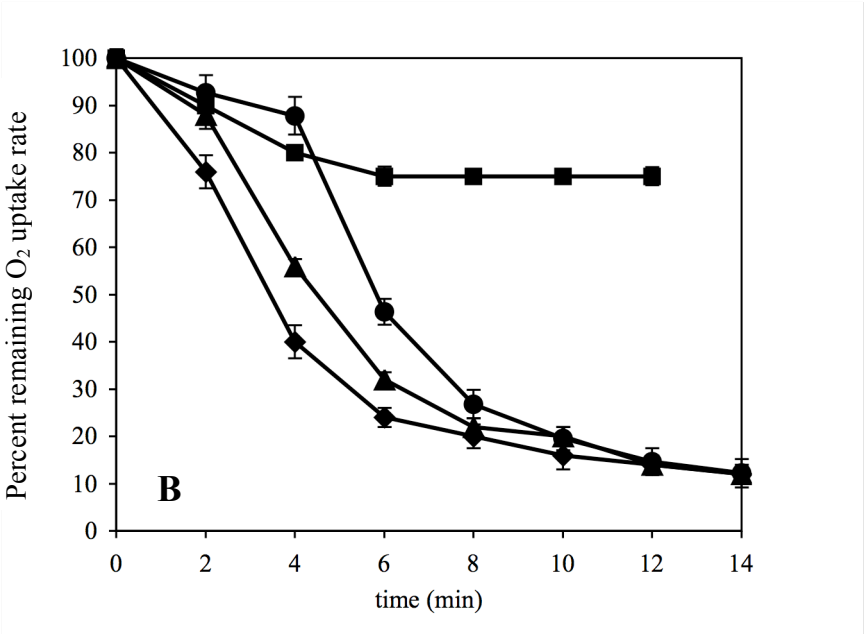

Figure 4.2. Differential effects of 1,1 DCE (A) and 1,2 *cis*-DCE (B) degradation on general cellular respiration in mutant strains of *P. butanovora.* Butane-grown cells were provided 3 mM lactate and 13 μM 1,1 DCE or 10 μM 1,2 *cis*-DCE. Slopes of tangents drawn to progress curves obtained during the assays were measured at the indicated time points to determine rates of O_2 uptake. Values are expressed as percentages of the initial rate of respiration immediately following addition of DCE. Symbols: Mutant strain G113N (■), L279F (●), Rev WT (◆), F321Y (▲).

3.5 min, which is about the same time that the substrate was completely consumed. Mutant strain F321Y had a similar response to the control. However, the rate of O_2 uptake in mutant strain L279F did not drastically decline until all available 1,2-*cis* DCE was consumed (at about 4 min). Although mutant strain G113N consumed the available 1,2-*cis* DCE in 8 min, its O_2 uptake rate was only reduced 25% after 12 min. The differential sensitivities of general respiration to DCE turnover in strains G113N and L279F relative to Rev WT suggest that specific amino acid substitutions in BMO affected CE turnover-product distribution such that the mutant strains experienced a dramatic reduction in cellular toxicity.

DISCUSSION

Mutant strains of *P. butanovora* containing single amino acid substitutions in BMOH-α have facilitated structure-function studies that are expanding our understanding of BMO-dependent oxidation reactions (Halsey *et al.*, 2006). To further probe the oxidative reactions of BMO we investigated both product formation and physiological responses of butane-grown mutant and wild type (Rev WT) strains of *P. butanovora* during exposure to chlorinated ethenes (Alvarez-Cohen and McCarty, 1991b; Doughty *et al.*, 2005; Halsey *et al.*, 2005; van Hylckama Vlieg *et al.*, 1997). Although TCE degradation causes inactivation of sMMO (Hanson and Hanson, 1996) and BMO (Halsey *et al.*, 2005), the short half-life of TCE epoxide has prevented detailed information of the mechanism of inactivation. On-line GC detection of the formation and consumption of 1,2 *cis*-DCE epoxide in sMMO-expressing cells pinpointed turnover of the epoxide as the causative agent of the inactivation (van Hylckama Vlieg *et al.*, 1996). A pre-epoxide intermediate has also been implicated in the covalent binding of the CE to the activated oxygen species of sMMO (Green and Dalton, 1989). Although the mechanism by which monooxygenases oxidize CE epoxides has not been elucidated, it is plausible that altered BMOs varying in epoxide affinity, turnover-dependent inactivation, and partitioning ratios will be useful tools

for determining the key catalytic details that influence epoxide turnover products. For example, strain G113N was engineered to more closely resemble sMMO, and some of its phenotypes reflect an sMMO-like character: i.e., subterminal oxidation of propane and butane and 3.5-fold less inhibition by methanol of methane oxidation (Halsey *et al.*, 2006), yet strain G113N appears to be unable to oxidize 1,2 *cis*-DCE epoxide.

CE epoxide breakdown products include highly reactive acyl chlorides that likely contribute to losses in cell viability by nonspecific binding to nucleic acids or other essential macromolecules. In strains Rev WT, F321Y and L279F, 100% of the 1,2 *cis*-DCE degraded was accounted for as the corresponding epoxide. In contrast, only 48% of the 1,2 *cis*-DCE degraded by strain G113N was detected as epoxide. The differential sensitivities of the mutant strains to DCE turnover as measured by lactate-dependent O_2 uptake suggest that DCE oxidation by G113N yields products that are less toxic. Furthermore, the steep decline in O_2 uptake rate by strain L279F began after commencement of 1,2 *cis*-DCE epoxide turnover. However, this strain liberated less chloride than Rev WT, but lost its rate of O_2 uptake as fast as Rev WT. Taken together, these results suggest that the different products produced in strain L279F are very toxic but need to reach a critical concentration before causing cellular injury. Alternatively, the parent compound provides protection until it is depleted.

CE turnover by the strain carrying the G⇒N substituted BMO released at most 54% of the available chlorine, formed 48% 1,2 *cis*-DCE epoxide, and maintained greater than 75% of its lactate-dependent respiration when exposed to CEs. These results support the idea that strain G113N utilizes a different CE oxidative pathway than either wild-type BMO or sMMO during CE degradation. Because the loss of cellular respiration during CE degradation by wild-type *P. butanovora* is most severe during 1,1 DCE turnover (Doughty *et al.*, 2005), it was quite remarkable that respiration was unaffected by oxidation of 1,1 DCE in strain G113N. Interestingly, butane grown *M. vaccae* also shows resistance to oxidation of 1,1 DCE (unpublished data), suggesting that *M. vaccae* probably does not form the corresponding epoxide during CE degradation. Furthermore, organochlorines accounted for 25% of the total products formed during TCE degradation by propane-grown *M. vaccae*, and only 53%

of the available chlorine was released (Vanderberg and Perry, 1994; Vanderberg *et al.*, 1995).

The dramatic phenotypes described above were measured in mutant strains L279F and G113N which were previously shown to oxidize butane at the subterminal carbon at rates 5.5 to 279-fold greater, respectively, than Rev WT (Halsey *et al.*, 2006). Mutant strain F321Y oxidizes butane exclusively at the terminal position (Halsey *et al.*, 2006), and it formed stoichiometric amounts of 1,2 *cis*-DCE epoxide and was hypersensitive to 1,1 DCE degradation as measured by lactate-dependent O_2 uptake. It appears that strain F321Y skews oxidation of CEs even more specifically towards epoxide formation than Rev WT.

Although the transient enzyme intermediates characterized in the sMMO system have not yet been identified in BMO, we believe that using a combination of chloroethenes as substrate probes and the *P. butanovora* mutant strains has the potential to provide unprecedented insights into mechanisms of catalysis in the BMO system. For example, we can surmise that the reaction cycle established for sMMO (shown below) (Beauvais and Lippard, 2005a, 2005b; Zhang and Lipscomb, 2006; Zheng and Lipscomb, 2006) is similar between the two systems.

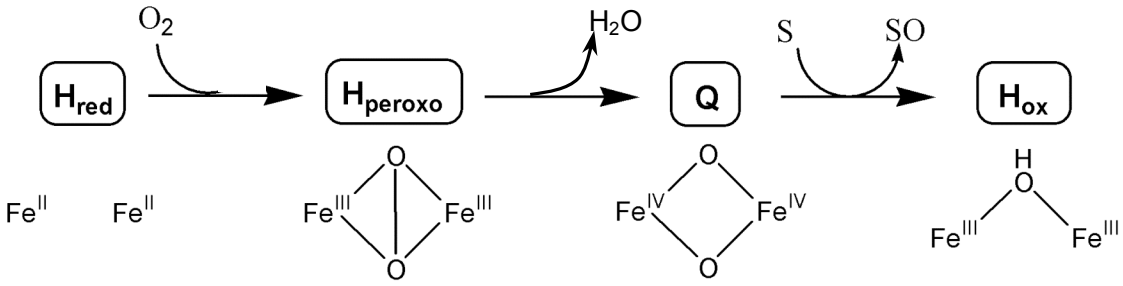

The boxed sMMO intermediates have been detected spectroscopically and refer to the different oxidative states of the diiron center. H_{ox} is reduced by the transfer of electrons from NADH restoring H_{red}. In sMMO, production of TCE epoxide and chloral are ascribed to two different oxidative reactions occurring at the enzymatic level (Fox *et al.*, 1990; Green and Dalton, 1989). sMMO oxidation of electron-rich alkenes such as propylene, is initiated by a two-electron transfer step followed by epoxidation of the substrate by the H_{peroxo} enzyme intermediate (Beauvais and

Lippard, 2005b). The results obtained in this study indicate that wild-type BMO also primarily oxidizes CEs via an H_{peroxo} intermediate forming unstable epoxides (Fig 4.3). The epoxides are either attacked by BMO or spontaneously degrade to reactive compounds leading to severe reductions in general cellular respiration and limiting CE transformation capacities. In sMMO, oxidation of alkanes such as methane, ethane, or propane progresses through the Q intermediate requiring two single electron abstraction steps and forming a carbocation product intermediate (Baik *et al.*, 2003; Brazeau and Lipscomb, 2000; Gherman *et al.*, 2001; Gherman *et al.*, 2004; Gherman *et al.*, 2005). In the case of CEs, subsequent rearrangement of the carbocation intermediate results in halide or hydride shift to the neighboring carbon. A similar mechanism has been demonstrated for attack of TCE by P-450 monooxygenases resulting in accumulation of chloral in vitro (Miller and Guengerich, 1982). Since strain G113N formed less epoxide, released less chloride and was less sensitive to CE degradation as measured by lactate-dependent O_2 uptake, we propose that its reaction with CEs utilizes the Q-state of the enzyme, and radical rebound chemistry to a greater extent than the wild-type BMO (Fig 4.3). Further work is needed to identify the specific products of CE degradation by BMO, and to confirm the hypothesis in vitro with purified enzyme.

We used CEs varying in substituent position and number to probe the enzymatic mechanism of *P. butanovora* BMOH-α mutants. The results are rationally explained by the presence of different oxidative pathways initiated by different enzymatic intermediates. Alteration of a single amino acid in BMOH-α appears to have created an enzymatic mechanism that oxidizes chloroethenes primarily via the Q enzymatic intermediate. The resulting product profiles of CE degradation also have significant physiological consequences that can be exploited for the purposes of sustainable bioremediation. Since biodegradation is limited by product toxicity in the form of enzyme inactivation or loss of cellular viability, the results obtained in this study indicate that the oxidative pathway favored by mutant strain G113N would promote more sustainable biodegradation of CEs.

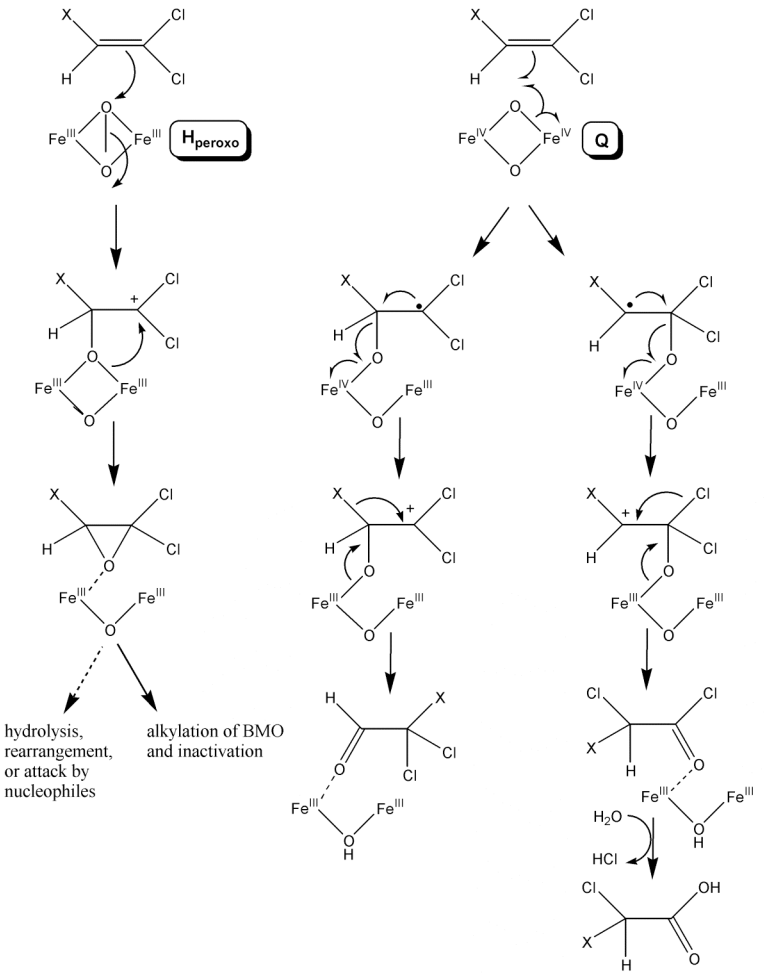

Figure 4.3. Proposed oxidative pathway of 1,1 DCE or TCE by BMO (X represents either Cl or H). Oxidation by the peroxodiiron(III) intermediate (H_{peroxo}) occurs by a two-electron transfer step and results in epoxide formation. Oxidation by the di(μ-oxo)diiron(IV) intermediate (Q) initiates at either carbon with electron transfer forming a cationic intermediate. The cationic intermediate may alkylate the active site resulting in enzyme inactivation, or leads to a chloride or hydride shift. Wild-type BMO primarily utilizes the H_{peroxo} enzyme intermediate for 1,1 DCE or TCE oxidation, and mutant strain G113N primarily utilyzes the Q enzyme intermediate.

ACKNOWLEDGEMENTS

This research was supported through a grant from the National Institutes of Health (5R01GM56128-06). This work was also supported by the office of Research and Development, U.S. Environmental Protection Agency, under Agreement # R-828772 through the Western Region Hazardous Substance Research Center.

CHAPTER 5.

SUMMARY

This work explores the basis of substrate specificity of butane monooxygenase (BMO) and chlorinated ethene toxicity in butane oxidizing bacteria. Monooxygenases like BMO, have characteristically large substrate ranges, making them valuable for use in biocatalysis and bioremediation. BMO can activate environmentally recalcitrant chlorinated compounds, but one factor limiting sustainable bioremediation is the toxicity of the BMO turnover products. The first chapter of this dissertation describes the kinetics of trichloroethylene turnover by BMO and the resulting effects on general cellular respiration and viability in three species of butane oxidizing bacteria (Halsey *et al*., 2005). This research demonstrated a range of toxicities resulting from trichloroethylene (TCE) turnover. Butane oxidizing bacteria harboring biochemically distinct BMOs oxidized TCE at different rates, with different transformation capacities, but remarkably similar apparent K_s values. Differences in cellular toxicities including moderate to severe mechanism based inactivation of BMO and zero to 83% reduction in cellular viability provide evidence for differences in the products released or the ratios of products released from the different BMOs.

Even though BMO is the closest known homologue to methane monooxygenase (MMO), previous research reported that BMO's substrate range excludes methane. The fundamental basis of methane restriction by BMO was investigated by engineering amino acid substitutions at key functional regions in the enzyme, analyzing the resulting biochemical phenotypes, and applying structural modeling. By measuring methanol accumulation during exposure to methane, BMO was shown to catalyze methane oxidation, but BMO is strongly inhibited by the product. One mutant strain, G113N, oxidized 4-fold more methane than the wild-type strain suggesting that alterations to the active site allowed methanol to release from the diiron center more readily. This was the first demonstration of methane oxidation by an enzyme other than MMO (Halsey *et al*., 2006). Changes to regiospecificity of

butane oxidation were also measured in the mutant strains. Although the wild-type strain oxidized butane primarily at the terminal position, butane was predominantly oxidized to 2-butanol in strain G113N. Propane oxidation was similarly affected in mutant strain G113N. This research demonstrated that single amino acid substitutions in BMO can modify regiospecificity of oxidation, methanol accumulation, and specific activity (Halsey *et al.*, 2006).

Differences in the altered BMO enzymes were further analyzed by utilizing chlorinated ethenes as mechanistic probes. BMO primarily oxidizes chlorinated ethenes via epoxide intermediates that are highly reactive contributing to turnover-dependent cellular toxicities. Experimental evidence suggested that altered BMOs can either directly hydroxylate chlorinated ethenes or cause intramolecular chloride migration (NIH shift). The different oxidative reactions have significant physiological ramifications. For example, the rate of O_2 uptake in mutant strain G113N was unaffected during 1,1 dichloroethylene (DCE) oxidation, but the wild-type strain and mutant strain F321Y rapidly lost their rates of O_2 uptake during 1,1 DCE oxidation. This research provides evidence that the mechanism of oxidation was altered in strain G113N. The data obtained in this research supports a model in which different enzymatic intermediates are utilized during CE oxidation by the altered BMO in G113N as compared to the wild-type BMO.

The single amino acid substitutions engineered in BMO in *P. butanovora* showed dramatic shifts in regiospecificity of oxidation and emphasized the importance of active site geometry to substrate specificity, regiospecificity, and regulation of activity. Experiments with the mutant strains and different butane-oxidizing genera emphasized the finely tuned nature of multicomponent monooxygenases. All together, this work combines mechanistic insights and physiological applications.

BIBLIOGRAPHY

Alvarez-Cohen, L., and McCarty, P.L. (1991a) A cometabolic biotransformation model for halogenated aliphatic compounds exhibiting product toxicity. *Environ Sci Technol* **25**: 1381-1387.

Alvarez-Cohen, L., and McCarty, P.L. (1991b) Product toxicity and cometabolic competitive inhibition modeling of chloroform and trichloroethylene transformation by methanotrophic resting cells. *Appl Enviro Microbio.* **57**: 1031-1037.

Arciero, D., Vannelli, T., Logan, M., and Hooper, A.B. (1989) Degradation of trichloroethylene by the ammonia-oxidizing bacterium *Nitrosomonas europaea*. *Biochem Biophys Res Commun* **159**: 640-643.

Arp, D.J. (1999) Butane metabolism by butane-grown *Pseudomonas butanovora*. *Microbiology* **145**: 1173-1180.

Arp, D.J., Yeager, C.M., and Hyman, M.R. (2001) Molecular and cellular fundamentals of aerobic cometabolism of trichloroethylene. *Biodegradation* **12**: 81-103.

Baik, M.H., Newcomb, M., Friesner, R.A., and Lippard, S.J. (2003) Mechanistic studies on the hydroxylation of methane by methane monooxygenase. *Chem Rev* **103**: 2385-2419.

Balendra, S., Lesieur, C., Smith, T.J., and Dalton, H. (2002) Positively charged amino acids are essential for electron transfer and protein-protein interactions in the soluble methane monooxygenase complex from *Methylococcus capsulatus* (Bath). *Biochemistry* **41**: 2571-2579.

Beauvais, L.G., and Lippard, S.J. (2005a) Reactions of the diiron(IV) intermediate Q in soluble methane monooxygenase with fluoromethanes. *Biochem Biophys Res Commun* **338**: 262-266.

Beauvais, L.G., and Lippard, S.J. (2005b) Reactions of the peroxo intermediate of soluble methane monooxygenase hydroxylase with ethers. *J Am Chem Soc* **127**: 7370-7378.

Beeman, R.E., and Bleckmann, C.A. (2002) Sequential anaerobic-aerobic treatment of an aquifer contaminated by halogenated organics: field results. *J Contam Hydrol* **57**: 147-159.

Belay, N., and Daniels, L. (1987) Production of ethane, ethylene, and acetylene from halogenated hydrocarbons by methanogenic bacteria. *Appl Environ Microbiol* **53**: 1604-1610.

Blazyk, J.L., Gassner, G.T., and Lippard, S.J. (2005) Intermolecular electron-transfer reactions in soluble methane monooxygenase: a role for hysteresis in protein function. *J Am Chem Soc* **127**: 17364-17376.

Brazeau, B.J., and Lipscomb, J.D. (2000) Kinetics and activation thermodynamics of methane monooxygenase compound Q formation and reaction with substrates. *Biochemistry* **39**: 13503-13515.

Brazeau, B.J., and Lipscomb, J.D. (2003) Key amino acid residues in the regulation of soluble methane monooxygenase catalysis by component B. *Biochemistry* **42**: 5618-5631.

Brazeau, B.J., Wallar, B.J., and Lipscomb, J.D. (2003) Effector proteins from P450(cam) and methane monooxygenase: lessons in tuning nature's powerful reagents. *Biochem Biophys Res Commun* **312**: 143-148.

Brzostowicz, P.C., Walters, D.M., Thomas, S.M., Nagarajan, V., and Rouviere, P.E. (2003) mRNA differential display in a microbial enrichment culture: simultaneous identification of three cyclohexanone monooxygenases from three species. *Appl Environ Microbiol* **69**: 334-342.

Brzostowicz, P.C., Walters, D.M., Jackson, R.E., Halsey, K.H., Ni, H., and Rouviere, P.E. (2005) Proposed involvement of a soluble methane monooxygenase homologue in the cyclohexane-dependent growth of a new *Brachymonas* species. *Environ Microbiol* **7**: 179-190.

Cadieux, E., Vrajmasu, V., Achim, C., Powlowski, J., and Munck, E. (2002) Biochemical, Mossbauer, and EPR studies of the diiron cluster of phenol hydroxylase from *Pseudomonas* sp. strain CF 600. *Biochemistry* **41**: 10680-10691.

Canada, K.A., Iwashita, S., Shim, H., and Wood, T.K. (2002) Directed evolution of toluene *ortho*-monooxygenase for enhanced 1-naphthol synthesis and chlorinated ethene degradation. *J Bacteriol* **184**: 344-349.

Chang, S.L., Wallar, B.J., Lipscomb, J.D., and Mayo, K.H. (2001) Residues in *Methylosinus trichosporium* OB3b methane monooxygenase component B involved in molecular interactions with reduced- and oxidized-hydroxylase component: a role for the N-terminus. *Biochemistry* **40**: 9539-9551.

Chu, K.H., and Alvarez-Cohen, L. (1999) Evaluation of toxic effects of aeration and trichloroethylene oxidation on methanotrophic bacteria grown with different nitrogen sources. *Appl Environ Microbiol* **65**: 766-772.

Coleman, N.V., Mattes, T.E., Gossett, J.M., and Spain, J.C. (2002) Biodegradation of *cis*-dichloroethene as the sole carbon source by a beta-proteobacterium. *Appl Environ Microbiol* **68**: 2726-2730.

Coleman, N.V., Bui, N.B., and Holmes, A.J. (2006) Soluble di-iron monooxygenase gene diversity in soils, sediments and ethene enrichments. *Environ Microbiol* **8**: 1228-1239.

DeLano, W.L. (2002) The PyMol Molecular Graphics System. San Carlos, CA, USA: DeLano Scientific.

DiSpirito, A.A., Gulledge, J., Shiemke, A.K., Murrel, J.C., Lidstrom, M.E., and Krema, C.L. (1992) Trichloroethylene oxidation by the membrane-associated methane monooxygenase in Type I, Type II and Type X methanotrophs. *Biodegradation* **2**: 151-164.

Doughty, D.M., Sayavedra-Soto, L.A., Arp, D.J., and Bottomley, P.J. (2005) Effects of dichloroethene isomers on the induction and activity of butane monooxygenase in the alkane-oxidizing bacterium "*Pseudomonas butanovora*". *Appl Environ Microbiol* **71**: 6054-6059.

Doughty, D.M., Sayavedra-Soto, L.A., Arp, D.J., and Bottomley, P.J. (2006) Product repression of alkane monooxygenase expression in *Pseudomonas butanovora*. *J Bacteriol* **188**: 2586-2592.

Dubbels, B.L., Sayavedra-Soto, L.A., and Arp, D.J. (accepted) Butane monooxygenase of *Pseudomonas butanovora*: purification and biochemical characterization of a terminal-alkane hydroxylating diiron monooxygenase. *J Microbiol.*

Elango, N., Radhakrishnan, R., Froland, W.A., Wallar, B.J., Earhart, C.A., Lipscomb, J.D., and Ohlendorf, D.H. (1997) Crystal structure of the hydroxylase component of methane monooxygenase from *Methylosinus trichosporium* OB3b. *Prot Sci* **6**: 556-568.

Ensign, S.A., Hyman, M.R., and Arp, D.J. (1992) Cometabolic degradation of chlorinated alkenes by alkene monooxygenase in a propylene-grown *Xanthobacter* strain. *Appl Environ Microbiol* **58**: 3038-3046.

Ensign, S.A. (1996) Aliphatic and chlorinated alkenes and epoxides and inducers of alkene monooxygenase nad epoxidase activities in *Xanthobacter* strain Py2. *Appl Environ Microbiol* **62**: 61-66.

EPA, U.S. (2001) Trichloroethylene health risk assessment: synthesis and characterization (external review draft). U.S. Environmental Protection Agency, Office of Research and Development, National Center for environmental Assessment, Washington Office, Washington, DC, EPA/600/P-01/002A, 2001.

Fiser, A., Do, R.K., and Sali, A. (2000) Modeling of loops in protein structures. *Prot Sci* **9**: 1753-1773.

Fishman, A., Tao, Y., Rui, L., and Wood, T.K. (2005) Controlling the regiospecific oxidation of aromatics via active site engineering of toluene *para*-monooxygenase of *Ralstonia pickettii* PKO1. *J Biol Chem* **280**: 506-514.

Fox, B.G., Froland, W.A., Dege, J.E., and Lipscomb, J.D. (1989) Methane monooxygenase from *Methylosinus trichosporium* OB3b. Purification and properties of a three-component system with high specific activity from a type II methanotroph. *J Biol Chem* **264**: 10023-10033.

Fox, B.G., Borneman, J.G., Wackett, L.P., and Lipscomb, J.D. (1990) Haloalkene oxidation by soluble methane monooxygenase from *Methylosinus trichosporium* OB3b: mechanistic and environmental implications. *Biochemistry* **29**: 6419-6427.

Fox, B.G., Liu, Y., Dege, J.E., and Lipscomb, J.D. (1991) Complex formation between the protein components of methane monooxygenase from *Methylosinus trichosporium* OB3b. Identification of sites of component interaction. *J Biol Chem* **266**: 540-550.

Froland, W.A., Andersson, K.K., Lee, S.K., Liu, Y., and Lipscomb, J.D. (1992) Methane monooxygenase component-B and reductase alter the regioselectivity of the hydroxylase component-catalyzed reactions - a novel role for protein-protein interactions in an oxygenase mechanism. *J of Biol Chem* **267**: 17588-17597.

Gassner, G.T., and Lippard, S.J. (1999) Component interactions in the soluble methane monooxygenase system from *Methylococcus capsulatus* (Bath). *Biochemistry* **38**: 12768-12785.

Gherman, B.F., Dunietz, B.D., Whittington, D.A., Lippard, S.J., and Friesner, R.A. (2001) Activation of the C-H bond of methane by intermediate Q of methane monooxygenase: a theoretical study. *J Am Chem Soc* **123**: 3836-3837.

Gherman, B.F., Baik, M.H., Lippard, S.J., and Friesner, R.A. (2004) Dioxygen activation in methane monooxygenase: a theoretical study. *J Am Chem Soc* **126**: 2978-2990.

Gherman, B.F., Lippard, S.J., and Friesner, R.A. (2005) Substrate hydroxylation in methane monooxygenase: quantitative modeling via mixed quantum mechanics/molecular mechanics techniques. *J Am Chem Soc* **127**: 1025-1037.

Gornall, A.G., Bardawill, C.J., and David, M.M. (1949) Determination of serum proteins by means of the Biuret reaction. *J Biol Chem* **177**: 751-766.

Gossett, J.M. (1987) Measurement of Henry's law constants for C_1 and C_2 chlorinated hydrocarbons. *Environ Sci Technol* **21:**202-208.

Green, J., and Dalton, H. (1985) Protein B of soluble methane monooxygenase from *Methylococcus capsulatus* (Bath). *J Biol Chem* **260**: 15795-15801.

Green, J., and Dalton, H. (1989) Substrate specificity of soluble methane monooxygenase. Mechanistic implications. *J Biol Chem* **264**: 17698-17703.

Halsey, K.H., Sayavedra-Soto, L.A., Bottomley, P.J., and Arp, D.J. (2005) Trichloroethylene degradation by butane-oxidizing bacteria causes a spectrum of toxic effects. *Appl Microbiol Biotechnol* **68**: 794-801.

Halsey, K.H., Sayavedra-Soto, L.A., Bottomley, P.J., and Arp, D.J. (2006) Site-directed amino acid substitutions in the hydroxylase alpha subunit of butane monooxygenase from *Pseudomonas butanovora*: Implications for substrates knocking at the gate. *J Bacteriol* **188**: 4962-4969.

Hamamura, N., Page, C., Long, T., Semprini, L., and Arp, D.J. (1997) Chloroform cometabolism by butane-grown CF8, *Pseudomonas butanovora*, and *Mycobacterium vaccae* JOB5 and methane-grown *Methylosinus trichosporium* OB3b. *Appl Environ Microbiol* **63**: 3607-3613.

Hamamura, N., Storfa, R.T., Semprini, L., and Arp, D.J. (1999) Diversity in butane monooxygenases among butane-grown bacteria. *Appl Environ Microbiol* **65**: 4586-4593.

Hamamura, N., and Arp, D.J. (2000) Isolation and characterization of alkane-utilizing *Nocardioides* sp. strain CF8. *FEMS Microbiol Lett* **186**: 21-26.

Hamamura, N., Yeager, C., and Arp, D.J. (2001) Two distinct monooxygenases for alkane oxidation in *Nocarioides* sp. strain CF8. *Appl Environ Microbiol* **67**: 4992-4998.

Hamamura, N., Olson, S.H., Ward, D.M., and Inskeep, W.P. (2006) Microbial population dynamics associated with crude-oil biodegradation in diverse soils. *Appl Environ Microbiol* **72**: 6316-6324.

Hanson, R.S., and Hanson, T.E. (1996) Methanotrophic bacteria. *Microbiol Rev* **60**: 439-471.

Hunt, J. (1996) *Petroleum Geochemistry and Geology, 2nd edn.* San Francisco: W.H. Freeman.

Hyman, M.R., and Wood, P.M. (1985) Suicidal inactivation and labeling of ammonia monooxygenase by acetylene. *Biochemistry* **227**: 719-725.

Infante, P.F., and Tsongas, T.A. (1983) Occupational reproductive hazards: necessary steps to prevention. *Am J Ind Med* **4**: 383-390.

Jahng, D., and Wood, T.K. (1994) Trichloroethylene and chloroform degradation by a recombinant pseudomonad expressing soluble methane monooxygenase from *Methylosinus trichosporium* OB3b. *Appl Environ Microbiol* **60**: 2473-2482.

Kao, C.M., and Prosser, J. (1999) Intrinsic bioremediation of trichloroethylene and chlorobenzene: field and laboratory studies. *J Hazard Mater* **69**: 67-79.

Kim, Y., Semprini, L., and Arp, D.J. (1997) Aerobic cometabolism of chloroform and 1,1,1-trichloroethane by butane-grown microorganisms. *Bioremediation* **1**: 135-148.

Kim, Y., Arp, D.A., and Semprini, L. (2000) Aerobic cometabolism of chlorinated methanes, ethanes, and ethenes by Butane-utilizing Microorganisms. *J Environm Engr* **126**: 934-942.

Kotani, T., Yurimoto, H., Kato, N., and Sakai, Y. (2006) A Novel acetone metabolism in a propane-utilizing bacterium *Gordonia* sp. strain TY-5. *J Bacteriol* (Epub ahead of print on Oct 2006).

Landa, A.S., Sipkema, E.M., Weijma, J., Beenackers, A.A.C.M., Dolfing, J., and Janssen, D.B. (1994) Cometabolic degradation of trichloroethylene by *Pseudomonas cepacia* G4 in a chemostat with toluene as the primary substrate. *Appl Environ Microbiol* **60**: 3368-3374.

Lau, P.C., Sung, C.K., Lee, J.H., Morrison, D.A., and Cvitkovitch, D.G. (2002) PCR ligation mutagenesis in transformable streptococci: application and efficiency. *J Microbiol Methods* **49**: 193-205.

Leahy, J.G., Batchelor, P.J., and Morcomb, S.M. (2003) Evolution of the soluble diiron monooxygenases. *FEMS Microbiol Rev* **27**: 449-479.

Lee, S.K., Nesheim, J.C., and Lipscomb, J.D. (1993) Transient intermediates of the methane monooxygenase catalytic cycle. *J Biol Chem* **268**: 21569-21577.

Lenczewski, M., Jardine, P., McKay, L., and Layton, A. (2003) Natural attenuation of trichloroethylene in fractured shale bedrock. *J Contam Hydrol* **64**: 151-168.

Liebler, D.C., and Guengerich, F.P. (1983) Olefin oxidation by cytochrome P-450: evidence for group migration in catalytic intermediates formed with vinylidene chloride and trans-1-phenyl-1-butene. *Biochemistry* **22**: 5482-5489.

Lipscomb, J.D. (1994) Biochemistry of the soluble methane monooxygenase. *Annual Review of Microbiology* **48**: 371-399.

Liu, K.E., Wang, D.L., Huynh, B.H., Edmondson, D.E., Salifoglou, A., and Lippard, S.J. (1994) Spectroscopic detection of intermediates in the reaction of dioxygen with the reduced methane monooxygenase hydroxylase from *Methylococcus capsulatus* (Bath). *J Amer Chem Soc* **116**: 7465-7466.

Lontoh, S., Zahn, J.A., DiSpirito, A.A., and Semrau, J.D. (2000) Identification of intermediates of in vivo trichloroethylene oxidation by the membrane-associated methane monooxygenase. *FEMS Microbiol Lett* **186**: 109-113.

Lovley, D.R. (2001) Bioremediation. Anaerobes to the rescue. *Science* **293**: 1444-1446.

Mahendra, S., and Alvarez-Cohen, L. (2006) Kinetics of 1,4-dioxane biodegradation by monooxygenase-expressing bacteria. *Environ Sci Technol* **40**: 5435-5442.

Marti-Renom, M.A., Stuart, A., Fiser, A., Sanchez, R., Melo, F., and Sali, A. (2000) Comparative protein structure modeling of genes and genomes. *Annu Rev Biophys Biomol Struct* **29**: 291-325.

McClay, K., Streger, S.H., and Steffan, R.J. (1995) Induction of toluene oxidation activity *in Pseudomonas mendocina* KR1 and *Pseudomonas* sp. strain ENVPC5 by chlorinated solvents and alkanes. *Appl Environ Microbiol* **61**: 3479-3481.

Merkx, M., Kopp, D.A., Sazinsky, M.H., Blazyk, J.L., Muller, J., and Lippard, S.J. (2001) Dioxygen Activation and Methane Hydroxylation by Soluble Methane Monooxygenase: A Tale of Two Irons and Three Proteins. *Angew Chem Int Ed Engl* **40**: 2782-2807.

Miller, R.E., and Guengerich, F.P. (1982) Oxidation of trichloroethylene by liver microsomal cytochrome P-450: evidence for chlorine migration in a transition state not involving trichloroethylene oxide. *Biochemistry* **21**: 1090-1097.

Murrell, J.C., Gilbert, B., and McDonald, I.R. (2000) Molecular biology and regulation of methane monooxygenase. *Arch Microbiol* **173**: 325-332.

Newman, L.M., and Wackett, L.P. (1997) Trichloroethylene oxidation by purified toluene 2-monooxygenase: products, kinetics, and turnover-dependent inactivation. *J Bacteriol* **179**: 90-96.

Paulsen, K.E., Liu, Y., Fox, B.G., Lipscomb, J.D., Munck, E., and Stankovich, M.T. (1994) Oxidation-Reduction potentials of the methane monooxygenase hydroxylase component from *Methylosinus trichosporium* OB3b. *Biochemistry* **33**: 713-722.

Phillips, W.E., and Perry, J.J. (1974) Metabolism of *n*-butane and 2-butanone by *Mycobacterium vaccae*. *J Bacteriol* **120**: 987-989.

Pikus, J.D., Studts, J.M., McClay, K., Steffan, R.J., and Fox, B.G. (1997) Changes in the regiospecificity of aromatic hydroxylation produced by active site engineering in the diiron enzyme toluene 4-monooxygenase. *Biochemistry* **36**: 9283-9289.

Prior, S.D., and Dalton, H. (1985) Acetylene as a suicide substrate and active site probe for methane monooxygenase from *Methylococcus capsulatus* (Bath). *FEMS Microbiol Lett* **29**: 105-109.

Qian, H., Edlund, U., Powlowski, J., Shingler, V., and Sethson, I. (1997) Solution structure of phenol hydroxylase protein component P2 determined by NMR spectroscopy. *Biochemistry* **36**: 495-504.

Rasche, M.E., Hyman, M.R., and Arp, D.J. (1991) Factors limiting aliphatic chlorocarbon degradation by *Nitrosomonas europaea:* cometabolic inactivation of ammonia monooxygenase and substrate specificity. *Appl Environ Microbiol* **57**: 2986-2994.

Rosenzweig, A.C., Brandstetter, H., Whittington, D.A., Nordlund, P., Lippard, S.J., and Frederick, C.A. (1997) Crystal structures of the methane monooxygenase hydroxylase from *Methylococcus capsulatus* (Bath): implications for substrate gating and component interactions. *Proteins* **29**: 141-152.

Rouviere, P.E., and Chen, M.W. (2003) Isolation of *Brachymonas petroleovorans* CHX, a novel cyclohexane-degrading beta-proteobacterium. *FEMS Microbiol Lett* **227**: 101-106.

Rui, L., Reardon, K.F., and Wood, T.K. (2005) Protein engineering of toluene *ortho*-monooxygenase of *Burkholderia cepacia* G4 for regiospecific hydroxylation of indole to form various indigoid compounds. *Appl Microbiol Biotechnol* **66**: 422-429.

Sali, A., and Blundell, T.L. (1993) Comparative protein modeling by satisfaction of spatial restraints. *J Mol Biol* **234**: 779-815.

Sayavedra-Soto, L.A., Byrd, C.M., and Arp, D.J. (2001) Induction of butane consumption in *Pseudomonas butanovora*. *Arch Microbiol* **176**: 114-120.

Sayavedra-Soto, L.A., Doughty, D.M., Kurth, E.G., Bottomley, P.J., and Arp, D.J. (2005) Product and product-independent induction of butane oxidation in *Pseudomonas butanovora*. *FEMS Microbiol Lett* **250**: 111-116.

Sazinsky, M.H., Bard, J., Di Donato, A., and Lippard, S.J. (2004) Crystal structure of the toluene/*o*-xylene monooxygenase hydroxylase from *Pseudomonas stutzeri* OX1. Insight into the substrate specificity, substrate channeling, and active site tuning of multicomponent monooxygenases. *J Biol Chem* **279**: 30600-30610.

Sazinsky, M.H., and Lippard, S.J. (2005) Product bound structures of the soluble methane monooxygenase hydroxylase from *Methylococcus capsulatus* (Bath): protein motion in the alpha-subunit. *J Am Chem Soc* **127**: 5814-5825.

Sazinsky, M.H., Dunten, P.W., McCormick, M.S., Didonato, A., and Lippard, S.J. (2006) X-ray Structure of a Hydroxylase-Regulatory Protein Complex from a Hydrocarbon-Oxidizing Multicomponent Monooxygenase, *Pseudomonas* sp. OX1 Phenol Hydroxylase. *Biochemistry* **45**: 15392-15404.

Sazinsky, M.H., and Lippard, S.J. (2006) Correlating structure with function in bacterial multicomponent monooxygenases and related diiron proteins. *Acc Chem Res* **39**: 558-566.

Seah, S.Y., Labbe, G., Kaschabek, S.R., Reifenrath, F., Reineke, W., and Eltis, L.D. (2001) Comparative specificities of two evolutionarily divergent hydrolases involved in microbial degradation of polychlorinated biphenyls. *J Bacteriol* **183**: 1511-1516.

Semprini, L. (1995) In situ bioremediation of chlorinated solvents. *Environ Health Perspect* **103 Suppl 5**: 101-105.

Semprini, L. (1997) Strategies for the aerobic co-metabolism of chlorinated solvents. *Curr Opin Biotechnol* **8**: 296-308.

Semprini, L.G.D., Hopkins, and McCarty, P.L. (1994) In-situ aerobic treatment of trichloroethylene by phenol-utlizing microorganisms: Results of transient formate addition studies. Extended Abstract in I&EC Special Symposium American Chemical Society, Altanta, GA, Sept. 19-21, pp. 1330-1333.

Shennan, J. (2006) Utilization of C_2-C_4 gaseous hydrocarbons and isoprene by microorganisms. *J Chem Tech and Biotech* **81**: 237-256.

Shields, M.S., Montgomery, S.O., Cuskey, S.M., Chapman, P.J., and Pritchard, P.H. (1991) Mutants of *Pseudomonas cepacia* G4 defective in catabolism of aromatic compounds and trichloroethylene. *Appl Environ Microbiol* **57**: 1935-1941.

Shinohara, Y., Uchiyama, H., and Kusakabe, I. (1998) Oxidation of some alkanes and trichloroethylene by H_2O_2/Hydroxylase system of soluble methane monooxygenase from *Methylocystis* sp. M. *J Ferm and Bioeng* **85**: 266-270.

Silverman, R.B. (1988) Introduction. In *Mechanism-based enzyme inactivation: chemistry and enzymology*. Vol. 1. Boca Raton: CRC Press, pp. 3-30.

Sluis, M.K., Sayavedra-Soto, L.A., and Arp, D.J. (2002) Molecular analysis of the soluble butane monooxygenase from '*Pseudomonas butanovora*'. *Microbiology* **148**: 3617-3629.

Smith, T.J., Slade, S.E., Burton, N.P., Murrell, J.C., and Dalton, H. (2002) Improved system for protein engineering of the hydroxylase component of soluble methane monooxygenase. *Appl Environ Microbiol* **68**: 5265-5273.

Smith, T.J., and Dalton, H. (2004) Biocatalysis by methane monooxygenase and its implications for the petroleum industry. In *Studies in Surface Science and Catalysis*. Vol. 151. Vazquez-Duhalt, R. and Qintero-Ramirez, R. (eds). Amsterdam: Elsevier B. B., pp. 177-192.

Steffan, R.J., and McClay, K.R. (2000) Preparation of enantio-specific epoxides. patent WO/2000/073425.

Takahashi, J. (1980) Production of intracellular and extracellular protein from *n*-butane by *Pseudomonas butanovora* sp. nov. *Adv Appl Microbiol* **26**: 117-127.

Takahashi, J., Ichikawa, Y., Sagae, H., Komura, I., Kanou, H., and Yamada, K. (1980) Isolation and identification of a *n*-butane-assimilating bacterium. *Agric Biol Chem* **44**: 1835-1840.

Taylor, L.A., and Rose, R.E. (1988) A correction in the nucleotide sequence of the Tn903 kanamycin resistance determinant in pUC4K. *Nucleic Acids Res* **16**: 358-362.

Tsein, H.-C., Brusseau, G.A., Hanson, R.S., and Wackett, L.P. (1989) Biodegradation of trichloroethylene by *Methylosinus trichosporium* OB3b. *Appl Environ Microbiol* **55**: 3155-3161.

Urgun-Demirtas, M., Pagilla, K.R., Stark, B.C., and Webster, D. (2003) Biodegradation of 2-chlorobenzoate by recombinant *Burkholderia cepacia* expressing *Vitreoscilla* hemoglobin under variable levels of oxygen availability. *Biodegradation* **14**: 357-365.

van Hylckama Vlieg, J., De Koning, W., and Janssen, D. (1997) Effect of Chlorinated Ethene Conversion on Viability and Activity of *Methylosinus trichosporium* OB3b. *Appl Environ Microbiol* **63**: 4961-4964.

van Hylckama Vlieg, J.E., and Janssen, D.B. (2001) Formation and detoxification of reactive intermediates in the metabolism of chlorinated ethenes. *J Biotechnol* **85**: 81-102.

van Hylckama Vlieg, J.E.T., deKoning, W., and Janssen, D.B. (1996) Transformation kinetics of chlorinated ethenes by *Methylosinus trichosporium* OB3b and detection of unstable epooxides by on-line gas chromatography. *Appl Environ Microbiol* **62**: 3304-3312.

Vanderberg, L.A., and Perry, J.J. (1994) Dehalogenation by *Mycobacterium vaccae* JOB-5: role of the propane monooxygenase. *Can J Microbiol* **40**: 169-172.

Vanderberg, L.A., Burback, B.L., and Perry, J.J. (1995) Biodegradation of trichloroethylene by *Mycobacterium vaccae*. *Can J Microbiol* **41**: 298-301.

Vangnai, A.S., and Arp, D.J. (2001) An inducible 1-butanol dehydrogenase, a quinohemoprotein, is involved in the oxidation of butane by *Pseudomonas butanovora*. *Microbiology* **147**: 745-756.

Vangnai, A.S., Arp, D.J., and Sayavedra-Soto, L.A. (2002) Two distinct alcohol dehydrogenases participate in butane metabloism in *Pseudomonas butanovora*. *J Bacteriol* **184**: 1916-1924.

Vardar, G., and Wood, T.K. (2004) Protein engineering of toluene-*o*-xylene monooxygenase from *Pseudomonas stutzer*i OX1 for synthesizing 4-methylresorcinol, methylhydroquinone, and pyrogallol. *Appl Environ Microbiol* **70**: 3253-3262.

Vardar, G., and Wood, T.K. (2005) Protein engineering of toluene-*o*-xylene monooxygenase from *Pseudomonas stutzeri* OX1 for enhanced chlorinated ethene degradation and *o*-xylene oxidation. *Appl Microbiol Biotechnol* **68**: 510-517.

Wackett, L.P., and Householder, S.R. (1989) Toxicity of trichloroethylene to *Pseudomonas putida* F1 is mediated by toluene dioxygenase. *Appl Environ Microbiol* **55**: 2723-2725.

Wallar, B.J., and Lipscomb, J.D. (2001) Methane monooxygenase component B mutants alter the kinetics of steps throughout the catalytic cycle. *Biochemistry* **40**: 2220-2233.

West, C.A., Salmond, G.P., Dalton, H., and Murrell, J.C. (1992) Functional expression in Escherichia coli of proteins B and C from soluble methane monooxygenase of *Methylococcus capsulatus* (Bath). *J Gen Microbiol* **138**: 1301-1307.

Whittington, D.A., and Lippard, S.J. (2001) Crystal structures of the soluble methane monooxygenase hydroxylase from *Methylococcus capsulatus* (Bath) demonstrating geometrical variability at the dinuclear iron active site. *J Am Chem Soc* **123**: 827-838.

Whittington, D.A., Rosenzweig, A.C., Frederick, C.A., and Lippard, S.J. (2001a) Xenon and halogenated alkanes track putative substrate binding cavities in the soluble methane monooxygenase hydroxylase. *Biochemistry* **40**: 3476-3482.

Whittington, D.A., Sazinsky, M.H., and Lippard, S.J. (2001b) X-ray crystal structure of alcohol products bound at the active site of soluble methane monooxygenase hydroxylase. *J Am Chem Soc* **123**: 1794-1795.

Wiegant, W.W., and deBont, J.A.M. (1980) A new route for ethylene glycol metabolism in *Mycobacterium* E44. *J Gen Microbiol* **120**: 325-331.

Yanisch-Perron, C., Vieira, J., and Messing, J. (1985) Improved M13 phage cloning vectors and host strains: nucleotide sequences of the M13mp18 and pUC19 vectors. *Gene* **33**: 103-119.

Yeager, C.M., Bottomley, P.J., and Arp, D.J. (2001) Cytotoxicity associated with trichloroethylene oxidation in *Burkholderia cepacia* G4. *Appl Environ Microbiol* **67**: 2107-2115.

Zhang, J., and Lipscomb, J.D. (2006) Role of the C-terminal region of the B component of *Methylosinus trichosporium* OB3b methane monooxygenase in the regulation of oxygen activation. *Biochemistry* **45**: 1459-1469.

Zhang, J., Wallar, B.J., Popescu, C.V., Renner, D.B., Thomas, D.D., and Lipscomb, J.D. (2006a) Methane monooxygenase hydroxylase and B component interactions. *Biochemistry* **45**: 2913-2926.

Zhang, J., Zheng, H., Groce, S.L., and Lipscomb, J.D. (2006b) Basis for specificity in methane monooxygenase and related non-heme iron-containing biological oxidation catalysts. *J Mol Catal A: Chem* **251**: 54-65.

Zheng, H., and Lipscomb, J.D. (2006) Regulation of methane monooxygenase catalysis based on size exclusion and quantum tunneling. *Biochemistry* **45**: 1685-1692.